ACTA UNIVERSITATIS SZEGEDIENSIS

PARS CLIMATOLOGICA ET CHOROLOGICA
SCIENTIARUM NATURALIUM

Curat: János Unger

ACTA CLIMATOLOGICA ET CHOROLOGICA

TOMUS XLIX-L.

SZEGED (HUNGARIA)

2016

IN MEMORIAM PROF. GYÖRGY KOPPÁNY

The retired professor of our department, Dr. György Koppány passed away on 13 April 2016, in the 84th year of his life.

He was born on 31 March 1932 in Bajmok, in the territory of the former Yugoslavia. He started his grammar school studies in Subotica and continued them in Hungary from 1948.

He graduated as a meteorologist in 1956 from Eötvös Loránd University, Budapest and in September the same year he got a job at the Hungarian Meteorological Institute. From the beginning his interest turned to the macro-scale, hemispheric atmospheric processes that cause fundamental and long-term changes in Hungary's weather. From 1957 his studies have been published. in the journal Időjárás, and later in different referred journals. In 1963 he received university doctorate degree defending his dissertation of the title "The 24-hour strong changes in the atmospheric pressure in the area between the Rocky Mountains and Western Siberia'. In 1966 he got a one-year United Nations scholarship. In this context, he spent 6 months in the Soviet Union and 6 months in the United States studying the Soviet and American long-term prognostic methods.

75-year-old greeting (Department of Climatology and Landscape Ecology, 2007)

In 1985 he was declared Doctor of the Geographical Sciences (Meteorology). His doctoral dissertation dealt with the long-term predictability of the weather. In 1986 he was appointed professor, and Head of Department in Szeged, at the Department of Climatology, József Attila University (in 2000 renamed University of Szeged). After his appointment, in addition to traditional meteorological and climatological subjects new directions appeared in both research and education at the department, such as renewable energy sources and historical climatology. He published several textbooks in these subjects (e.g. Atmospheric Resources, JATE, Szeged, 1989; Will the Earth Remain Habitable? Academic Publishers, Budapest, 1993; Introduction to the Paleoclimatology, JATEPress, Szeged, 1996).

In the early 90s his research interest was directed to the development of a method by which drought in the following year could be predicted. In order to quantify drought he applied Pálfai's index because its physical dimensions are the temperature and precipitation therefore it is climatologically meaningful. He led the department until 1995. He retired in 1998, but did not cut ties with the university; he held optional lessons, educational lectures and shared his thoughts related to some problems of humanity's future in another book (Foresight, divination and meteorology, Book Masters 2002 Publishing House, 2010).

During the whole of his career he was an active member of the Hungarian Meteorological Society. He was the secretary of the Society from 1957 until 1966. In 1987 he was awarded the Lajos Steiner Memorial Medal, rewarding outstandingly successful academic and social work over a long period in the Society. In 2006 he was elected to the Honorary Members of the Society. For his internationally recognized and long-term climate-related literature activities he was awarded the Kabos Hegyfoky Memorial Medal in 2012.

Between Dr. Pál Ambrózy and Academician Dr. György Major (Hungarian Academy of Science, 2011)

Christmas Party (Department of Climatology and Landscape Ecology, 2013)

In 1974 he became a member of the Climatological Subcommittee of the Hungarian Academy of Sciences for several years. In 2002 he received the Guidó Schenzl Award from the Environmental Secretary in recognition of his meteorological activities.

A Memorial Mass was celebrated in honor of him, in the Cathedral of Szeged, 30th April 2016. We keep his memory in our thoughts, may he rest in peace!

His former colleagues
Department of Climatology and Landscape Ecology, University of Szeged

ACTA CLIMATOLOGICA ET CHOROLOGICA
Universitatis Szegediensis, Tomus 49-50, 2016, 9-20

ASSESSMENT OF TREE OF HEAVEN (*AILANTHUS ALTISSIMA*) SPREAD DYNAMICS ON EXAMPLE OF SZEGED (HUNGARY)

ÁK CSETE, E TANÁCS and Á GULYÁS

Department of Climatology and Landscape Ecology, University of Szeged, P.O.Box 653, 6701 Szeged, Hungary
Email: cseteaki@gmail.com

Summary: The spread of invasive species means a serious ecological problem worldwide. The modified environmental conditions in the cities significantly influence (mostly impair) the urban vegetation. In these circumstances, invasive species with a wide ecological tolerance enjoy a significant advantage. In our study, the possible spreading factors of the Tree of heaven (*Ailanthus altissima*) were examined on the example of Szeged (Hungary). The survey was based on the Local Climate Zone (LCZ) system. Several important characteristics of urban space parameters were processed, such as potential direct irradiation, the land cover and the urban heat island. We found not too strong correlation for example between the land cover type or the heat island intensity in June and the number of trees.

Key words: urban invasive species, Tree of Heaven (*Ailanthus altissima*), spatial analysis, urban built-up investigation

1. INTRODUCTION

The global anthropogenic transformation has significant local implications as well. This includes a particularly dangerous environmental phenomenon, the spread of invasive species worldwide (Walter and Gillet 1998). The diminishing role of geographical distance will further facilitate the expansion of these species.

The complex surface structure of cities, the different heat capacity and run-off properties of the artificial materials used in the built environment have caused the change of climatic conditions in urban areas (Unger et al. 2014). This usually leads to heat excess in the cities. These environmental conditions have significantly influenced the composition of the urban vegetation. The cumulative anthropogenic effects create unnatural habitat conditions for species that can tolerate relatively little. Thus, invasive species with a wide ecological tolerance enjoy a significant advantage (Bartha 2002, Gulyás and Kiss 2007). Heat and drought tolerant tree species, such as the tree of heaven (*Ailanthus altissima*) may have a serious advantage over native species. Temperature trends due to climate change are likely to favour species with an aggressive growth strategy, which the urban impacts of climate change can strengthen even further. The urban problem of invasive species is a very complex topic since the negative effects of urbanization and climate change are summed up.

Ailanthus is one of the most dangerous invasive species in the Central European flora area (Landenberger et al. 2009). It has all the features that enable a plant to withstand the changed circumstances in both natural and anthropogenic environment (Udvardy and Zagyvai 2012). The aggressive growth strategies of the species make it capable of significant propagation, thus it plays a role in not only degrading urban vegetation, but it also contributes

to significantly reducing biodiversity outside the city in near natural vegetation (Lawrence et al 1991, Kowarik and Sämuel 2007, Csiszár et al. 2012). Due to a strong root sprouting ability, it can cause severe damage in the urban environment, i.e. to roads, sidewalks, walls, damaging the building structure as well (Udvardy 2004). Despite the seriousness of this problem, very little research has so far been conducted on the subject. However, the many ecosystem disservices caused by this species require examination. In our research, we examine what methods can be used to address this complex urban environmental issue. In order to prevent the spread of the species it is necessary that we know the factors most influencing propagation.

2. THE STUDY AREA AND METHODS

2.1. Description of study area

Our study area is located in southern Hungary, Szeged. In Trewartha's system the country is classified as category D1 (continental climate with longer warm seasons), and within this the Great Plain is characterized by warm, dry climate. Thus, the climate in the immediate environment of Szeged is also characterized by high summer heat, when drought can also develop, high levels of sunshine duration, low humidity and cloud cover (Péczely 1979). Szeged is the largest city in the Southern Great Plains, both spatially (281 km^2) and in terms of population size (~ 162,000 capita) (KSH 2015). It is a strongly urbanized area, a significant part built-up. The sample areas were chosen in the area of the city called 'Ó-Szeged', northwest of the river Tisza, because this area well reflects the classic city structure and built-up types of Szeged. As the assessment of the whole area of the city was not an option, we settled for a representative, area-proportional sampling method, which represents the variety of urban structures well.

On the basis of literature data we assumed that the urban spread of the thermophilic *Ailanthus* is influenced by the local climate-modifying effect of the urban environment in addition to the background climatic conditions (Kowarik and Säumel 2007, Kowarik 2008). Therefore, in the course of the designation of sample areas we took into account the already developed Local Climate Zone (LCZ) system in Szeged. The LCZ system is a relatively new method aiming to refine the study of urban climate, which takes into account the urban surface reactions and thermal parameters in a complex manner (Unger et al. 2014). The elements of the LCZ are a few hundred meters to several kilometres areas that are characterized with more or less uniform land cover, structure, material types and anthropogenic energy emissions. The method has the advantage that the number of subtypes is relatively low and they are objectively separable from each other. Each LCZ type has a characteristic temperature distribution, which manifests itself most prominently over relatively flat and dry surface, calm and clear nights (Stewart and Oke 2012). Because of the built-up conditions of Szeged, only 6 LCZ types were isolated in the city (LCZs 2, 3, 5, 6, 8, 9), of the internationally agreed LCZ types (Unger et al. 2014) (Fig. 1).

The applied survey method somewhat combines a sampling method used in open areas with those matching urban structures well. Accordingly, the sampling areas are located inside of the third (and outmost) boulevard. Within the LCZ types 200-m radius circle sampling plots were designated based on random sampling (30 plots in all). The number and overall area of the plots in each LCZ reflects the areal proportion of that particular LCZ type. In the

sample plots we examined *Ailanthus* individuals located in public areas, because access was not possible on private property. Field surveys were carried out between June and September in the summer of 2014. All accessible trees were recorded according to a standard wood cadastral if their diameter at breast height (DBH) exceeded 5 cm. The height, trunk height, DBH, crown diameter, and different parameters of the health condition of the trees were recorded. These data were analysed using SPSS 22 statistical software.

Fig. 1 LCZ types of Szeged and sample plots of the investigation

2.2. Potential direct irradiation investigation

The maximum potential amount of light available for photosynthesis was estimated using a potential direct insolation map. We defined potential direct insolation as the amount of direct irradiation, which may come from the sun at the specific geographical location, at a given time of day and season of the year, regardless of the state of the atmosphere. In order to prepare this we used a digital terrain model of Szeged, including the buildings. The aim of the process is to show how much shadows the buildings cast over the surrounding areas, and how they limit the incoming direct radiation. The analysis was carried out for the average growing season of the *Ailanthus* (between April 1 and October 31), with a time step of 7 days and 5 hours within the day. For this analysis, we used the SAGA GIS software. As a result we got the values for each cell of the DTM and calculated the average, minimum and maximum value for each plot. The resulting potential direct insolation values and the appearance of *Ailanthus* within the sample areas were compared in order to look for a connection between the two phenomena. The direct irradiation data relating to individual trees, and averages of the LCZs and the sample areas were calculated using QGIS software.

2.3. The effect of built-up area

In order to prepare a simple surface cover map (concentrating on built-up/green space) we used the Department of Climatology and Landscape Ecology's building database of Szeged, a 0.5 m resolution orthophoto created from 4-band (IRGB) UltraCamD aerial images as well as a surface model generated from that (Gál and Unger 2012).

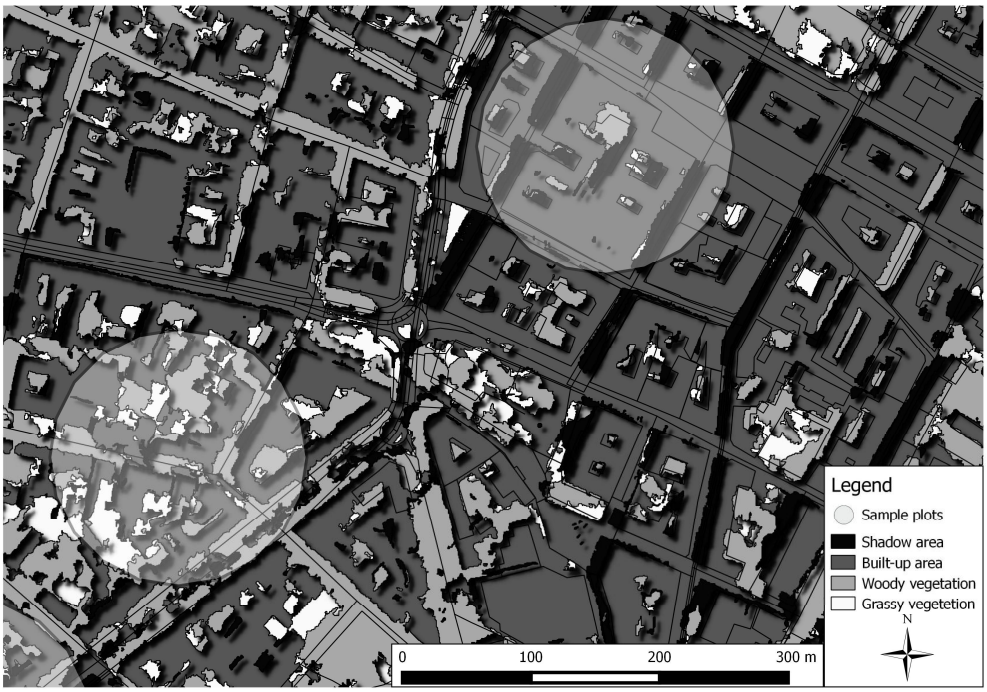

Fig. 2 Surface cover categories according to eCognition classification

The classification was carried out with eCognition 8.7 software, with a simple set of rules using thresholds. Four categories have been identified: grassy vegetation, woody vegetation, built-up area and shadowed areas (Fig. 2). The green areas were determined using the vegetation index NDVI. Due to the light conditions at the time of taking the photos, there were strong shadows of the buildings and trees on their northwest side. In these locations determining the actual land cover was really precarious and difficult, so overshadowed areas are considered lack of data from the point of view of the analysis. The situation is somewhat similar with ground under trees, some of these areas may be suitable for *Ailanthus* colonization, however but the chances to determine such places from above are limited.

2.4. Heat island investigation

The urban heat island (UHI) is one of the most important effects of climate change in urban areas; it is excess heat appearing at certain times. The heat island is best characterized by its intensity, which is very closely related with the landcover and built-up area (Balázs et al. 2009, Lelovics et al. 2013). The temperature differences show inherent high spatial heterogeneity within the city as well. We tried to find a relationship between heat island

intensity and the presence and health conditions of *Ailanthus*. The temperature data for heat island intensity were obtained from the Urban-Path project's climate stations (Unger et al. 2014) (22 monitoring stations with average and maximum heat island intensity data, with a monthly temporary resolution from March to August 2015). We carried out an IDW (Inverse Distance Weighted) interpolation on these point data using QGIS software, in order to prepare simple maps of the monthly average and maximum heat island intensity in Szeged.

3. RESULTS AND DISCUSSION

During the field survey 184 adult specimens of *Ailanthus* were measured. In the downtown areas (LCZs 2, 3) the occurrence of *Ailanthus* is characterized by a uniform distribution and a low number of specimens (Table 1). A possible reason for that is the high proportion of built-up areas, which does not provide favourable living conditions for any plant.

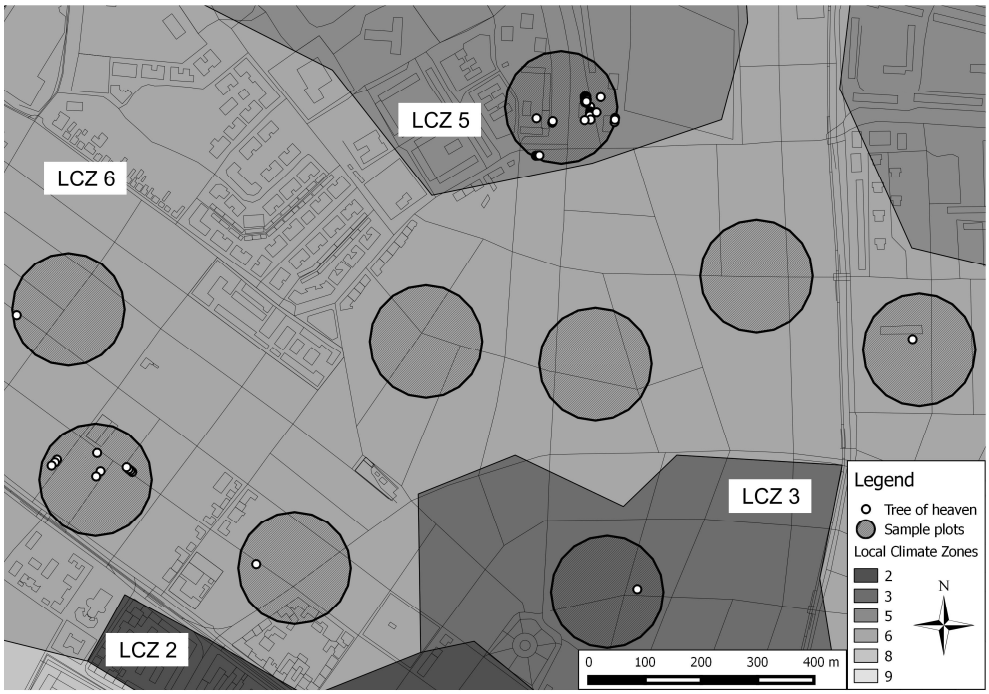

Fig. 3 Distribution of tree of heaven in some sample plots

However, the spatial distribution of the trees could be influenced by the fact that public green surfaces are better kept in the downtown areas, so there is a higher chance that unwanted *Ailanthus* specimens would be removed than in suburban areas. The highest population density (tree per hectare) was observed at LCZ 5 (open construction, medium-height buildings), and it was also in this type that the most individuals (in absolute term) were recorded. Within the LCZ, the distribution is uneven; it is the most dense in the eastern and

northern part of the city. In our experience, most of the trees occur in disturbed housing estate areas.

Table 1 Distribution of *Ailanthus* by LCZ areas and population density per hectare (total area= 10,509.94 ha, 1 sample spot=3.09 ha)

LCZ	Area %	Tree count	Sample plots area (ha)	Tree count/ha
2	5.99	1	6.18	0.16
3	6.34	4	6.18	0.65
5	23.71	128	18.54	6.90
6	56.15	44	52.53	0.84
8	6.10	7	6.18	1.13
9	1.71	0	3.09	0

LCZ 6 and 8 are not characterized by a large number of specimens. In the open and less built-up areas (e.g LCZ 5) more specimens are found, than in the city centre, probably because there is more space for growth (Fig. 3).

During the field survey we noted (and on the survey map it is also outlined) that along the boulevards the amount trees is higher. Therefore, the busy boulevards, meaning a major disturbance seem to increase the number of *Ailanthus* trees.

3.1. Health conditions

According to the standard wood cadastral mapping method, on which our survey was based, the state of the tree can be defined on the basis of the health conditions of the tree trunk and the canopy. During the survey we recorded the trunk injuries (eg. bark injuries, rot, cavity) and the canopy damage (eg. broken branches, decay of the top, crown base injuries, cavity) and tree health conditions were characterized as the sum of these. A deteriorating health status can inform about environmental conditions that do not correspond to the trees' needs.

Despite *Ailanthus* being described in the literature as an urbanophile species, in the city its health conditions were far from perfect. Looking at all the trees, the condition larger or smaller care gaps predominated. Well-tended for specimens were not found, and only approx. 8% of the total population (184) could be classified as one of the two better conditions (tended and care gaps category). The majority (74.73%) fell into the category serious care deficiencies (serious care gap category). Trees in the worst condition (the untended for category) represent 17.03% of the total (Fig. 4).

The health conditions of trees vary according to LCZ as well. Because each LCZ zone has similar land cover structure and urban climate features, the differences in the health conditions of the trees between the different zones may be informative. Tended trees (i.e. individuals developing healthily in most respects) are only found in LCZs 5 and 6. In these zones, the picture is the most heterogeneous, because the number of samples is the largest. In the other LCZs the low number of individuals distorts the evaluation, although it is striking that in LCZ 8 a significant part of the trees is in the untended for category.

The more neglected and deteriorated the studied areas are the worse the health conditions of the trees. In the housing estate areas (LCZ 5) green space is usually less tended than in the city centre, so the trees are not in such good condition either. The detached houses area (LCZ 6) is similar with the difference that here the number of tended trees is slightly greater. The trees of LCZ 8 are in the worst condition, but these are industrial sites, where green surface management is not a priority.

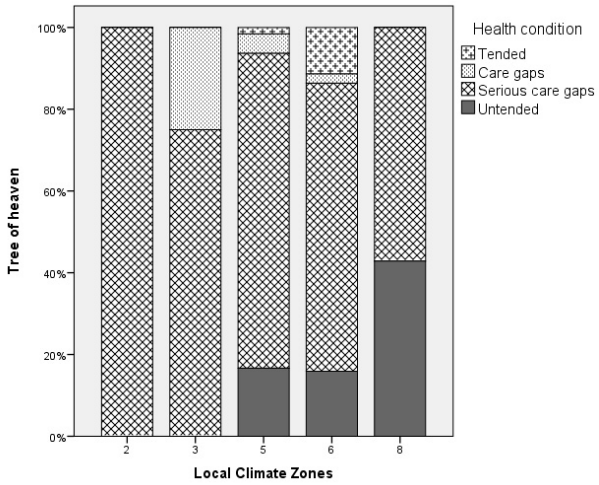

Fig. 4 The health conditions of trees by LCZs

Ailanthus often responds to urban conditions by drying. We observed that the main and smaller branches started drying in the case of several individuals of different sizes, but often even the tree top dieback is apparent. Further typical injuries include trunk rot and longitudinal cracks, which subsequently further aggravate the health conditions of the trees. Root growth is confined by the narrow space so the *Ailanthus* often develops its roots pushing the surrounding pavement, however in turn it does not grow at a healthy pace. Cavities are not typical for *Ailanthus*.

3.2. Potential direct irradiation investigation

We investigated the influence of irradiation on the number of trees at several scales. At the tree-level, the individual tree characteristics (size and health conditions) were compared with the potential direct irradiation for the whole study area. Then the relationship between the number of trees and the plot-level irradiation characteristics was examined for both the whole area and the LCZs separately.

Concerning the dimensional characteristics of the *Ailanthus* in the study area small specimens are the most typical, a DBH of 15–25 cm and a height of 7–8 m are the most common; larger individuals are rarely found in the surveyed area. Based on statistical analysis neither DBH, height, nor the proportion of dead tissue shows appreciable correlation with direct irradiation. There are also no significant differences in the amounts of maximum potential insolation and the tree's site according to tree condition. This was the expected result, since the trees dimensional properties depend mainly on age and the habitat, which can be considered practically homogeneous within the city.

Next, we examined the plot-level relationship between the number of trees within the plot, and potential direct irradiation using Spearman's rank correlation. For the entire area (30 sample plots), the number of trees only showed a significant (negative) correlation with the maximum of the radiation ($r = -0.469$). This can be explained with the fact that the highest potential irradiation values appeared on building tops (due to the simplified building database, in which all roofs are flat) and in larger squares (of which there are few in the city).

Therefore, the highest maximum potential irradiation values occurred where there are large and tall buildings, mainly in the well built-up city centre, where there are few *Ailanthus* trees.

When considering the LCZs separately, there are only two zones (5 and 6), where the number of plots was sufficient in order to calculate correlation. LCZ 5 contains less plots but more trees whereas in LCZ 6 there are more plots with much less individual trees. In LCZ 5, the number of trees showed a strong positive correlation ($r = 0.829$) with the potential direct irradiation averaged for the plot. These results are more easily interpretable and they correspond to our experience in the field as well. In LCZ 5 we find more *Ailanthus* where there is more available amount of light. This LCZ is dominated by housing estates, i.e. high buildings and large, open areas with high amounts of light, where the *Ailanthus* has optimal growth area.

3.3. The effect of built-up area

One important difference between urban and natural habitats is that the former has varying degrees of built-up area, which greatly limits the spread of a species. Such abiotic limiting factors are rare in natural habitats. The land cover map of the area used four categories (grassy vegetation, woody vegetation, built-up, and shadow area). The category grassy vegetation is low green surfaces, typically grasses or small bushes. The woody areas include all mature trees. The built-up category contains all the artificial surface elements: sidewalks, roads, buildings and bridges. The creation of the shadow category was necessary in order to indicate lack of data – the shading effect of the buildings and large trees could not be eliminated. The analysis was carried out in 29 plots within LCZs 2, 3, 5, 6 and 8 (Fig. 5).

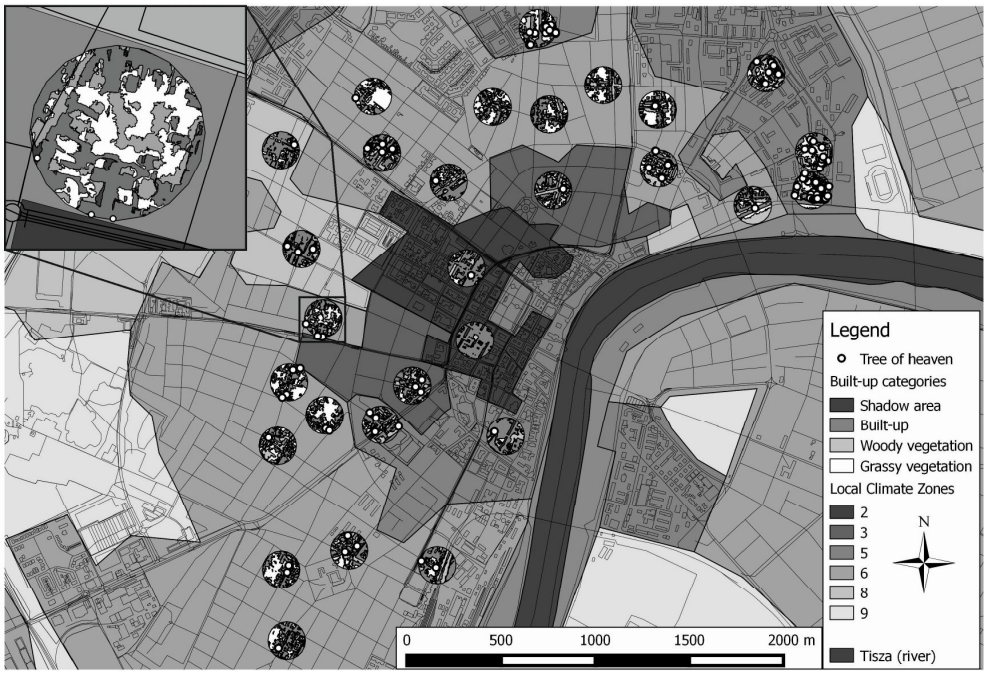

Fig. 5 The surface cover categories in sample plots and the LCZ background

The built-up rates are different within the various LCZs (Fig. 6), LCZs 2 and 8 have the highest proportion of built-up areas. At the same time, in LCZ 2 the ratio of the shadows is very high, due to the presence and shading effect of high buildings. In the other LCZs, the built-up ratio is lower by almost 30%. In LCZs 5 and 6, the built-up areas show similar proportions, however the LCZ 5 has slightly higher proportion of woody vegetation.

In the correlation analysis (including all 29 plots) the relationship between the total area of the categories (per plot) and the number of *Ailanthus* trees in the plot was examined. Weak to moderate correlation was detected between the number of trees and the ratio of woody vegetation-covered areas. This is partly (but not entirely) due to the fact that the *Ailanthus* trees themselves have fallen into the woody vegetation category. In addition, it is also implied that small trees may often spring up at the foot of larger trees. Examining the LCZs individually, it is only in LCZ 5 that a strong positive correlation could be detected between the number of trees and the grass vegetation area. In this LCZ housing estates are frequent with major open grassy areas between the buildings. In order to refine this analysis, further surveys will be needed, including increasing the number of sample plots.

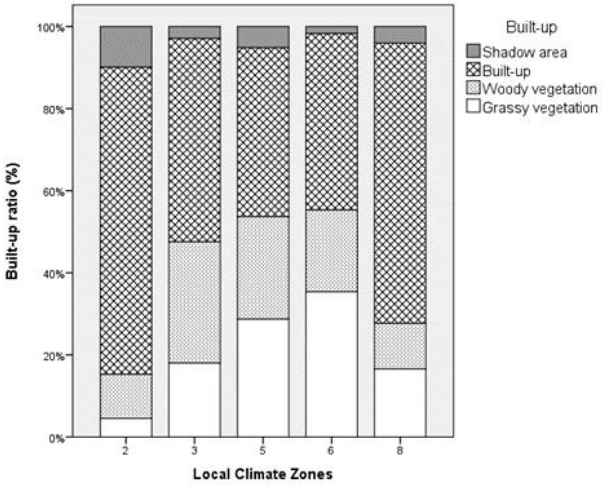

Fig. 6 The built-up categories by LCZs

3.4. Heat island investigation

The temperature differences show a high spatial heterogeneity within the city, and this is why we chose to compare the heat island intensity with the occurrence and health status of *Ailanthus* trees. Heat island intensity varies according to season but the values are generally higher in the downtown areas. In many cases, however, such as the maximum value of the May heat island intensity can be high in the outer zones LCZ 5 as well. The number of *Ailanthus* trees in the plot and the heat island intensity generally showed no significant correlation, except for the June average heat island intensity with which it showed a weak negative relationship.

The sample plots characterized by greater number of *Ailanthus* trees are mostly located in low heat island intensity areas (Fig. 7) (the relationship is significant at the 10% level, the specific value was 5.2%). This result is presumably linked with the ratio of built-up areas, as heat island intensity is usually greater in the more densely built-up areas. In such areas growth possibilities for trees are also limited by the lack of available space.

We carried out further analysis concerning the relationship between heat island intensity and tree health conditions. We plotted the average values of heat island intensity in

the vicinity of the trees according to the health conditions categories (Fig. 8). The results were verified using the Mann-Whitney U test.

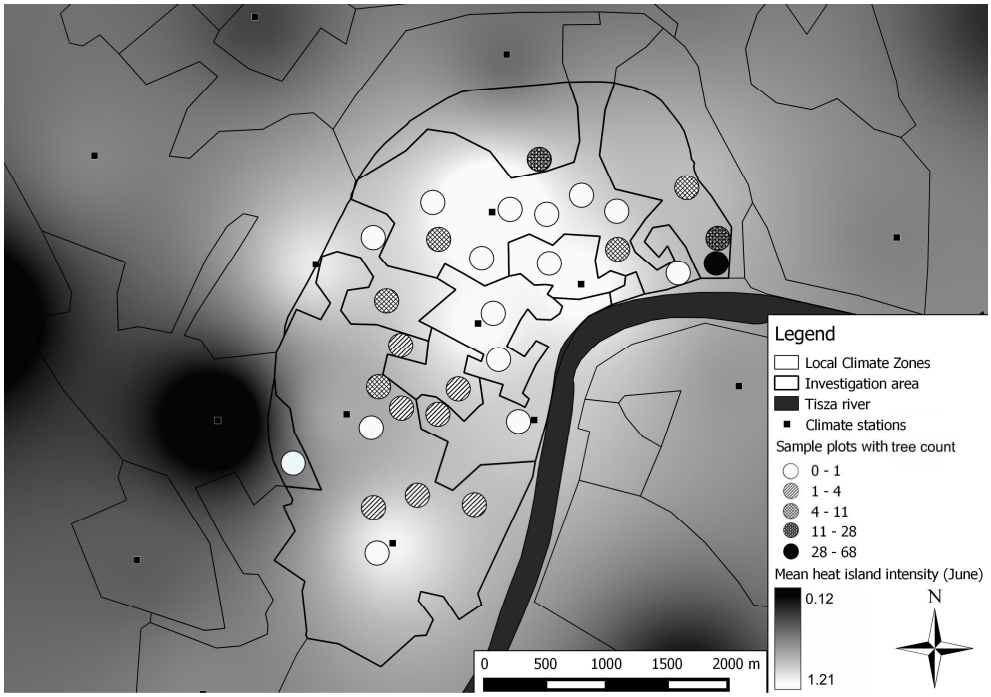

Fig. 7 The average heat island intensity (°C) in June 2014 with the tree numbers in the sample plots

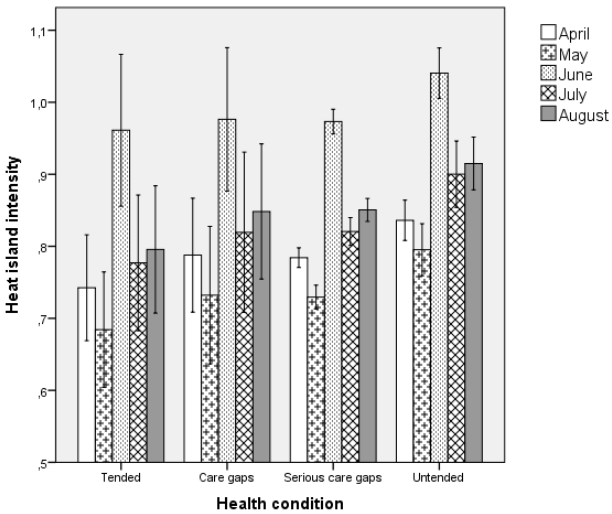

Fig. 8 The heat island intensity (°C) and the health conditions of trees
(Error bars represent the 95% confidence interval)

Based on the results, the trees in worse conditions have higher heat island intensity values associated. The highest means were found where trees were in the worst condition (untended). It is clear that for trees in a bit better condition (serious care gaps category) this value is lower. Although the other two categories seem to follow a similar trend, there are too few trees and consequently too high standard deviation. We can conclude that trees considered to be in worse condition were typically found in areas characterized with higher heat island intensity. This analysis was run both with the monthly average and the monthly maximum heat island intensity values, and the results were the same.

Overall, the strongest relationship with both the number of trees per plot and the health conditions were found with the June heat island intensity data, when the UHI is strongest. The correlation with the number of trees is mostly not significant, but it is significant for the June data at the 10% significance level. The weak relationship probably originated from the fact that (1) heat island intensity can be one of several factors influencing the condition of the trees (2) the heterogenity of the actual UHI intensity is probably greater than that represented by our interpolated map. The trees occur less in areas with higher heat island intensity, as these are also the most densely built-up areas, least suitable for colonization for any type of vegetation. When investigating the relationship between tree condition and heat island intensity it can be seen that trees in worse conditions are usually found in areas with a higher heat island intensity (considering both the monthly average intensity and the maximum). The fact that there is a difference between individual months, however, suggests that there is a real link between the microclimate and the studied species.

4. CONCLUSIONS

The analysis of the urban appearance of invasive species is a complex and little-researched area. In our research, we tested a method often used in natural environments, in order to find out whether it is suitable to examine the spread of the *Ailanthus* in an urban environment. As a city has extremely complex ecological relationships, the results are not always clear. In this phase of the study it can be seen that in the densely built-up areas of the city centre, the chance of *Ailanthus* occurrence is small. This has several, interconnected reasons, from the quantity of available light to the extent of heat island intensity, which probably affect the trees in a complex manner. The trees have a very heterogeneous distribution and it is difficult to clearly explain the large differences in density.

The accuracy of the results could be achieved by further increasing the number of sample plots, as a large and representative volume of data provides more reliable and general results. Additional parameters e.g. precipitation at the plots or the amount of nutrients available could improve the complexity of the research.

REFERENCES

Balázs B, Unger J, Gál T, Sümeghy Z, Geiger J, Szegedi S (2009) Simulation of the mean urban heat island using 2D surface parameters: empirical modeling, verification and extension. Meteorol Appl 16: 275-287

Bartha D (2002) Adventív fa- és cserjefajok Magyarországon. [Adventive tree- and srhub species in Hungary. (in Hungarian)] Erdész Lapok 137:63-65

Csiszár Á, Korda M, Schmidt D, Šporčić D. Teleki B, Tiborcz V, Zagyvai G, Bartha D (2012) Néhány inváziós és potenciálisan inváziós neofiton allelopátiás hatásának vizsgálata. [Examination of some invasive and potentially invasive neophytes allelopathic effect. (in Hungarian)] Bot Közlem 99:159-171

Gál T, Unger J (2012) Surface geometry mapping for SVF calculation in urban areas. In: Proc 8th Int Conf on Urban Climate and 10th Symp on Urban Environ, Dublin, Ireland. Paper 168

Gulyás Á, Kiss T (2007) Városi élőhelyek és élőlények. [Urban habitat and live being. (in Hungarian)] In: Mezősi G (eds) Városökológia. JATE Press, Szeged

Kowarik I, Säumel I (2007) Biological flora of Central Europe: Ailanthus altissima (Mill.) Swingle. Perspect Plant Ecol 8:207-237

Kowarik I (2008) On the role of alien species in urban flora and vegetation. In: Marzluff JM, Shulenberger E, Endlicher W, Alberti M, Bradley G, Ryan C, Simon U, ZumBrunnen C (eds) Urban ecology: an international perspective on the interaction between humans and nature. Springer-Verlag, New York

KSH (2015) Helységnévtár. [Gazetteer (in Hungarian)]

Landenberger RE, Warner TA, McGraw JB (2009) Spatial pattrns of female Ailanthus altissima across an urban-to-rural land use gradient. Urban Ecosyst 12:437-448

Lawrence JG, Colwell A, Sexton OJ (1991) The ecological impact of allelopathy in Ailanthus altissima (Simaroubaceae). Am J Bot 78:948-958

Lelovics, Unger J, Gál T (2013) A lokális klímazónák termikus sajátosságainak elemzése– szegedi esettanulmány. [Evaluation of the thermal features of the Local Climate Zones – a case study in Szeged. (in Hungarian)] Légkör 58:140-144

Péczely Gy (1979) Éghajlattan. [Climatology. (in Hungarian)] Nemzeti tankönyvkiadó, Budapest

Udvardy L (2004) Bálványfa (Ailanthus altissima [Mill.] Swingle). [Tree of Heaven (Ailanthus altissima [Mill.] Swingle). (in Hungarian)] In: Mihály B, Botta-Dukát Z (eds) Biológiai inváziók Magyarországon. Özönnövények. – A KvVM Természetvédelmi Hivatalának Tanulmánykötetei 9, TermészetBÚVÁR Alapítvány Kiadó, Budapest

Udvardy L, Zagyvai G (2012) Mirigyes bálványfa (Ailanthus altissima [Mill.] Swingle). [Tree of heaven (Ailanthus altissima [Mill.] Swingle) (in Hungarian)] In: Csiszár Á (ed.) Inváziós növényfajok Magyarországon. Nyugat-magyarországi Egyetem Kiadó, Sopron

Unger J, Lelovics E, Gál T, Mucsi L (2014) A városi hősziget fogalom finomítása a lokális klímazónák koncepciójának felhasználásával – példák Szegedről. [Refining the concept of urban heat island using Local Climate Zones classification – examples from Szeged (in Hungarian)] Földrajzi Közlemények 138:50-63

Stewart ID, Oke TR (2012) Local Climate Zones for urban temperature studies. B Am Meteorol Soc, 93:1879-1900

Walter K and Gillett H (1998) 1997 IUCN Red list of threatened plants. IUCN

ACTA CLIMATOLOGICA ET CHOROLOGICA
Universitatis Szegediensis, Tomus 49-50, 2016, 21-32

CALCULATION OF SKY VIEW FACTOR AND ROUGHNESS PARAMETERS IN A MEDIUM SIZED CITY

T GÁL and J UNGER

Department of Climatology and Landscape Ecology, University of Szeged, POBox. 653, 6701 Szeged, Hungary
E-mail: tgal@geo.u-szeged.hu

Summary: Studying the altered urban environment is important because of the high number of the involved inhabitants. In urban areas surface cover and geometry differ from the rural surfaces, and the water and energy balances are modified. As a result the thermal environment and the airflow conditions are modified, and these modifications affect the energy consumption and wind energy potential in urban areas. The evaluation of the urban surface geometry and its parameters are not straightforward, and still a rapidly developing field of research. In this paper new software methods for the calculations of urban surface parameters are presented. These software tools enable us to evaluate the building and tree-crown databases from spectral and elevation data, and to use these two datasets to calculate SVF and roughness parameters. These software tools were applied for the study area in Debrecen, Hungary, in order to test the methods and to gather information about the variance of the urban surface in this city. Using the results the heating/cooling energy demand of the households and the wind energy potential can be estimated in urban areas.

Key words: building and tree datasets, mapping tools, surface geometry, urban climate

1. INTRODUCTION

Studying the altered urban environment is important because of the high number of the involved inhabitants. The surface cover and geometry differ from the rural surfaces, and the water and energy balances are modified (Oke 1987). Urban climate research focuses on this modified local climate. This is a priority topic since the prediction of the possible impacts of global climate change for urban areas is impossible without an in-depth knowledge of the features of urban climate. The two most important modifications of the climate in these areas are the altered thermal environment and the different airflow conditions, and both of these climate modifications are primarily connected with the alteration of the geometry and material characteristics of the surface (Oke 1987).

The thermal modification often appears in urban temperatures being higher than in the surrounding rural areas (urban heat island − UHI). The largest UHI, which is the strongest urban-rural temperature contrast, generally appears at night, while during the daytime the difference is moderate or absent. The main reason of the UHI is the urban-rural difference in the nocturnal cooling processes, which are primarily forced by outgoing long wave radiation. In urban areas the 3D geometrical configuration of the surface plays an important role in the restriction of long-wave radiative heat loss, and contributes to intra-urban temperature variations below roof level (Oke 1981). The sky view factor (SVF) is the most appropriate parameter describing the urban geometry (Oke 1981, Svensson 2004). SVF is defined as the

ratio of the radiation received (or emitted) by a planar surface and the radiation emitted (or received) by the entire hemispheric environment (Watson and Johnson 1987). It is a dimensionless measure between zero and one, representing totally obstructed and free spaces, respectively (Oke 1988). This parameter is also essential for the estimation of the solar potential in urban areas because the higher the SVF at a surface point the greater its openness to the sky thus the larger its solar potential too.

Due to the increased drag of the surface the average wind speed is lower in the cities than in the surrounding rural areas (Oke 1987). For describing the geometry or texture of the surface and as a consequence its roughness several parameters are known (Grimmond and Oke 1999). The connection between the wind and the drag force of the obstacles (buildings, vegetation) can be characterized by the zero-plane displacement height (z_d) and the aerodynamical roughness length (z_0) (Counihan 1971). These are the key parameters in studying the urban atmosphere, and at the same time these are the basic parameters for the estimation of intra-urban wind energy potential.

There are several options to calculate SVF values in urban environment (see Unger (2009) and Chen et al. (2012) for brief reviews). One way is the application of computer algorithms that requires a 3D surface database about the examined area. These methods can be separated by the input data used (raster or vector). Most of them utilize high resolution raster digital surface models containing the terrain and the buildings for computing patterns of continuous sky view factor (Lindberg 2007). Their advantage is that the roof of buildings can be managed more easily; however the accuracy of the results is significantly affected by the selection of the resolution of the input data (Gál et al. 2009). There are some examples for vector-based methods as well (Souza et al. 2003, Gál et al. 2009, Matzarakis and Matuschek 2010). These scripts calculate the SVF values more accurately because the buildings are in vector format, thus the locations of the building walls are unequivocal and do not depend on the resolution.

The determination of the roughness length (z_0) and displacement height (z_d) is not straightforward and remains problematic however there are numerous ways for their assessment or calculation. Three generalized classes of these methods are available: (1) micrometeorological methods using field observations of wind and turbulence, (2) roughness classification methods using roughness classes and visual estimation, (3) morphometric (or geometric) methods using measures of surface morphometry. The most common micrometeorological methods use data of field observations from one or a few installed and instrumented tall towers for the computation of z_0 and z_d based on the log-law (Grimmond and Oke 1999). The micrometeorological methods are unsuitable for detailed roughness mapping; however they are suitable for the validation of the other surface roughness calculation procedures. With the classification methods roughness can be estimated based on earlier measurements of the roughness values in a similar terrain elsewhere. The well-known Davenport method distinguishes eight roughness classes and it uses the eye as integrator of photographs or land use maps (Davenport et al. 2000). This method is based on the decisions of the researcher who evaluates the input data, thus it is not suitable for the development of a roughness calculation software. There are several morphometric methods using surface morphology data (Counihan 1971, Bottema 1997, Grimmond and Oke 1999). These methods are based on empirical relations from wind tunnel studies concerning flows over regular building arrangements and there are only a few examples of their generalization.

The roughness parameters are widely used for wind speed reduction in urban sites where in situ measurements are not available. Wind speed at 2 or 10 m above ground level is a key input parameter for microclimate modeling for example in ENVI-met (Lahme and Bruse 2003, Égerházi et al. 2013) or in the RayMan model (Matzarakis et al. 19), and it is also applied for the

calculation or modeling of human thermal comfort parameters (Spangolo and de Dear 2003, Kántor and Unger 2011, Bröde et al. 2012).

The aims of this study are (i) to present a new automatic software method for the calculation of sky view factor and roughness parameters, and (ii) to apply these methods in a medium sized city (Debrecen, Hungary).

2. STUDY AREA AND THE APPLIED DATABASE

The study area is located in Debrecen (47.5°N, 21.5°E). The city lies at a height of 120 m above sea level on nearly flat terrain in the Great Hungarian Plain, which is favorable for UHI development (Fig. 1). It is the second largest city in Hungary with a population of 220 000. Debrecen is the cultural, academic and economic centre of the northeastern region of the country.

The city's region belongs to the Köppen climate type Cfb on the basis of the 1961–90 climate normal, but it has a significant year-by-year fluctuation. The annual amount of precipitation is about 550 mm and its variation shows a maximum in May and June. Generally, the summer is sunny and warm, with an average temperature above 20 °C. The winter is cold; it is around -2 °C and it is often snowy. The wind speed is usually around 3 ms^{-1} and the prevailing wind direction is northeasterly (Bottyán et al. 2005).

The study area was divided to 1 km × 1 km grid and the roughness parameters were calculated for the center points of each grid (Fig. 1). The SVF varies at the local scale therefore it is not reasonable to present its intra-urban variation in the entire city area. So three grid cells representing the most important built-up types of the city were selected (Fig. 1): compact midrise, open midrise and open low-rise.

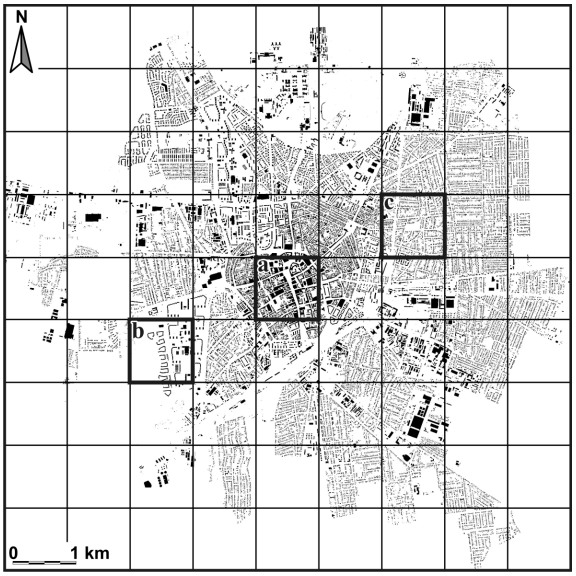

Fig. 1 Study area with the 1 km grid for roughness calculation and the areas (a: compact midrise, b: open midrise, c: open low-rise) for SVF calculation

Detailed building and tree-crown databases were used as inputs for the SVF and roughness calculations in the study area. These databases were calculated with a tree-crown mapping tool (TCM) (Fábián 2012, Gál et al. 2013). This standalone automatic software tool was developed in C++ language and it is compatible with Windows and Linux environments.

The basic parameter for tree crown mapping was the Normalized Vegetation Index (NDVI). NDVI is calculated from the red and near infrared pixel values of the aerial image, it is between -1 and +1 and the values between 0.2 and 1 represent the areas where the amount vegetation (biomass) is high (Lillesand and Kiefer 1987). Elevation information was stored in comma-separated text files and the outputs of the software were in two shapefiles containing the building and tree crown databases (Gál et al. 2013). The NDVI represents the ratio of the vegetation thus it is important for deciding whether a point (a pixel in an aerial photograph) belongs to a building or to a tree. If the NDVI indicates that this point is a part of a tree crown, it is classified as tree crown, even if there is a building roof under it.

In this case the source of the elevation data was a 3D point cloud calculated by photogrammetric method. For the evaluation of the 3D point cloud and calculation of NDVI 4-band digital aerial photographs were used, taken by the Hungarian Institute of Geodesy, Cartography and Remote Sensing in 2007. The resolution of the photographs is approximately 0.5 m and they have 4 spectral bands (3 visible and 1 near infrared). Due to their spectral and spatial resolution these bands are suitable for calculating high resolution spectral indices (e.g. NDVI), also for applying photogrammetric methods for height measurements at the same time. This kind of aerial photographs are commonly used for cartographical issues, and they can be accessed easily in most of the countries (Gál and Unger 2012). The evaluation of the aerial photographs was carried out with the Leica Photogrammetry Suit, and for the height measurements its enhanced Automatic Terrain Extraction (eATE) tool was used.

As an optional input the TCM can use building footprints and tree-crown border lines in ESRI shape files. If these files are available the calculation time can be significantly shorter. In our case a building footprint database was applied as an input, which was calculated from the digital cadastral map of Debrecen.

The localization of the tree-crowns is based on the NDVI values. The shapes of the tree-crowns are calculated by using Thiessen (or Voronoi) polygons (Aurenhammer 1991) around the points in the 3D point cloud. Tree crown points are localized by the software. All points in the 3D point cloud were identified as tree points, if the NDVI value in the same location was higher than 0.35 and grass areas if it is between 0.15 and 0.35. These values are based on a test in selected aerial photographs. During the test we calculated the NDVI values for several typical tree crowns and for typical other vegetation patches (grass, etc). Also, the method selects tree points in a small area, where there are no other (non-tree) points inside the perimeter of this selection, and the difference of the elevation of the points is below a threshold (0.5 m in this case). Finally, a Voronoi polygon was plotted around of this set of tree points. Within all of these polygons two different elevation values are calculated: (i) tree top height (the average of the highest 5% of the measured elevations), (ii)

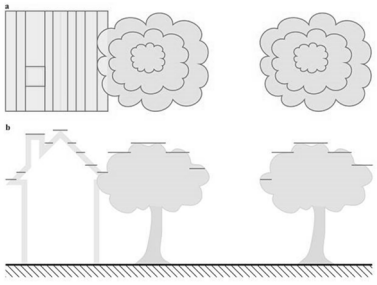

Fig. 2 Concept of the building and tree-crown databases (a: footprint, b: side view)

tree perimeter height (the average of the lowest 5% of the measured elevations). Hereinafter we use only this second elevation value.

The obtained building and tree-crown databases contain polygons (bordered by not only straight but curved lines too) representing the parts of the roofs or trees where the elevation values are approximately the same (Fig. 2). In our case the building database was calculated using the building footprints, thus we have only 2 height values for each building (roof top and eaves heights).

The building and tree-crown databases were evaluated for the whole study area. Fig. 3 illustrates a small part of it in the center of Debrecen.

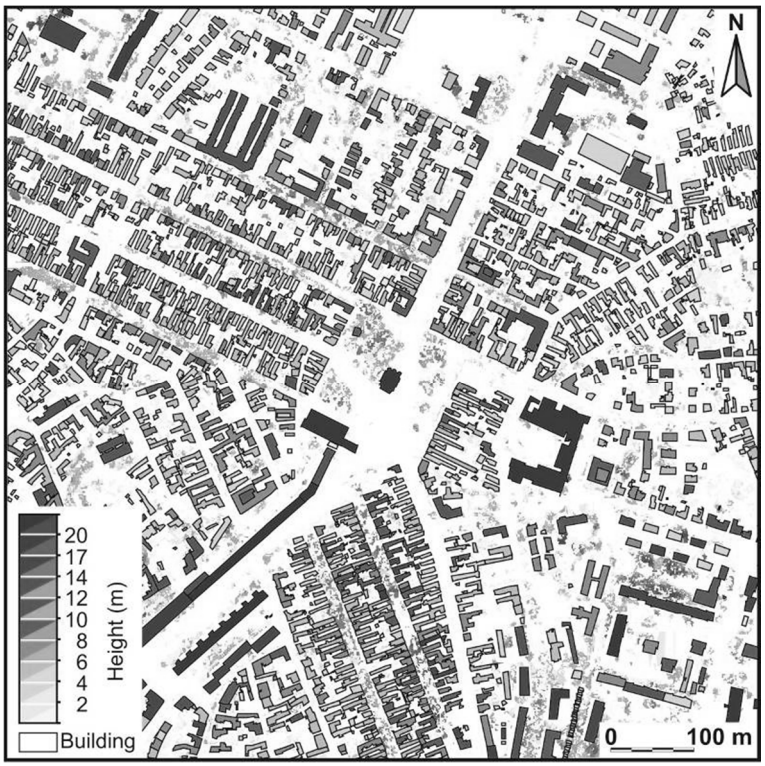

Fig. 3 Building and tree-crown databases in the center of the whole study area

3. NEW CALCULATION METHODS

3.1. SVF mapping tool

The calculation of the SVF is based on a modified form of the equation by Unger (2009) and Gál et al. (2009). It takes into account the effect of different object types on the SVF. These objects are: building (B) with the highest elevation angle (β) in a given direction from a given point, tree (T_1) with the highest elevation angle (β + γ) in the same direction, and tree (T_2) with the highest zenith angle (δ) of the crown overlapping the point where the SVF calculation was made (Fig. 4).

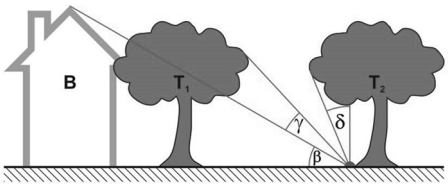

Fig. 4 Elevation angles for the different objects in a given direction

The value of the SVF for a given point is equal to one minus the sum of the view factors (VF) of different objects (B, T_1, T_2) in all directions (ω):

$$SVF = 1 - \left(\int_0^{2\pi} VF_B \, d\omega + \int_0^{2\pi} \tau \cdot VF_{T_1} d\omega + \int_0^{2\pi} \tau \cdot VF_{T_2} d\omega \right) \quad (1)$$

where τ is the transparency of the tree crowns. This transparency is considered to be constant and it describes the average transparency of the different tree species in the study area. In order to estimate the transparency we carried out field measurements and we obtained a τ value of 0.863591 (Gál and Unger 2012, 2014).

The calculations of the three different view factors were based on the equation for the calculations of SVF in a regular circle basin given by Oke (1987). For a regular basin, where β is the elevation angle from the centre to the wall, the SVF value (referring to the basin centre) is: $SVF_{basin} = \cos^2\beta$. So the view factor of a basin with the same elevation angle β is $VF_{basin} = 1 - \cos^2\beta = \sin^2\beta$. Therefore, if we have a regular circular building around the point of interest the view factor of this building is $VF_B = \sin^2\beta$. Similarly, the view factor of the first type trees is calculated using the angle γ with the following equation: $VF_{T1} = \sin^2(\beta + \gamma) - \sin^2\beta$ (Figs. 4 and 5). For the second type trees δ is used for calculation: $VF_{T2} = \sin^2 90° - \sin^2(90° - \delta) = 1 - \sin^2(90° - \delta)$.

In real situations the angular height of the objects is not equal in all directions; therefore the projection of the objects on the hemisphere is not a circle. In this case the three angular heights vary as a function of the direction (ω), so the Eq. 1 is modified:

$$SVF = 1 - \left(\int_0^{2\pi} \sin^2 \beta \, d\omega + \int_0^{2\pi} \tau \cdot \left(\sin^2(\beta + \gamma) - \sin^2 \gamma \right) d\omega + \int_0^{2\pi} \tau \cdot \left(1 - \sin^2(90° - \delta) \right) d\omega \right) \quad (2)$$

To develop a computer algorithm, the utilization of Eq. 2 is not appropriate therefore the SVF value of this equation is estimated by using discrete sections of the hemisphere. The width of these sections is defined by the rotation angle α (Fig. 5) that determines the resolution of the calculation. If the value α decreases, i.e. the hemisphere is divided in small parts, the resolution and precision of the method increases since these describe the real layout of the objects around the point of interest more precisely.

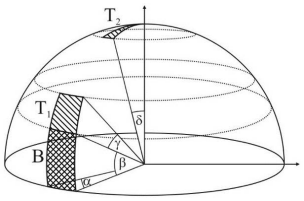

Fig. 5 Polygons on the hemisphere corresponding to a building (B) and to the two types of tree-crowns (T_1 and T_2) (for explanation of angles see the text)

Using the angle α, Eq. 2 can be approximated with Eq. 3, where n is the number of divisions of the circle (n = 360°/α). In all directions only the elevation

angles (β, γ, δ) (Figs. 5 and 6) have to be determined for the calculation using the building and tree-crown databases.

$$SVF = 1 - \left(\sum_{i=1}^{n} \frac{\alpha}{2\pi} \cdot \sin^2 \beta_i + \sum_{i=1}^{n} \tau \cdot \frac{\alpha}{2\pi} \cdot \left(\sin^2 (\beta_i + \gamma_i) - \sin^2 \beta_i \right) + \sum_{i=1}^{n} \tau \cdot \frac{\alpha}{2\pi} \cdot \left(1 - \sin^2 (90° - \delta_i) \right) \right) \quad (3)$$

For the implementation of this calculation we developed a new software method in Java language. It is compatible with both Windows and Linux platforms, and it does not need any GIS software to operate (Gál and Unger 2014). This software reads the geometry and attributes information from the input building and tree crown shape files. For each SVF calculation point it scans the elements of the building and tree-crown databases with a projection line in a given (user defined) distance. The first direction of scanning line is North and then rotated clockwise by (user defined) angle α. The software calculates the highest elevation angles β and γ, and the largest zenith angles δ for all scanning lines; it also calculates the view factors for the different objects (B, T_1, T_2). The software applies a user defined constant transparency value (τ) during calculations. The calculation time is significantly low, the calculation of the SVF for one point takes only approximately 0.6 s in a common PC (Core i3 processor and 4 GB memory).

3.2. Roughness mapping tool

In our earlier research we have developed a new implementation for roughness calculation (Gál and Unger 2009). With this approach the calculation of the roughness parameters is possible not only for regular arrays of buildings and houses but also for irregular building groups as well as real urban sites (Gál and Unger 2009). The basis of the roughness length (z_0) computations is in accordance with the method of Bottema (1997). His basic model equation was originally designed for regular building groups:

$$z_0 = (h - z_d) \exp\left(-\frac{\kappa}{\sqrt{0.5 \cdot C_{Dh} \cdot \lambda_F}} \right) \quad (4)$$

where C_{Dh} is the drag coefficient for isolated obstacles and it is considered constant (0.8) (Bottema 1997), and λ_F is the frontal area ratio of an elementary area. The formula of the zero displacement height (z_d), which is necessary for Eq. 4, is a simple power-law approximation of the regular-group-model: $z_d = h \cdot (\lambda_P)^{0.6}$, where λ_P is the plan area ratio of an elementary area. In the case of irregular arrangements it gives an approximate value for z_d without taking the volume of the buildings and their recirculation zones into account.

The basis of the calculation of the input parameters is the building block; therefore the buildings touching each other were merged into blocks. As a next step we divided the study area into polygon-shape areas based on these blocks, which is a kind of extension of the approach used by Grimmond and Oke (1999). Each polygon consists of the set of points closer to the central building block than to the other blocks.

We defined the total surface area or lot area (A_T) as the area of a polygon. The sum of the areas of building footprints is the plan area for buildings (A_{Pb}). For the tree-crown parts in each polygon we have done the same in order to obtain the plan area for trees (A_{Pt}). The wind flow blocking attributed to the tree-crowns can be described using the porosity (p), which is a simple ratio of the perforated area to the total area of an obstacle (Heisler and DeWalle 1988). This p value for buildings is 0 but for deciduous trees it is characteristically

0.2 in winter and or 0.6 in summer owing to the variation of leaf cover. Using the porosity values the plan area ratio (λ_P) referred to a polygon is:

$$\lambda_P = (A_{Pb} + (1-p) \cdot A_{Pt}) / A_T \quad (5)$$

In order to determine the frontal area ratio (λ_F) we have to compute the frontal area of each building and tree-crown (Fig. 6). The frontal areas of buildings and trees depend on the direction of the airflow. The basis of the calculation is the frontal projection of the buildings and the tree-crowns within a lot polygon. This frontal projection could be calculated using projection lines with a given resolution (Δx). For each lines two height values are obtained: z_t for trees and z_b for buildings (Fig. 6). The frontal area for buildings (A_{Fb}) is the sum of the $\Delta x \cdot zb$ values in each projection lines. The calculation of the frontal area of tree-crowns (A_{Ft}) is similar (sum of $\Delta x \cdot zt$) if the value of z_t is higher than the value of z_b. In the case when the projection of a building is higher, the tree-crown is omitted from the calculation, because it has insignificant effect for the airflow compared to the building. The frontal area ratio referred to a polygon (and to an orientation) is:

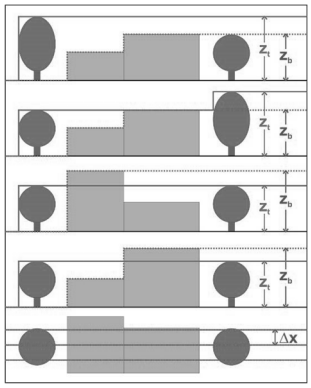

Fig. 6 Concept of the frontal area calculation in a few different cases (for explanation of symbols see the text)

$$\lambda_F = (A_{Fb} + (1-p) \cdot A_{Ft}) / A_T \quad (6)$$

The calculation of the volumetrically averaged building height needs the volumes (V_{b1}, V_{b2}, V_{b3}, …, V_{bn}) and heights (h_{b1}, h_{b2}, h_{b3}, …, h_{bn}) of each building and also of tree-crowns (V_{t1}, V_{t2}, V_{t3}, …, V_{tn} and h_{t1}, h_{t2}, h_{t3}, …, h_{tn}) in each building block:

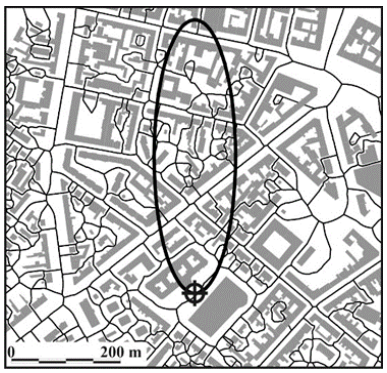

Fig. 7 Illustration of the fetch in an urban area (the cross shows the measurement site)

$$h = \frac{\sum_{i=1}^{n} V_{bi} \cdot h_{bi} + \sum_{j=1}^{n} \left(V_{tj} \cdot (1-p)\right) \cdot h_{tj}}{\sum_{i=1}^{n} V_{bi} + \sum_{j=1}^{n} \left(V_{tj} \cdot (1-p)\right)} \quad (7)$$

The final step is to take into account the effect of the surrounding areas. For this purpose we applied the concept of fetch (Liu et al. 2009). With this concept the effect of the source area (Schmidt 1994) for the airflow can be included into the calculation of the roughness parameters. In their work (Liu et al. 2009) the roughness length was calculated with four different morphometric methods in an elliptical area. The major and minor axis of these fetch were 500 and 150 m, respectively. The major axis was parallel to the wind direction, and the near endpoint of the windward placed fetch was at the measurement site (Fig. 7).

In our new method we use the similar approach. The roughness calculation refers to a point grid with an arbitrary resolution. For each point the roughness parameters are calculated with the following formulas:

$$z_0 = \frac{\sum_{i=1}^{n} z_{0i} \cdot A_i}{\sum_{i=1}^{n} A_i} \ , \ z_d = \frac{\sum_{i=1}^{n} z_{di} \cdot A_i}{\sum_{i=1}^{n} A_i} \tag{6}$$

where A_i is the overlapping area, z_{0i} is the roughness length, z_{di} is the displacement height of each lot polygon from the group of the polygons overlapping with the fetch (Fig. 7).

4. RESULTS

4.1. Intra-urban SVF patterns

The main characteristics of the spatial patterns of the calculated SVF values in the three different urban areas are significantly different. In the compact midrise area (Fig. 8a) the dominant range of SVF is 0.1–0.5, and only a few wide streets and urban squares have higher values. The dominance of the low SVF indicates that the long wave emission of the surface is mostly blocked in the urban canopy layer, thus at nighttime the cooling rate is moderate compared to the rural area.

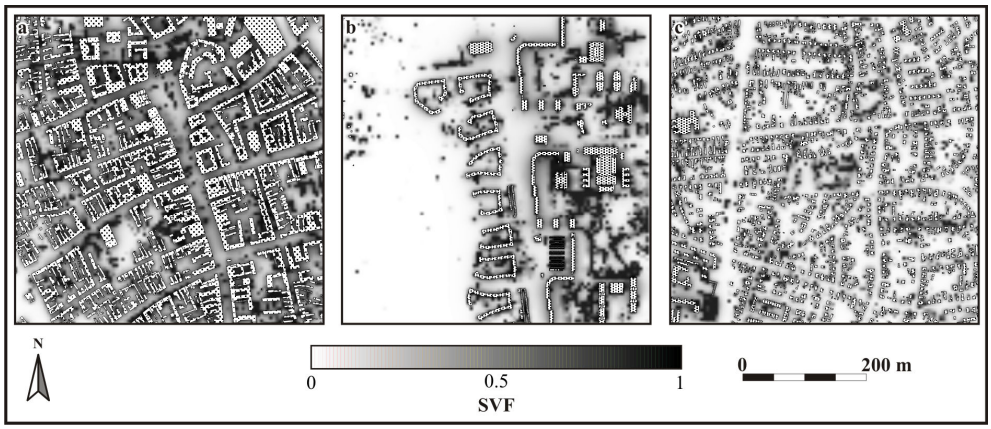

Fig. 8 Spatial patterns of the SVF in the three different urban areas
(a: compact midrise, b: open midrise, c: open low-rise)

In the open midrise area (Fig. 8b) the buildings are not smaller than in the compact midrise area, but the dominant range of the SVF decreased significantly. The values around 0.1–0.5 appear only in the close proximity of the buildings or in the urban parks with significant tree cover. In most of the streets the typical values are around 0.5–0.7. This difference indicates that the radiation balance and thermal reactions of this area are not so different from the rural ones like in the case of the compact midrise area.

In the open low-rise area (Fig. 8c) the typical SVF values are around 0.4–0.7, only some parts – with significant tree crown cover – have 0.1–0.3 values. The streets have 0.5–0.8 values and most of the backyards have the same or higher SVF because in these areas mostly low vegetation is present. These SVF values indicate that this kind of urban area has the least modified thermal properties and radiation balance within the presented types.

With the help of the obtained results of SVF calculation the thermal characteristics of the different built-up types can be identified. The compact midrise areas (city core) possibly have lower cooling rates at nighttime, thus the energy consumption of the households decreases in winter and increases in summer. This difference is less characteristic in the open midrise areas (housing estates) and the open low-rise (houses with gardens) areas. These results may help to calculate the energy consumption of these building types, which is essential for planning the necessary production by the renewable energy sources.

4.2. Roughness parameters in the study area

In the urbanized area of Debrecen the two most important roughness parameters show an almost concentric shape (Fig. 9). The zero displacement height (Fig. 9a) increases at the edge of the urban area and in the mostly open low-rise areas of the city it is around 2–5 m. At the edge of the inner city there is a rapid increase and in the city core its value reaches 12 m.

Roughness length increases rapidly in the edge of the city (Fig. 9b), the highest z_0 values appear in the center and in the open midrise areas (thanks to the 10-story buildings). In the center it reaches 2.5 m and in most of the city core it is larger than 1.5 m.

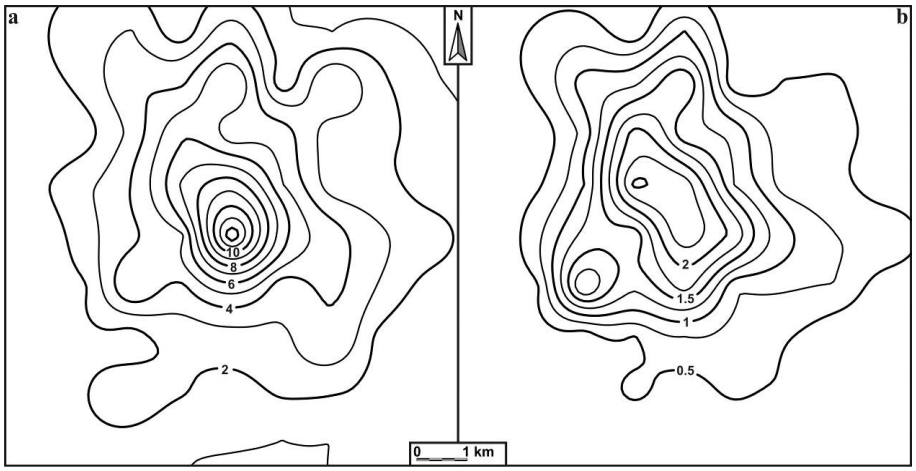

Fig. 9 Spatial distribution of displacement height (a) and roughness length (b) in m

Using these spatial patterns of the roughness parameters the most suitable areas for the development of the household-scale small wind turbines are mostly the open low-rise areas in the suburbs owing to the small enough z_0 and z_d values here. The tops of the high buildings in the open midrise areas may be also considered in this respect because of the relatively small roughness parameters. However, the city core is not appropriate for this purpose, namely the roughness parameters indicate high drag and decreased wind speed near the top of the buildings.

4. CONCLUSIONS

We presented new software methods for the calculation of urban surface parameters. These software tools enable us to evaluate the building and tree-crown database from spectral and elevation data, and using these two datasets to calculate SVF and roughness parameters. In this study we applied these software tools for a study area in Debrecen, Hungary, in order to test the methods and to gather information about the variance of the urban surface in this city. Using the results of this study the heating/cooling energy demand of the households and the wind energy potential can be estimated in urban areas.

Acknowledgements: The study was supported by the TÁMOP-4.2.2.A-11/1/KONV-2012-0041 project co-financed by the European Union and the European Social Fund, as well as by the Hungarian Scientific Research Fund (OTKA PD-100352) and by the János Bolyai Research Scholarship of the Hungarian Academy of Sciences.

REFERENCES

Aurenhammer F (1991) Voronoi diagrams – A survey of fundamental geometric data structure. ACM Comput Surv 23:345-405

Bottema M (1997) Urban roughness modelling in relation to pollutant dispersion. Atmos Environ 31:3059-3075

Bottyán Z, Kircsi A, Szegedi S, Unger J (2005) The relationship between built-up areas and the spatial development of the mean maximum urban heat island in Debrecen, Hungary. Int J Climatol 25:405-418

Bröde P, Fiala D, Błażejczyk K, Holmér I, Jendritzky G, Kampmann B, Tinz B, Havenith G (2012) Deriving the operational procedure for the Universal Thermal Climate Index (UTCI). Int J Biometeorol 56:481-494

Chen L, Ng E, An X, Ren C, Lee M, Wang U, He Z (2012) Sky view factor analysis of street canyons and its implications for daytime intra-urban air temperature differentials in high-rise, high-density urban areas of Hong Kong: a GIS-based simulation approach. Int J Climatol 32:121-136

Counihan J (1971) Wind tunnel determination of the roughness length as a function of fetch and density of three-dimensional roughness elements. Atmos Environ 5:637-642

Davenport AG, Grimmond CSB, Oke TR, Wieringa J (2000) Estimating the roughness of cities and sheltered country. In: Proc 12th Conf Appl Climatol, Boston, USA. 96-99

Égerházi LA, Kovács A, Unger J (2013) Application of microclimate modelling and onsite survey in planning practice related to an urban micro-environment. Adv Meteorol 251586

Fábian PÁ (2012) Derivation of tree-crown database using spectral and height information in an urban area (in Hungarian). MSc Thesis, University of Szeged, Szeged, Hungary

Gál T, Unger J (2009) Detection of ventilation paths using high-resolution roughness parameter mapping in a large urban area. Build Environ 44:198-206

Gál T, Unger J (2012) Surface geometry mapping for SVF calculation in urban areas. In: Proc 8th Int Conf on Urban Climate and 10th Symp on Urban Environ, Dublin, Ireland. Paper 168

Gál T, Unger J (2014) A new software tool for SVF calculations using building and tree-crown databases. Urban Clim 10:594-606

Gál T, Lindberg F, Unger J (2009) Computing continuous sky view factor using 3D urban raster and vector databases: comparison and an application for urban climate. Theor Appl Climatol 95:111-123

Gál T, Unger J, Kiss M (2013) An automatic method to create an urban vegetation database using 4 band aerial photographs for Sky View Factor calculation – A case study in Szeged, Hungary. In: Proc. Two hundred years of urban meteorology in the heart of Florence: Int Conf on Urban Climate and History of Meteorol, Florence, Italy. 124-132

Grimmond CSB, Oke TR (1999) Aerodynamic properties of urban areas derived from analysis of surface form. J Appl Meteorol 34:1262-1292

Heisler GM, DeWalle DR (1988) Effect of wind break structure on wind flow. Agr Ecosyst Environ 22-23:41-69

Kántor N, Unger J (2011) The most problematic variable in the course of human-biometeorological comfort assessment – the mean radiant temperature. Cent Eur J Geosci 3:90-100

Lahme E, Bruse M (2003) Microclimatic effects of a small urban park in densely built-up areas: Measurements and model simulations. In: Proc. 5th Int Conf on Urban Climate, Lodz, Poland. P.5.1

Lillesand TM, Kiefer RW (1987) Remote sensing and image interpretation. J. Wiley and Sons, Hoboken

Lindberg F (2007) Modelling the urban climate using a local governmental geo-database. Meteorol Appl 14:263-273

Liu G, Sun J, Jiang W (2009) Observational verification of urban surface roughness parameters derived from morphological models. Meteorol Appl 16:205-213

Matzarakis A, Matuschek O (2010) Sky View Factor as a parameter in applied climatology – Rapid estimation by the SkyHelios Model. Meteorol Z 20:39-45

Matzarakis A, Rutz F, Mayer H (2007) Modelling radiation fluxes in simple and complex environments - application of the RayMan model. Int J Biometeorol 51:323-334

Oke TR (1981) Canyon geometry and the nocturnal urban heat island: comparison of scale model and field observations. J Climatol 1:237-254

Oke TR (1987) Boundary layer climates. Routledge, London-New York

Oke TR (1988) Street design and urban canopy layer climate. Energ Buildings 11:103-113

Schmid HP (1994) Source areas for scalars and scalar fluxes, Bound-Lay Meteorol 67:293-318

Souza LCL, Rodrigues DS, Mendes JFG (2003) The 3DSkyView extension: an urban geometry acces tool in a geographical information system. In: Proc 5th Int Conf on Urban Climate, Lodz, Poland. O.31.3

Spagnolo JC, de Dear RJ (2003) A human thermal climatology of subtropical Sydney. Int J Climatol 23:1383-1395

Stewart ID, Oke TR (2012) Local Climate Zones for urban temperature studies. B Am Meteorol Soc 93:1879-1900

Svensson M (2004) Sky view factor analysis – implications for urban air temperature differences. Meteorol Appl 11:201-211

Unger J (2009) Connection between urban heat island and sky view factor approximated by a software tool on a 3D urban database. Int J Environ Pollut 36:59-80

Watson ID, Johnson GT (1987) Graphical estimation of sky view-factors in urban environments. J Climatol 7:193-197

ACTA CLIMATOLOGICA ET CHOROLOGICA
Universitatis Szegediensis, Tomus 49-50, 2016, 33-39

FIRST RESULTS OF ALLOMETRIC AND GROWTH INVESTIGATIONS IN HUNGARIAN URBAN TREE STANDS IN AN ECOSYSTEM SERVICE CONTEXT

Z GYŐRI, J PIKÓ, Á GULYÁS, Z PÁDÁR and M KISS

Department of Climatology and Landscape Ecology, University of Szeged, P.O.Box 653, 6701 Szeged, Hungary
E-mail: gyorizsa@gmail.com

Summary: The methodology of evaluating urban ecosystem services gains much importance in the context of global climate change and international policy processes. Urban trees provide important climate-related regulating services, which can be evaluated using specifically developed models. Some of these approaches need location-specific data about the growth characteristics of frequently planted tree species in urban circumstances, for exact ecosystem service quantification and indicator development. One main task is to accurately calculate biomass growth, in order to quantify service provision more precisely in life-cycle assessments. Besides, mathematical relations between different size parameters of trees might be needed for the background calculations of some model applications. In this paper, we present some methodological investigations and preliminary results for these purposes. Growth curves of carbon storage potential and potential leaf area were developed for two important urban tree species (Common hackberry**,** Japanese pagoda tree). The results highlight the need to take worse tree condition at high ages into account in further improvements and real applications. In the second part of the study, we present the first results of allometric models to predict crown diameter from diameter at breast height of the trees, based on the tree cadastre dataset of the city of Szeged.

Key words: urban trees, ecosystem services, leaf area, carbon storage, allometric relations

1. INTRODUCTION

The evaluation of ecosystem services is gaining a major role in environmental sciences and practical environment management (MEA 2005, TEEB 2010). Their purpose is to enable the quantification of resources used by humans directly or indirectly from the perspective of securing human welfare (Termorshuizen and Opdam 2009, Kovács et al. 2011, Gómez-Baggethun et al. 2013). Ecosystem services are divided into four different groups. They are: maintenance (supportive), provisional, regulatory and cultural services. The most important task of the new methodology, which evaluates the natural resources from the perspective of contributing to human welfare, is the technical support of the environmental protection goals and biodiversity protection. In recent years more and more research is being conducted on the green space ecosystem services of urban areas (Haase et al. 2012, Hubacek and Kronenberg 2013). Their benefits, originating from their regulating services are of paramount importance, like climate regulation by the shading and evapotranspiration of trees, decreasing stormwater runoff, air pollution removal and carbon sequestration (Kirnbauer et al. 2013, Nowak et al. 2013, Jim and Chen 2014). In the case of urban green areas we are talking about ecosystems suffering from strong anthropogenic impact which affect the life

quality for many people in densely populated areas, so that they can also be an important subject of monetary or non-monetary evaluations.

The appearance of the methodology is more and more frequent at a policy level too, proved by the fact that the first thematic TEEB report dealt with urban environment management (TEEB 2011). Besides, the Green Infrastructure Development Goal which is part of the EU Biodiversity Strategy 2020, specifically mentions the urban green areas, highlighting their contribution to the health and a number of other factors of the well-being of the population. The evaluation of ecosystem services is performed by developing and mapping indicators or integrating them into more complex models.

The quantitative assessment of the regulating ecosystem services of urban trees can be realized on a model basis. Several specific models have been created in different parts of the world primarily for the evaluation of climate-related services (i-Tree 2014, Peng et al. 2008). Most of these assessment tools, like the Eco package of the most elaborated i-Tree software, are only suitable for static evaluation. Nevertheless in many cases, the analyses of the services provided by the tree would be required to consider the life-cycle i.e. monitoring these services in parallel with the growth of trees. For example for the installation of urban trees or green areas it would be needed to know in how much time will they be able to provide the same service volume as their predecessor tree stands. Certain model applications have been made specifically for that purpose, for example the i-Tree Design application that is easy to use (on a web interface) by non-professional users. This application is suitable for the calculations of the provided services by a tree of a selected species (also in economic terms) installed at a predetermined location in an arbitrary period of time. However this application is designed for the USA. The growth of trees and deposition of pollutants are significantly affected by climatic conditions, therefore applications developed for local conditions would be needed to use more descriptive functions of ecosystem services under the local conditions.

Furthermore, in certain applications the specification of additional tree parameters may be required. It has to be noted that some of those measurements are more difficult to carry out (e.g. the measurement of the crown diameter which is necessary to calculate the shading capability of trees, thereby to estimate the energy savings of heating and cooling). Another possible use is the estimation of trunk parameters from crown parameters derived from photogrammetric investigations. The relations between these tree size parameters are given by so-called allometric equations. Nowak (1996) has developed regression equations to calculate the leaf area and leaf biomass of urban trees. These equations form the base e.g. for the widely used i-Tree model suite (i-Tree 2014 – formerly UFORE – Urban Forest Effects Model). The aim of the works of Peper et al. (2001a, 2001b) was to develop prediction models for diameter at breast height (DBH) based on age, and that the tree height, crown diameter, crown height, and leaf area are based on DBH. Logarithmic regression models were used for all variables except for leaf area predictions, for which a nonlinear exponential model was used.

In line with these general goals, the aim of our study is to pave the way for the development of model applications that take into account the above mentioned aspects and local conditions, therefore especially suit the data needs regarding common tree species in Hungary. On the one hand the change of the ecosystem services provided by the trees are examined during their lifecycle. On the other hand, some allometric models predicting a crown size parameter from the DBH are tested.

2. METHODS

In the first part of the study, we present the life cycle curves of two important ecosystem service indicators, the amount of stored carbon in tree biomass (indicating carbon sequestration), and the leaf area (which is a widely used indicator of air pollutant removal and stormwater runoff reduction). In the calculation process of the i-Tree Eco model, the so-called standardized growth is used. It is quantified based on an average constant growth rate (in DBH), and is corrected based on climatic parameters. Crown light exposure and tree condition are used as correction factors. In our calculation, we used the growth observations used in Hungarian horticultural and green space management practice (Radó 1999). These growth curves are based on measurements of trunk diameter in relation with the tree's age, using a dataset of thousands of tree individuals in Hungary.

For calculations of carbon storage and leaf area, our methodology is mainly based on the workflow of commonly used methods (e.g. in i-Tree Eco). From multiplying the DBH and the shading factor by the regression coefficients we obtained the natural logarithm of the leaf area from which the leaf area was calculated by a simple exponent function (Nowak 1996). Equations based on the DBH are of the following form:

$$\ln Y = b_0 + b_1 X + b_2 S \quad (1)$$

where Y is the leaf area (m^2), X is the DBH (cm), b_0-b_2 are the regression coefficients and S (percentage of light intensity intercepted by foliated tree crowns) is the average shading factor for the individual species (McPherson 1984). We made the calculations for two commonly planted street and park tree species, Common hackberry (*Celtis occidentalis*) and Japanese pagoda tree (*Sophora japonica*). The shading factors are 0.88 for hackberry and 0.78 for pagoda tree. The calculation of the stored amount of carbon was based on species-specific equations, using the DBH as a single parameter (CUFR 2008, Liu and Li 2012).

Table 1 The species investigated with allometric investigations

Common name	Scientific name	Number of trees
Goldenrain tree	*Koelreuteria paniculata*	23
Silver lime	*Tilia tomentosa*	148
Japanese pagoda tree	*Sophora japonica*	41
Small-leaved lime	*Tilia cordata*	42
Early maple	*Acer platanoides*	32
Ash	*Fraxinus excelsior*	27
Big-leaf linden	*Tilia platyphyllos*	24
Common hackberry	*Celtis occidentalis*	63
Maple Leaf plane	*Platanus hybrida*	32
Total		432

In the second part of our research, allometric models were tested to predict one of the most important size parameter of tree crowns, the crown diameter, from the more easily measurable parameter of DBH. The statistical calculations were based on a field-based tree database for the downtown area of Szeged (Hungary). The selection of specimens was carried from the tree cadastral database created and maintained by the Department of Climatology and Landscape Ecology of the University of Szeged, in cooperation with the local

environmental management company (Takács et al. 2015). For allometric investigations, trees in a good condition should be chosen. The selection criteria were the following: the place of the tree is a typical urban location (mainly street trees); missing crown ratio does not exceed 10%. The whole tree cadastre database contains several parameters (tree size parameters, health-related attributes, location information). For the purposes of this study, the DBH and average crown diameter data were used. Crown diameter was measured with Vertex III equipment. From the total tree cadastre database, 432 specimens fulfilled the criteria, the surveyed species are summarized in Table 1.

Curve fitting algorithms were executed to test the fit of different regression models for the trees of different species. The calculations were carried out in SPSS 19.0 software, the used functions are summarized in Table 2.

Table 2 The tested allometric models to predict crown diameter (CD, m) from diameter at breast height (DBH, cm), b_0-b_3 are regression coefficients

The type of function	Equation
Linear	$CD = b_0 + b_1 \cdot DBH$
Logarithmic	$CD = b_0 + b_1 \cdot \ln DBH$
Inverse	$CD = b_0 + b_1 / DBH$
Parabolic	$CD = b_0 + b_1 \cdot DBH + b_2 \cdot DBH^2$
Cubic	$CD = b_0 + b_1 \cdot DBH + b_2 \cdot DBH^2 + b_3 \cdot DBH^3$
Power	$CD = b_0 \cdot DBH^{b1}$
Exponential	$CD = b_0 \cdot b_1^{DBH}$
Sigmoidal	$CD = e^{b0 + b1 / DBH}$
Growth	$CD = e^{b0 + b1 \cdot DBH}$

The values of the adjusted coefficients of determination (R^2_{adj}) were calculated, together with standard error of estimate (SEE) values.

3. RESULTS AND DISCUSSION

The potential leaf area and carbon storage of the two tree species in relation with age can be seen on Fig. 1, the results will be discussed focusing on the state achieved at high ages (around 55 years). The higher growth was observed in the case of pagoda tree, which may potentially exceed 1200 m^2 in leaf area and 1400 kg of stored carbon at high ages. The leaf area values for common hackberry are around 1000 m^2 and below 1000 kg. In our field-based dataset, containing individual-based estimates calculated with the growth equations of the i-Tree Eco model (Kiss et al. 2015), we can see that there are only some trees in the complete inventory for the city centre with the above-mentioned values. The main reason for this might be that street trees at high ages have high values of missing crown parts and crown dieback (beacuse of bad health status in urban circumstances, and because of pruning and other management activities – the mentioned reference database is the total tree cadastre inventory, which contains trees in bad condition as well). This decreases mainly the leaf area, and the amount of biomass (and consequently the stored carbon) to a high extent. Therefore, there are very few tree specimens with these quite high values in our city. It is the case in particular for the pagoda tree, its population is in a considerably bad condition in the investigated stands

according to the i-Tree categorization (Kiss et al. 2015). The management of old-growth urban trees is a very important topic in urban green space management. These trees are in a worse condition which results in higher management costs. But meanwhile they provide a very high amount of ecosystem services, as it might be indicated by the growth curves presented in our study for climate-related regulating services.

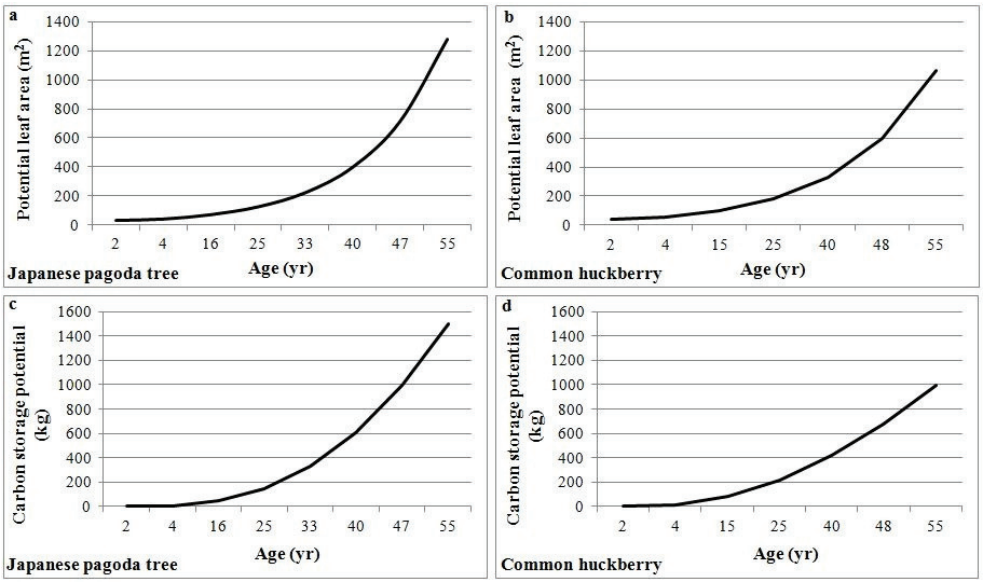

Fig. 1 Potential leaf area (a, b) and carbon storage potential (c, d) depending on the age at the two investigated species

Table 3 Best fitting models and their parameter estimates relating crown diameter and DBH for the investigated species

Species	Model	Fitting		The function parameters	
		R^2_{adj}	SEE	b0	b1
Big-leaf linden	power	0.862	0.208	44.838	0.841
Silver linden	power	0.866	0.203	28.566	0.940
Golden rain tree	power	0.529	0.327	42.488	0.819
London plane	power	0.620	0.200	57.031	0.733
Common hackberry	power	0.628	0.253	130.707	0.543
Ash	power	0.661	0.309	75.472	0.642
Japanese pagoda tree	exponential	0.666	0.271	431.611	0.018
Early maple	sigmoidal	0.801	0.275	7.106	-11.693
Small-leaved linden	power	0.788	0.315	50.199	0.788

Table 3 shows the best predictive models for the crown diameter of trees of the investigated species (with the highest R^2 values, together with low SEE). Four species have a model with a relatively good fit ($R^2_{adj}>0.70$, $p<0.01$) to the measured dataset. For most species, the power function seems to be the best model to predict the investigated parameter,

and it might be considered as a possible general model type. Linden species have better fitting models, which can be explained by their relatively healthy crowns. In contrast, pagoda trees have a sparse canopy structure with high variation in crown diameter, which makes curve fitting harder. Worse fits might be caused in general by heterogeneity in the tree locations (which affects the forms of the crowns and other growth characteristics of the trees). Besides that, although trees had been chosen with crowns in a good condition, the shapes of the crowns are affected by light exposure and may be affected by pruning and other management activities, which might cause greater variation in the investigated size parameter. Further investigations from other cities in this climate zone would increase the reliability of the models for practical applications.

4. CONCLUSION

We carried out some background studies on some aspects of the growth and allometric relationships of urban trees in the context of ecosystem services. The main aims were to correct the models for calculating two important climate-related ecosystem service indicators (leaf area and stored carbon) based on Hungarian growth functions. Based on our results and their comparison with the field-based estimates of the referring values, we consider that our approach is usable for planning targeted simulation modeling tools. Further research is needed for suitable methods to take the loss of biomass at high ages into account, if the ecosystem service providing capacity of old trees is in the focus of investigations. Another goal was to test curve fitting algorithms to form a base for allometric equations describing relations between two size parameters of trees. The models should be refined based on more extended datasets. We consider that management-oriented tree cadastres are suitable for determining allometric models for predicting certain size parameters or biomass indicators from more easily measurable parameters.

REFERENCES

CUFR (2008) CUFR Tree Carbon Calculator – Documentation. US Forest Service, Washington DC

Gómez-Baggethun E, Barton DN (2013) Classifying and valuing ecosystem services for urban planning. Ecol Econ 86:235-245

Haase D, Schwarz N, Strohbach M, Kroll F, Seppelt R (2012) Synergies, trade-offs, and losses of ecosystem services in urban regions: an integrated multiscale framework applied to the Leipzig-Halle region, Germany. Ecol Soc 17:22

Hubacek K, Kronenberg J (2013) Synthesizing different perspectives on the value of urban ecosystem services. Landscape Urban Plan 109:1-6

I-Tree (2014) i-Tree Eco User Manual v5.0

Jim CY, Chen WY (2014) Assessing the ecosystem service of air pollutant removal by urban trees in Guangzhou (China). J Environ Manage 88:665-676

Kirnbauer MC, Baetzb BW, Kenneyc WA (2013) Estimating the stormwater attenuation benefits derived from planting four monoculture species of deciduous trees on vacant and underutilized urban land parcels. Urban For Urban Gree 12:401-407

Kiss M, Takács Á, Pogácsás R, Gulyás Á (2015) The role of ecosystem services in climate and air quality in urban areas: Evaluating carbon sequestration and air pollution removal by street and park trees in Szeged (Hungary). Morav Geogr Rep 3:36-46

Kovács E, Pataki Gy, Kelemen E, Kalóczkai Á (2011) Az ökoszisztéma-szolgáltatások fogalma a társadalomkutató szemszögéből. [Concept of ecosystem services from the perspective of the sociologist. (in Hungarian)] Magyar Tudomány 7:780-787

Liu C, Li X (2012) Carbon storage and sequestration by urban forests in Shenyang, China. Urb For Urb Green 11:121-128
McPherson, EG (1984) Planting design for solar control. Energy-conserving site designe. American Society of Landscape Architects, Washington, DC, 141-164
MEA (2005) Millennium Ecosystem Assessment: Ecosystems and Human Well-being –Synthesis. Island Press, Washington, DC
Nowak D (1996) Estimating leaf area and leaf biomass of open-grown deciduous urban trees. Forest Sci 42:504-507
Nowak DJ, Greenfield EJ, Hoehn RE, Lapoint E (2013) Carbon storage and sequestration by trees in urban and community areas of the United States. Environ Pollut 178:229-236
Peng L, Chen S, Liu Y, Wang J (2008) Application of CITYgreen model in benefit assessment of Nanjing urban green space in carbon fixation and runoff reduction. Fron Forest China, 3:177-182
Peper P, McPherson E, Mori S (2001a) Equations for predicting diameter, height, crown width, and leaf area of San Joaquin Valley street trees. J Arboric 27:306-317
Peper P, McPherson E, Mori S (2001b) Predictive equations for dimensions and leaf area of coastal southern california street trees. J Arboric 27:169
Radó D (1999) Bel- és külterületi fasorok EU-módszer szerinti értékelése. [Urban and suburban alleys evaluated by the EU-method. (in Hungarian)] Lélegzet 7-8:1-12
Takács Á, Kiss M, Tanács E, Varga L, Gulyás Á (2015) Investigation of tree stands of public spaces in Szeged. J Env Geogr 8:33-39
TEEB (2010a) The Economics of Ecosystems and Biodiversity: Mainstreaming the Economics of Nature. A synthesis of the approach, conclusions and recommendations of TEEB. Earthscan, London-Washington
TEEB (2010b) The Economics of Ecosystems and Biodiversity: Mainstreaming the Economics of Nature. Ecological and Economic Foundations. Earthscan, London-Washington
TEEB (2011) TEEB Manual for Cities: Ecosystem Services in Urban Management. Earthscan, London-Washington
Termorshuizen JW, Opdam P (2009) Landscape services as a bridge between landscape ecology and sustainable development. Landscape Ecol 24:1037-1052

ACTA CLIMATOLOGICA ET CHOROLOGICA
Universitatis Szegediensis, Tomus 49-50, 2016, 41-48

MODELING ENVIRONMENTAL PROCESSES WITH BAYESIAN NETWORKS, BASED ON THE EXAMPLE OF EUTROPHICATION OF KARSTIC LAKES

M KISS[1], A SAMU[2], E TANÁCS[1] and I BÁRÁNY-KEVEI[1]

[1]*Department of Climatology and Landscape Ecology, University of Szeged, P.O.Box 653, 6701 Szeged, Hungary*
[2]*TETT Association, Holló str. 2., 6723 Szeged, Hungary*
E-mail: kiss.marton@geo.u-szeged.hu

Summary: Bayesian networks are more and more frequently used tools in environmental sciences. The advantage of the methodology is the possibility of handling conditional probabilities, thus they are able integrate expert knowledge and information from different knowledge domains. There are several examples for the use of the approach from the fields of water management, climate and land use change modeling. The evaluation of ecosystem services is an interdisciplinary research field, for which Bayesian networks have much potential. In our case study, we present a model examining the eutrophication process of karstic lakes, focusing on the share of toxic ammonia. It is important from the point of view of the health status of fish populations, which is an important indicator of ecosystem state and service providing capacity. The sensitivity analysis revealed that pH and water temperature have the most important role in the investigated process. The model is suitable for evaluating management alternatives and other types of decision support.

Key words: environmental modeling, Bayesian networks, eutrophication, fish populations, ammonia

1. INTRODUCTION

1.1. Bayesian networks

Bayesian networks are useful tools of environmental science and decision support applications. The use of artificial intelligence related graphic mathematical models spread at first for medical diagnostics (e.g. Kahn et al. 1997), but now they are also used in many other domains as well, like solving telecommunicational (Devitt et al. 2006) and financial problems (Gemela 2001). Bayesian networks describe relations between variables by conditional probabilities. In the graphic interpretation of the Bayesian networks, variables are marked by nodes, while causal relations are marked by edges. The relations among variables are defined in the related conditional probability tables (Fig. 1). (The whole probability table contains the combination of each relevant variable's every possible value.)

Conditional probability tables must contain discrete values, so continuous variables have to be partitioned in intervals. The networks may contain so-called utility variables as well. By assigning utility scores to different possible values of end variables in complex models, the setting of parent variable values can be optimized using the known probabilities. Using costs as benefit variables makes it possible to examine the cost efficiency of investments or environmental interventions as well. Besides direct value input, conditional probability values can be calculated by summarizing a sufficient amount of measured data as

well. This is how medical diagnostics applications generally operate, just as the case study hereby presented. Besides conditional probability, there is a possibility to include equation-defined deterministic relations as well.

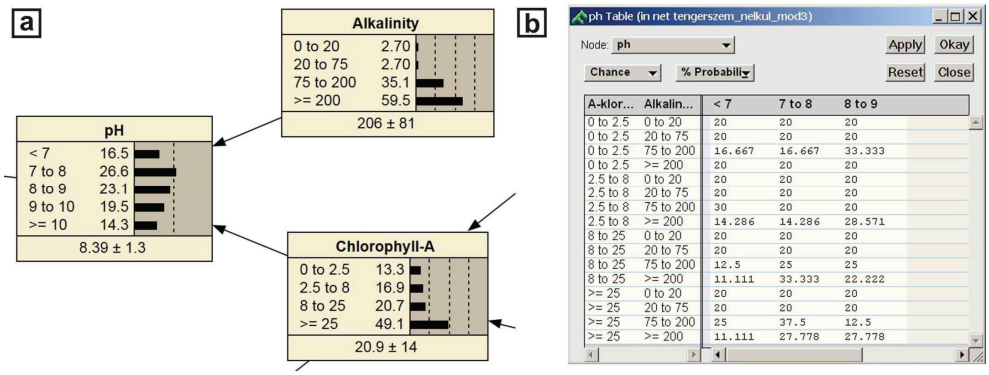

Fig. 1 A variable and its parent variables in the graphic model (a), with the relevant conditional probability table (b)

1.2. Bayesian networks in environmental and ecosystem service modeling

There are several fields of landscape and environmental research, for which Bayesian networks may serve as a useful tool, in case of theoretical problems and practical applications as well. The possibility to include information from different domains was presented in the study of Carmona et al. (2011). It provides a decision support model in water management, which is one the most frequent domains where Bayesian networks are applied. Beyond the quantitative and qualitative aspects of surface and groundwater bodies, economic and social issues are also worth taking into account in this domain. Moreover, processes, and, this way, the results of different strategies of treatment are subject to significant uncertainty, which again justifies the usage of Bayesian networks. The possibility of including expert decisions may be useful in land use change modeling, since decision-making influence land use change but they are hard to incorporate in the models. Bayesian networks may offer a solution for this issue as well (e.g. Aalders 2008). The conditional probability values are mostly based on known quantitative interrelations, calculations or submodels, but may be provided by expert decisions as well. In the study mentioned, natural aspects influencing land use change are completed by the age distribution of inhabitants and farmers, and the presence of heirs to continue managing the farms. Besides modeling the environmental and landscape processes themselves, Bayesian networks may be suitable for creating decision support systems, through drawing up relevant abstract problems, and particularly through relations of and/or character. These are well-illustrated by the study of Newton (2010), providing a decision network facilitating the Red List classification of species.

Bayesian networks are useful tools in modeling ecosystem services as well (Landuyt et al. 2013). The focus of this approach is on the contribution of environmental attributes to human well-being. It is an interdisciplinary field, where several advantages of Bayesian networks may be utilized. The possibility to include information from different knowledge domains make it possible to evaluate cultural services (Shaw et al. 2016). As the delivery of services is mainly a complex process, all the elements and flows may not be exactly

discovered and quantified. The integration of expert knowledge could have a significant added value, as it is the case with several supporting and regulating services (Grêt-Regamey et al. 2013). And the decision support systems may also be developed in an ecosystem service context, with the help of Bayesian networks (Villa et al. 2014). The aim of our paper is the presentation of a decision support oriented application of the Bayesian networks, on the example of a well-known environmental issue, the eutrophication of freshwater systems. The study was carried out in an environmentally sensitive landscape type.

1.3. Eutrophication of surface waters

Eutrophication and the related issues began emerging more vigorously in the middle of the previous century. The nutrient load, increased as a result of human activity, caused deterioration in water quality, which at the beginning manifested itself only in the loss of some functions, and finally it led to the total disappearance of their function in the ecosystem. The initial changes had worried only the experts, but later, when algal blooms, water discoloration, various odours and sometimes fish die-offs (Somlyódy and van Straten 1986), threatening public use occurred, a demand to stop and reverse the process emerged. After the exploration of the drivers different measures were carried out with more or less success in order to prevent the pollution, or in many places, to rehabilitate the water bodies. To find the best management alternatives, it is important to know the effects of different natural and anthropogenic factors in the eutrophication process. It highlights the need for targeted model development.

The lakes and their fish stock have a crucial role in providing many ecosystem services. The filling up process of the karstic lakes causes reduction in the diversity of landscapes and in the value of the scenery. Fish have a significant role in the lakes' ecosystem processes and thus provide important supporting services. The proliferation or decline of fish species on the different levels of the food chain influences the flow of elements and the population of other species, and through terrestrial fish consumers they can also affect the processes of other habitats as well (Holmlund and Hammer 1999).

In the present study we present a Bayesian network examining the eutrophication processes of karstic lakes in Hungary. One aim is to aid decision-making through seeking the influence of the different factors on one important attribute in the eutrophication process, the share of toxic ammonia. Besides that, we would like to give an example for the usage of Bayesian networks with the approach of estimating condition probabilities based on measurement datasets. It might be a usable approach in modeling supporting and other types of ecosystem services too.

2. METHODS AND STUDY AREA

Our research is carried out in the Gömör-Torna karst region. Our goal is the examination of the still waters in the area, and the quantification of the environmental conditions affecting them. These examinations are especially reasonable in karstic areas, as water is an important forming factor of the karstic system, it infiltrates fast, and thus it affects groundwater quality, underground wildlife and formations, especially caves (e.g. speleothem degradation). Contamination from human land use accumulates in the water gathered in different karstic depressions, becoming obvious firstly through the change in water quality,

while later it gets transported underground. The fact that in the last few decades several still water bodies got in the state of being filled up or even disappeared in the area, also justifies the investigation. Shallow, small-scale ponds are in increased risk of eutrophication, as in their case the decrease in water quality can be followed by complete termination. In dry, karstic plateaus it means an even greater loss, firstly in terms of human use, but also in terms of decreasing biodiversity, as these ponds serve as the habitat and breeding place of several (often protected) species. The subjects of our investigation were Lake Papverme, Lake Vörös, Lake Kender and Lake Aggteleki. A three-year measurement series was carried out, from which we used data from the year 2009, from April to October.

In our study we examined the changes in the amount of ammonia, which affects the health of fish stock. Ammonia is excreted by plants and animals, and it occurs in the water due to the decomposition of living organisms, industrial emissions, and fertilizer washing-in (Randall and Tsui 2002). Ammonia is a free, non-ionic form, which can permeate through most of the biological membranes, and it affects living organisms as a neurotoxin (Szilágyi 2007). It is formed from ammonium with a higher rate in case of higher pH and higher water temperature. Algae blooms, occurring in waters overloaded with nutrients, cause assimilational alkalisation, leading to alkaline pH. Areas with limestone bedrock are especially vulnerable in this respect, as they may further increase this effect. Therefore, especially in the summer, concentrations toxic to the fish can occur.

The sampling points in the lakes were chosen in 4 or 2 directions according to the points of the compass, near the shores, because in the case of lakes, coastal water quality is decisive. In addition, samples were taken from where inflows reach the lakes. According to this, in the case of Lake Papverme 8, in the case of Lake Tengerszem 4 sampling points were marked, and 2–2 in the case of the other lakes. In the field tests we used a WTW pH/Cond 340i instrument for measuring pH and conductivity. Water temperature was measured with a Hach Lange thermoluminescent dissolved oxygen meter. The measurement of ortophosphate, nitrate and ammonium were carried out in a lab, by a Fia Star 5000 meter. The determination of alkalinity was based on the MSZ EN ISO 9963-1:1998 standard. Chlorophyll-a content was measured by the North Hungarian Environmental Protection and Water Management Inspectorate.

3. RESULTS AND DISCUSSION

3.1. Structure of the model

The probability network (Fig. 2) generated on the basis of our data illustrates one of the possible consequences of euthrophic conditions in the lakes formed and already stabilized as a result of nutrient stress, and its contribution to achieving this consequence. This means the share of toxic ammonia, converted from the potentially present ammonium, which depends on the level of alkalinity and the rise of water temperature. Ammonia, and especially its permanent presence, may be harmful to the health condition of fish, even in small quantities. In those lakes, where fish farming is going on this presents a serious problem, while in other lakes it indicates that the ecosystem is not capable of supporting higher forms of life, so species diversity decreases. The direct contribution of nutrient load to the higher rate of ammonia mainly means a higher ammonium-input, but also works indirectly: the algae proliferating due to the abundance of nutrients shift the pH towards an alkaline environment

with their photosynthetic activity, and they also increase turbidity, which increases another important factor of ammonia-formation, the water temperature. The particles suspended in the water (soil, algae) absorb and scatter the sunlight, so the surface temperature of these waters increases (especially at noon) (Paaijmans et. al. 2008). Therefore, the model is built from parameters influencing the ammonia rate directly, and of other parameters affecting them indirectly. These are the anthropogenic impact, expressed by the nutrient supply; the weather conditions, which can enhance anthropogenic effects (SPI drought index); and the air temperature, that directly affects the temperature of water. As an external influence, we can mention alkalinity, which affects the quantity of ammonia through the pH. As alkalinity increases pH, in waters where the level of alkalinity is high, the ammonia is more toxic (Wurts and Durborow 1992). The value of the SPI drought index affects the quantity of the 3 types of nutrients by providing information on the appearance and length of wet and dry periods. Especially during wetter periods the rate of diffuse pollution may increase. The calculation of the index is based on the amount of precipitation of a chosen base period (McKee et al. 1993). Precipitation data are from the meteorological stations of Jósvafő and Silica, the index was calculated for the period 1958-2009. In the model, the values are valid for one-month periods; the categories used are moderately, very, or extremely wet and dry periods.

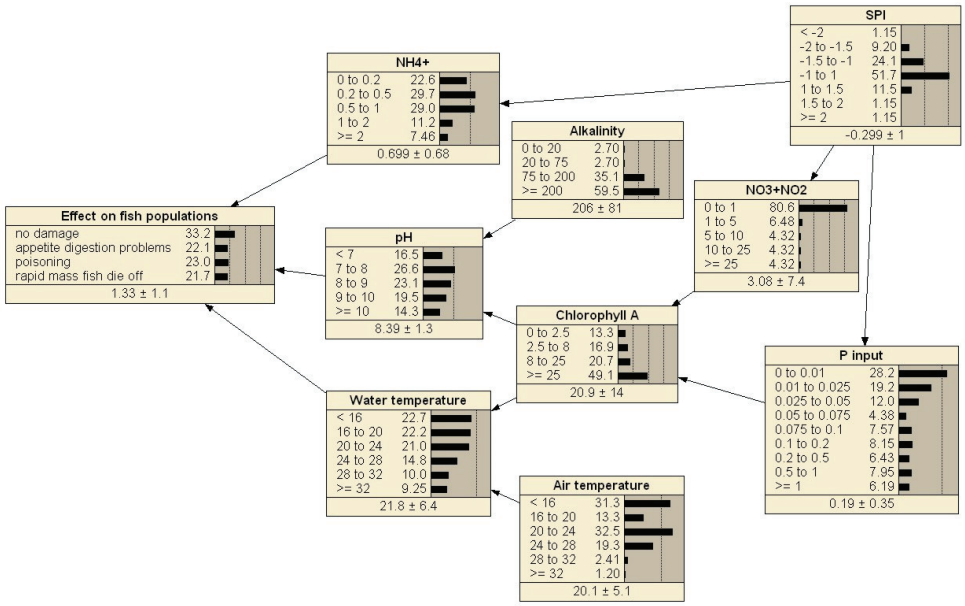

Fig. 2 Euthropication model of the lakes in Gömör-Torna karst

The next step in the model is the chlorophyll-a quantity, which is influenced by the nitrate and phosphorus content. The threshold limit values of ammonium and nitrate are given based on the no. MSZ 12749:1993 standard, in five water quality categories (from excellent to highly polluted). The limit values connected to ortophosphate are given based on the trophic state (Szilágyi and Orbán 2007). The chlorophyll-a levels were classified on the basis of OECD's (1982) trophity-grades. The limit values of alkalinity were determined based on

Wurts and Durborow (1992), according to the ideal level present in a lake ecosystem. The limit values of air and water temperature were designated arbitrarily; the lower limit is the temperature which may be relevant in terms of ammonia formation and durability of persistence. This was also the basis of the pH value categorization. The possible categories of ammonia levels were determined according to the health effects on fish, four classes were made: when there is no damage; when some irritations occur (loss of appetite, or degradation of digestion); when poisoning occurs; and the rapid development of mass fish die-off (Szakolczay 1997). For the latter there was no example amongst our measurements, but our researches led us to the conclusion that in the examined lakes at certain times (especially on summer days), there's a risk of that extreme condition occurring.

3.2. Sensitivity analysis

With the help of the sensitivity test of the program it is possible to determine in the multi-factor system of the constructed Bayesian network, how much each factor influences the final outcome, or the development of any (other) chosen variable. By this method we can test if the constructed structure is adequate or not (this has an especially high importance in the case of Bayesian networks which are based on experts' knowledge). As a result of the sensitivity analysis that was executed on the variable 'effect on fish populations' we found that in accordance with the preliminary assumptions the fish were the most sensitive to the pH and the water temperature. The next most important parameter was the ammonium rate. The chlorophyll-a amount precedes both air temperature and alkalinity. It means that this parameter plays a more important role through its effect on pH and water temperature than the air temperature or the alkalinity. Following air temperature, the drought index is the first parameter that does not have a direct impact on the two most important parameters, but its extensive impact justifies its place in the list. The health state of the fish is the least sensitive to the alkalinity, and to the nitrate and phosphate rate. Considering the initial independent variables in this respect the climate parameters – especially air temperature – are determining, in contrast with the bedrock and the atmospheric CO_2-content, which influence the alkalinity.

When measured data are used, in addition to the determination of the model structures' 'goodness' the result of the sensitivity test can also help to decide which the most important and minimally necessary parameters are to be measured if we want to find out what causes the presence of ammonia in a certain place, how persistent it will be, and where we have to intervene in the system to eliminate the unfavourable state.

We checked the accuracy of the generated model with the help of a test file from the measurement data. During the verification process we eliminated a variable from the system, and the program estimated the result for each test case on the basis of the probabilities set up for the original cases. The estimation was compared with the real value, and an error rate was calculated from it. The error rate compares the number of estimation errors to the total number of test cases. The accuracy of classification can be defined by a confusion matrix, which shows the distribution of misclassifications between the categories. Based on the 15 test cases the error rate was estimated 20%, probably caused by the low number of test data, and the disproportionate distribution of cases between the categories. Based on similar results, Marcot et al. (2001) determined that the actual occurrence of rare events is underestimated, because the forecasts of the model are based on the most probable events. It is also true in case of the data we used, because in our measurements, the state when there is no harm to the fish is dominant. The model estimated this state correctly in every case, but in opposite, instead of the state of 'decline in appetite and digestion' 2 times out of 2, and

instead of the case of 'poisoning' once out of 3 'no damage' state was given as a result. For estimating the correctness of the model the software calculates even more indicators, one of them is the so-called 'spherical payoff' (Morgan and Henrion 1990, briefly introduced in. Marcot et al. 2001), its value varies between 0 and 1 (1 means the best possible model performance). In the case of our model the spherical payoff was 0.77 which, considering the low number of available data, is a relatively high value.

3. CONCLUSION

Based on our results, we consider Bayesian networks to be a useful tool in studies of water management and other environmental issues. Evaluations of ecosystem services need methods that can integrate interdisciplinary information. Bayesian networks may fulfil this need, and provide the possibility for developing decision support systems. The condition probability tables can be created based on known relationships, e.g. using measurement datasets. In this study, we gave an example for that, with an eutrophication model of karstic lakes in the Gömör-Torna Karst Region. We focused on a parameter having an effect on the health status of fish populations, which is an important element in the delivery of different ecosystem services. This approach may be used in modeling different types of ecosystem services. The model we built may need to be improved in several different aspects. Firstly, for specifying the different causal relations more precisely the model might need some changes, e.g. the use of some correlations which are not based on our own measurement data. Because of the possibility of including probability-based relations and experts' decisions in the model, Bayesian networks might be capable of handling also economical and sociological data, and might be able to examine the future tendencies as well. In the case of these karstic lakes it may mean applying the method of restoration costs for decision support: with the help of Bayesian networks different alternatives of treatment (for example dredging, protection from erosion, regional drainage) can be compared.

Acknowledgements: This research was supported by the Hungarian Scientific Research Fund in the frames of the project OTKA/048356.

REFERENCES

Aalders I (2008) Modeling land-use decision behavior with Bayesian belief networks. Ecol Soc 13: article 16

Carmona G, Varela-Ortega C, Bromley J (2011) The Use of Participatory Object-Oriented Bayesian networks and Agro-Economic Models for Groundwater Management in Spain. Water Resour Manage 25:1509-1524

Devitt A, Danev B, Matusikova K (2006) Constructing Bayesian networks Automatically using Ontologies. In: Second Workshop on Formal Ontologies Meets Industry (FOMI 2006), Trento, Italy

Gemela J (2001) Financial analysis using Bayesian networks. Appl Stochastic Models Bus Ind 17:57-67

Grêt-Regamey A, Brunner SH, Altwegg J, Christen M, Bebi P (2013) Integrating expert knowledge into mapping ecosystem services trade-offs for sustainable forest management. Ecol Soc 18: article 34

Holmlund CM, Hammer M (1999) Ecosystem services generated by fish populations. Ecol Econ 29:253-268

Kahn CE, Roberts LM, Shaffer KA, Haddawy P (1997) Construction of a Bayesian network for mammographic diagnosis of breast cancer. Comput Biol Med 27:19-29

Landuyt D, Broekx S, D'hondt R, Engelen G, Aertsens J, Goethals PLM (2013) A review of Bayesian belief networks in ecosystem service modelling. Environ Modell Softw 46:1-11

Marcot GB, Steventon JD, Sutherland GD, McCann RK (2006) Guidelines for developing and updating Bayesian belief networks applied to ecological modelling and conservation. Can J Forest Res 36:3063-3074

Morgan MG, Henrion M (1990) Uncertainty: a guide to dealing with uncertainty in quantitative risk and policy analysis. Cambridge Press, New York

Newton AC (2010) Use of a Bayesian network for Red Listing under uncertainty. Environ Modell Softw 25:15-23

OECD (Organization for Economic Cooperation and Development) (1982) Eutrophication of Waters. Monitoring assessment and control. Final Report. OECD Cooperative Programme on Monitoring of Inland Waters (Eutrophication Control). Environment Directorale, OECD, Paris

Paaijmans KP, Takken W, Githeko AK, Jacobs AFG (2008) The effect of water turbidity on the near-surface water temperature of larval habitats of the malaria mosquito Anopheles gambiae. Int J Biometeorol 8:747-753

Randall DJ, Tsui TKN (2002) Ammonia toxicity in fish. Mar Pollut Bull 45:17-23

Shaw E, Kumar V, Lange E, Lerner DN (2016) Exploring the utility of Bayesian networks for modelling cultural ecosystem services: A canoeing case study. Sci Total Environ 540:71-78

Somlyódy L, van Straten G (eds) (1986) Modelling and managing shallow lake eutrophication. With application to Lake Balaton. Springer-Verlag, Berlin

Szakolczay J (1997) Halegészségügyi alapismeretek. [The basics of fish health. (in Hungarian)] In: Tathy B (ed) Halgazdálkodás II. [Fish farming] MOHOSZ [Hungarian National Association of Anglers], Budapest. 457-487

Szilágyi F, Orbán V (eds) (2007) Alkalmazott hidrobiológia. [Applied hydrobiology. (in Hungarian)] Magyar Víziközmű Szövetség [Hungarian Water Utility Association], Budapest

Villa F, Bagstad KJ, Voigt B, Johnson GW, Portela R, Honzák M, Batker D (2014) A Methodology for Adaptable and Robust Ecosystem Services Assessment. Plos One 9:e91001

Wurts WA, Durborow RM (1992) Interactions of pH, carbon dioxide, alkalinity and hardness in fish ponds. Southern Regional Aquaculture Center Publication 464:1-4

ACTA CLIMATOLOGICA ET CHOROLOGICA
Universitatis Szegediensis, Tomus 49-50, 2016, 49-61

ANALYSIS OF LAND SURFACE TEMPERATURE AND NDVI DISTRIBUTION FOR BUDAPEST USING LANDSAT 7 ETM+ DATA

G MOLNÁR

Department of Climatology and Landscape Ecology, University of Szeged, P.O. Box 653, 6701 Szeged, Hungary
E-mail: molnarge@geo.u-szeged.hu

Summary: Urban areas considerably vary in land coverage, emission of pollutants and anthropogenic heat release from the natural surroundings. As a result, an alteration of meteorological variables (e.g. temperature, wind, moisture) is detected in the cities, which can fundamentally be observed with three methods: in-situ measurements, numerical mesoscale meteorological models and remote sensing products. In this work, a satellite imagery (single-channel algorithm) technique was utilized to investigate the spatial distribution of land surface temperature (LST) and normalized vegetation index (NDVI) for the capital city of Hungary. The high-resolution thermal infrared band (60 m) of Landsat 7 ETM+ (Enhanced Thematic Mapper Plus) provides a powerful tool to categorize different land cover zones and to determine the thermal properties of land surface. Two dates (2 and 18 August 2014) and 11 Local Climate Zones (LCZs) were selected to take into consideration the progress of vegetation and the dissimilarity of land coverage in LST modification. The results suggest that the presence of vegetation leads to a significant LST reduction. For instance, the thermal contrast between the LCZs of compact midrise (NDVI: 0.15) and dense trees (NDVI: 0.73) passed 40 °C on 02 August, 2014. On average, the LST approached 40 °C in case of three LCZs (compact midrise, compact low-rise, open midrise) and for 9% of the total study area.

Key words: Land surface temperature, Normalized Difference Vegetation Index, Landsat 7 ETM+, Local Climate Zones, Single-channel Algorithm, NDVI Threshold Method

1. INTRODUCTION

After the industrial revolution, the population started to increase explosively, and this process caused a rapid urbanization. Whilst 3% of the global population lived in urban areas in the 1800s, nowadays this ratio exceeds 50%. The tendency will likely continue in the forthcoming decades: according to some estimations (e.g. UN 2015), the expansion of urban areas can reach 66% by the 2050s. Urbanization contributes to the change of land-use and environmental factors. The natural landscape being replaced by artificial materials generated a remarkable change in physical features: roads, pavements have lower albedo, higher volumetric heat capacity and thermal conductivity compared to the natural sites.

The modification of the surface energy balance can also be observed in the urban areas. Because of the lower albedo, less incoming (shortwave) radiation is reflected from the ground, thus more heat (energy) is stored in the urban fabric. The reflected shortwave beam is strongly absorbed and backscattered by the pollutants. Long wave components are also attenuated by the absorbtion and re-emission of the aerosol particles. Traffic, industry, domestic energy usage (heating, cooling, cooking etc.) induces a large quantity of anthropogenic heat (AH) emission. Emission of stored and anthropogenic heat leads to an

energy surplus in the inner cities. Subsequently, a temperature difference occurs between the urban and rural areas, which is named the urban heat island (UHI) phenomenon. As reported by most studies (e.g. Miao et al. 2009, Wang et al. 2013, Chen et al. 2014), the proportion of AH release in a heat island may attain 30% depending on the land cover categories.

UHI is mostly developed under anticyclonic synoptic conditions, when the wind speed is low and the insolation is not interrupted by clouds. As a result of complex physical processes, the magnitude and the behavior of vertical heat island are diversified in the urban boundary layer. Features of the surface heat island (SUHI) depend on the amount of incoming radiation, hence the largest intensities can be found in summer at daytime, while the conventional (canopy layer) heat island is strongest at nighttime due to the heat emission from artificial materials. The frequency of heat waves tends to be higher in the forthcoming decades (Field et al. 2014). The existing heat island increases, even more enhancing the thermal load during the heat wave periods proportionally to the city-size (Gosling et al. 2007). The other significant environmental problem is the photochemical transformation of precursors (e.g. nitrogen-oxides, carbon monoxide, VOC). Consequently, the mortality rate of urban habitants becomes larger afterwards (WHO 2004), which urges the decision-makers to assign a reason to mitigation strategies. One of the most productive approach is the establishment of green areas. Vegetation lowers the temperature by the shading effect and reduces the air pollution by the stomatal exchange of CO_2/O_2. By the biophysical process of evapotranspiration, plants distract latent heat from the environment cooling their local area as well. Besides these direct effects, the greenery lowers the emission of pollutants by decreasing the energy consumption of AC systems. The advancement of remote sensing has opened a new dimension in the urban environment- and vegetation-related investigations. Nowadays, large datasets are available for scientific and educational purposes, because the satellites guarantee high-resolution and continuous data even where field observations are not applicable or do not exist.

Numerous researches examine the connection between the NDVI and the LST using Landsat 7 ETM+ data. Mallick et al. (2008) found reasonably strong relationship between the two variables. The land cover category of dense vegetation (forest) and high dense built-up showed the highest (R^2=-0.752) and the lowest (R^2=-0.394) correlation in Delhi (India). Alipour et al. (2008*)* compared the mono-window algorithm of Qin et al. (2001) and the single-channel method of Jimenez-Munoz and Sobrino (2003). The results argued that both algorithms captured the LST distribution well with an irrelevant difference ($\Delta R^2 \approx 0.06$). Senanayake et al. (2013) introduced the Environmental Criticality Index (ECI) based on the ratio of LST and NDVI. ECI presented inverse proportion to NDVI, thus the areas with lack of vegetation might have high 'environmental criticality'. Walawender et al. (2014) confirmed that the land-cover characteristics (e.g. shape of buildings, availability of vegetation) are the most decisive circumstances in the spatial distribution of LST. They emphasized that the largest influence on LST can be observed at the end of the vegetation period, when the greenery is greatly developed.

Urban environment research has been conducted in Budapest since the 1970s (Probáld 1974, 2014). The studies have generally been focused on the comparison of in-situ measurements and satellite observations. In the work of Pongrácz et al. (2010), a Terra/MODIS (Moderate Resolution Imaging Spectroradiometer) dataset was employed to study the thermal conditions in Budapest and other Central European cities (e.g. Belgrade, Bucharest, Milan, Munich, Sofia, Vienna, Warsaw, Zagreb). The largest SUHI appeared in summer at nighttime; the monthly mean values reached 3–4 °C in Budapest. Fricke et al.

(2014) investigated the relationship between LST and vegetation-cover on the district-scale. MODIS measurements indicated that the SUHI was, on average, 1.5–2 °C higher in the urbanized territories than in the encircling forests. Gábor and Jombach (2009) classified the land surface of Budapest into 14 classes and calculated LST and NDVI using Landsat 5 TM. The study showed that the highest LSTs were found in the categories of Intensive residential, Commercial and railway junctions. In addition, the average temperature difference achieved 14 °C between Woodland and Commercial classes.

The main objective of our investigation is to analyze the role of greenery in thermal load reduction by the comparison of NDVI and LST distribution in Budapest. To the best of the author's knowledge, Landsat 7 ETM+ data have not been applied to similar investigations yet, therefore this work aims to provide a beneficial basis for further research. In this study, after a short review of urban environment, the study area and the operation of Landsat 7 ETM+ are described in Section 2. Then the article gives a short explanation about the calculation of NDVI and LST using the images of red, near infrared and thermal infrared bands. Finally, maps and cross-section diagrams are represented to understand the spatial pattern of NDVI and LST distribution for the 11 Local Climate Zones (LCZs) (Stewart and Oke 2012) of Budapest.

2. MATERIALS AND METHODS

2.1. Description of the study area

Budapest (47,5°N, 19°E) is located in the Carpathian Basin in the northern part of Hungary with an area of 525.2 km^2. 1.76 million people have been living in the largest city of Hungary recently, but the population has decreased by 10% in the last 2 decades (Census of Hungary 2013). Budapest is surrounded by Pilis Mountainss and Szentendre Island in the north, Pesti Plain and Gödöllő Hills in the east, Csepel Island in the south and Tétény Uphill and Buda Hills in the west. The river Duna splits the city into two parts and creates the Óbuda Island, Margaret Island, Csepel Island. Buda Hills, the westernmost part of the study area contain steep hills (the highest point is 528 m), whilst on the east side of Duna River the relief is insignificant. The climate of Budapest is Cfb (Maritime temperate) and Dc (Temperate continental) according to Köppen and Trewartha (Köppen 1923, Peel et al. 2007) with a mean annual temperature and a precipitation of 11.3 °C and 533 mm, respectively.

11 Local Climate Zones were distinguished on the basis of the land cover of Budapest, following the work of Stewart and Oke (2012). This technique is based on uniform geometric (sky view factor, aspect ratio, building surface fraction, impervious surface fraction, natural surface fraction, pervious surface fraction, height of roughness elements, terrain roughness class) and thermal/radiative/metabolic (surface admittance, surface albedo, anthropogenic heat output) properties of a local (few kilometer expanse) area. The LCZ technique employs three aspects during the classification process (built types, land cover types, variable land cover properties) creating 20 categories (see more in Stewart and Oke 2012). Budapest was classified into 11 LCZs (Table 1) of which the largest is the LCZ of large low-rise (25.9%). The historical city center and its narrow environment are dominated by commercial and residential buildings with continuous urban fabric (compact midrise, compact low-rise). Large low-rise, open midrise and open low-rise categories are located in the outer residential belt, where the vast majority of the population lives. The southeastern and the southwestern

part of the city includes meadows, arable lands and agricultural areas (low plants, bare soil). The largest continuous forests are placed in the Buda Hills (dense trees), and remarkable vegetation is found in the major parks of Budapest (scattered trees: Orczy-park, Népliget, Városliget).

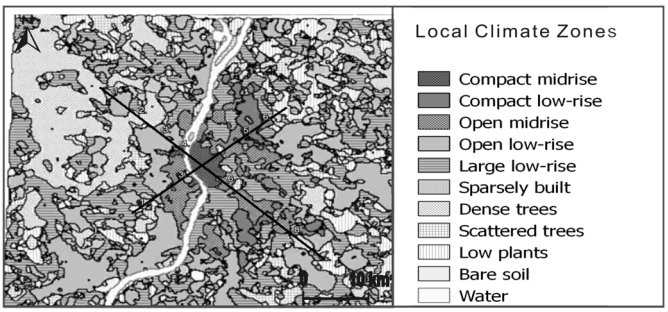

Fig. 1 Spatial distribution of the LCZs and the situation of the northwest-southeast and southwest-northeast cross-sections (detailed in Chapter 3.3.) in Budapest. The markers denote those places that have been numbered in Fig. 4 and Fig. 5

Table 1 Extension of the Local Climate Zones in Budapest

LCZ	LCZ name	Percentage of area
LCZ 2	compact midrise	1.1
LCZ 3	compact low-rise	2.4
LCZ 4	open midrise	5.6
LCZ 5	open low-rise	19.7
LCZ 8	large low-rise	25.9
LCZ 9	sparsely built	6.3
LCZ A	dense trees	15.2
LCZ B	scattered trees	9.6
LCZ D	low plants	10.5
LCZ F	bare soil	1.1
LCZ G	water	2.9

2.2. Description of the meteorological data and the Landsat 7 ETM+ satellite

As a result of the USGS (United States Geology Survey) data policy, Landsat 7 data can be downloaded free of charge since 1 October, 2008. The images are geometrically and radiometrically corrected in order to take the geolocation and the systematic (sensor) errors into account. In order to represent the urban effect and the peak period of vegetation, two distinct dates were chosen (2 and 18 August 2014). On both days, high-pressure formation dominated the Carpathian Basin. The maximum of 2-m temperature exceeded 25 °C (2 August: 31.9 °C; 18 August: 25.4 °C) and no precipitation occurred. The low cloud fraction (0 octa during the observations) favored for high insolation, therefore strong SUHI could be formed.

The Landsat satellites were constructed to satisfy various scientific interests in the field of agriculture, forestry, geology and meteorology. They have been operating since 1972, when the Landsat 1 was launched. Data acquisition of Landsat 7 has been started on 15 April 1999 on-board with the ETM+ (Enhanced Thematic Mapper Plus) sensor. Landsat 7 is on sun-synchronous orbit (inclined 98.2°) and supplies a temporal resolution of 16 days. ETM+

was originally developed for Landsat 6 and contains several improvements compared to the previous sensor (TM – Thematic Mapper; Landsat 4 and Landsat 5). This sensor possesses a new panchromatic band and a refined thermal infrared band with the spatial resolutions of 15 m and 30 m respectively and it consists of eight bands altogether. The scan line corrector (SLC) of ETM+ malfunctioned on 31 May 2001 resulting data-free black strips at the edge of images and about 22% data-loss for each pass (Chandler et al. 2009). A large number of methods (Storey et al. 2005 Zhang et al. 2007, Zeng et al. 2013) were constructed in order to recover missing pixels (e.g. kriging local histogram comparison method, weighted linear regression method, triangulation method) based on statistical comparison of the existing and the absent values.

2.3. Calculation of NDVI and LST

First, every pixel from the downloaded images was converted from DN (digital number) to spectral radiance (L_λ) in order to receive measurable physical quantities Eqs. 1, 2, 3. Before the calculation of spectral radiance, the theoretical maximum and minimum of digital numbers and spectral radiances have to be estimated with post-calibration creating the gain (G) and the bias (B) parameters.

$$G = \frac{L_{\max\lambda} - L_{\min\lambda}}{DN_{\max} - DN_{\min}} \tag{1}$$

$$B = L_{\min\lambda} - G \cdot DN_{\min} \tag{2}$$

$$L_\lambda = G \cdot DN - B \tag{3}$$

In order to determine the NDVI, the spectral radiance has to be converted into spectral reflectance (4) by employing the following equation for the red (0.631–0.692 μm) and the near infrared bands (0.772–0.898 μm):

$$\rho_\lambda = \frac{\pi \cdot L_\lambda \cdot d^2}{E_{SUN\lambda} \cdot \sin(\Theta_s)} \tag{4}$$

The sun elevation angle (Θ_s), the mean solar irradiance and the mean Sun-Earth distance (d) were obtained from metadata. The vegetation reacts separately for the different wavelength of electromagnetic radiation. The leaf pigments (chlorophyll) absorb the red (and the blue) portion of visible spectrum, while the near infrared part is reflected. It is worth noting that the phenological phase and the environmental conditions (heat and moisture stress) are primary factors in shaping the rate of reflection. In autumn, the leaves reflect less NIR (and more visible) radiation than in spring. Myriads of investigations (Jordan 1969, Rousse et al. 1974, Gitelson 2004) aimed to capture the step of reflection at the border of NIR and red spectrum of electromagnetic radiation. One of the most common index is NDVI, which can be estimated with this expression:

$$NDVI = \frac{\rho_{NIR} - \rho_{RED}}{\rho_{RED} + \rho_{NIR}} \tag{5}$$

The land surface emissivity (6) expresses the ability of thermal energy emission for a given material, thus this parameter is required to calculate the land surface temperature. Since

both the NDVI and the LSE are interpreted as a characteristic of land cover, the emissivity can be predicted with this vegetation index producing the so-called NDVI Threshold Method (hereinafter THM) (Sobrino et al. 2004). THM uses predetermined values of emissivity and NDVI for soil ($\varepsilon_{s\lambda}$=0.92, $NDVI_s$=0.2) and vegetation ($\varepsilon_{v\lambda}$=0.99, $NDVI_v$=0.5). To take the water and urban surfaces into consideration, new LSE values (ε_w=0.96, ε_u=0.92) were introduced.

$$\varepsilon_\lambda = \begin{cases} \varepsilon_{s\lambda} & NDVI < NDVI_s \\ \varepsilon_{s\lambda} + (\varepsilon_{v\lambda} - \varepsilon_{s\lambda}) P_v & NDVI_s < NDVI < NDVI_v \\ \varepsilon_{v\lambda} & NDVI < NDVI_v \end{cases} \quad (6)$$

The P_v term (7) is the fractional vegetation cover on mixed land cover areas (Carlson and Ripley 1997), and ranging from 0 ($NDVI=NDVI_s$) to 1 ($NDVI=NDVI_v$):

$$P_v = \left(\frac{NDVI - NDVI_s}{NDVI_v - NDVI_s} \right)^2 \quad (7)$$

Sobrino et al. (2008) found that the THM underestimates the emissivity of water, snow, ice and rocks. To consider the limitation of method for water bodies, a new emissivity value (0.97) was set, when NDVI is less than -0.3. Besides the THM, the TES (Temperature emissivity separation; Gillespie et al., 1998) and the TISI (Temperature independent spectral indices; Becker and Li 1990) algorithms are also valuable tools to compute the LSE. Oltra-Carrió et al. (2012) analyzed the land surface temperature pattern with different emissivity estimations for grass, bare soil and artificial surfaces and showed that the TES (RMSE=1.6 K) and the TISI (RMSE=1.7 K) performed better than the THM (RMSE=2.3 K). Nevertheless, the TES can only be used with at least four TIR image, and the TISI is designed with observations from daytime and nighttime, therefore the THM tends to be the most suitable method in our case.

Several methods were designed to calculate LST temperature by using satellite observations such as the single-channel algorithm (Jiménez-Munoz and Sobrino 2003), the mono-window algorithm (Qin et al. 2001), the split-window algorithm (Qin and Karnieli 1999) and the dual-angle method (Gu and Gillespie 2000). In this study, the single-channel algorithm (hereinafter SC) was applied, because this method does not employ such atmospheric parameters as water vapor content, effective mean temperature or at least 2 thermal bands like the mono-window and split-window algorithms. Only three parameters (band average atmospheric transmission, effective bandpass downwelling and upwelling radiance) are required for SC, which are provided by the MODTRAN atmospheric correction parameter calculator (Barsi et al. 2003). The MODTRAN claims the date (in YMDM format) and the location (latitude, longitude) compulsorily, since the surface conditions (e.g. altitude, air temperature, pressure and relative humidity) may be given optionally. If the surface conditions are not available, the values are interpolated from the observations of NCEP (National Center for Environment Prediction).

To derivate the surface temperature with SC, first, the brightness (or at-sensor) temperature (T_B) can be computed by inverting the Planck's Function:

$$T_B = \frac{K_2}{\ln\left(\frac{K_1}{L_\lambda} + 1\right)} \tag{8}$$

where K_1 (666.09 W m^{-2} sr^{-1} μm^{-1}) and K_2 (1282.71 K) are Landsat 7-specific calibration constants. In the next step, the MODTRAN outputs are used to determine ψ_1, ψ_2, ψ_3 atmospheric functions and γ, δ parameters as follows:

$$\psi_1 = \frac{1}{\tau} \tag{9}$$

$$\psi_2 = -L^{\downarrow} - \frac{L^{\uparrow}}{\tau} \tag{10}$$

$$\psi_3 = L^{\downarrow} \tag{11}$$

$$\gamma = \left\{ \frac{c_2 L_\lambda}{{T_B}^2} \left[\frac{\lambda^4 L_\lambda}{c_1} + \frac{1}{\lambda} \right] \right\}^{-1} \tag{12}$$

$$\delta = -\gamma \cdot L_\lambda + T_B \tag{13}$$

where c_1 (1.19104 10^8 W μm^4 m^{-2} sr^{-1}) and c_2 (1.43877 10^4 μm K) are constants and λ is the effective wavelength of Landsat 7 for band 6 (λ=11.27 μm) (NASA 2015). Finally, the equation of land surface temperature can be obtained:

$$T_S = \gamma \left[\frac{1}{\varepsilon} \left(\psi_1 L_\lambda + \psi_2 \right) + \psi_3 \right] + \delta \tag{14}$$

3. RESULTS

3.1. NDVI distribution patterns and quantitative results

On the two distinct dates (2 and 18 August 2014), the NDVI distribution indicated a positive gradient from the downtown (0.1–0.3) to the suburb (0.4–0.6), where the compact built-up structure is replaced with detached houses, in addition, the presence of natural surfaces becomes dominant (Fig. 2). The inner districts (e.g. Terézváros, Józsefváros, Ferencváros, Lipótváros) are characterized by the lowest NDVI (around 0.1), while areas with higher elevation (e.g. Buda Hills) and larger forests showed greater values (around 0.6). Green spots in the inner city, with a typical NDVI value of 0.5, refer to the major parks (e.g. Népliget, Városliget, Orczy-park) and recreational areas of Budapest (e.g. Margaret Island, Gellért Hill). Transport junctions, logistic centers, industrial territories are responsible for the isolated low-valued points in the suburb. Despite the similarities between the two dates, the vegetation reached the peak of its phenologic phase and biological activity on 2 August, accordingly higher NDVI were calculated at this time.

This assumption is confirmed by the NDVI values for the 11 LCZs, shown in Table 2. On 2 August, the average NDVI was 0.44, which is 16% higher than on 18 August (0.37).

The land cover zone of compact midrise indicated the lowest NDVI values (0.15 and 0.02) due to the presence of dense and large buildings and high impervious surface fraction. On the other hand, the greatly vegetated areas such as dense trees (0.73 and 0.70) or scattered trees (0.61 and 0.58) presented the highest NDVI. Areas with high NDVI can be interpreted as the most homogeneous region of Budapest based on the standard deviation rates (e.g. dense trees 0.09 and 0.11). Contrarily, the transitional categories (e.g. open low-rise, large low-rise) displayed the most complex land features (standard deviations: 0.12 and 0.16 for open low-rise; 0.18 and 0.23 for large low-rise) due to the mixture of medium-density residential and natural surfaces.

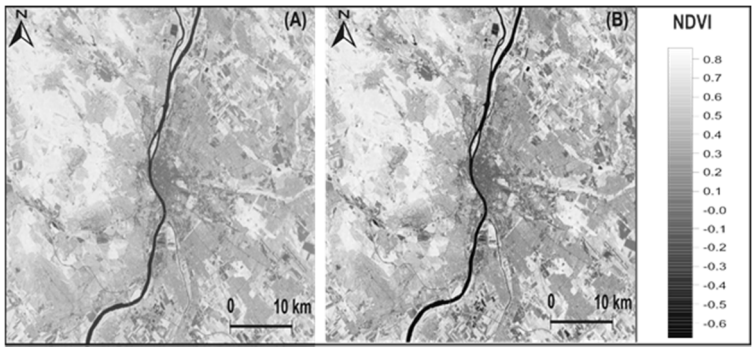

Fig. 2 Spatial distribution of the Normalized Difference Vegetation Index in Budapest on 2 (a) and 18 (b) August 2014

Table 2 Mean and standard deviation of NDVI in 11 Local Climate Zones of Budapest on 2 and 18 August 2014

LCZ name	02.08.2014.		18.08.2014.	
	Mean	Std. dev.	Mean	Std. dev.
compact midrise	0.15	0.11	0.02	0.14
compact low-rise	0.38	0.09	0.28	0.12
open midrise	0.39	0.13	0.31	0.16
open low-rise	0.47	0.12	0.39	0.16
large low-rise	0.46	0.18	0.39	0.23
sparsely built	0.55	0.12	0.50	0.16
dense trees	0.73	0.09	0.70	0.11
scattered trees	0.61	0.14	0.58	0.17
low plants	0.54	0.13	0.51	0.17
bare soil	0.48	0.20	0.40	0.25
water	0.07	0.38	-0.11	0.49

3.2. Distribution of land surface temperature

The 30-m resolution of the thermal band enables to determine the spatial pattern and the magnitude of the LST distribution in Budapest. It is clearly seen in Fig. 3 that the diversity of surface geometry generates a 30 °C interval in LST temperature on 2 and 18 August as well. The historical city center suffers a significant heat surplus because of high building and impervious surface fraction. By increasing the natural surface fraction, the surface temperature decreases rapidly, therefore the lowest LST can be found in the woodlands of

Buda Hills and in the outer districts. The local parks act as oases with high LST gradient along their border creating an ideal venue for recreational and leisure activities. Islands of Budapest (e.g. Margaret Island, Csepel Island) are also designated as cold spots for the sake of higher natural surface fraction and the cooling effect of the River Danube. The higher LSTs occurred on 2 August, when the maximum of 2-m temperature was the greatest as stated in the Bulletin of Hungarian Meteorological Service (Table 2). By this time, the thermal contrast decreased between the different land cover categories. It is worth pointing out that the LST values remained lower during the pass time of satellite in the downtown. Partly, this effect may likely be explained by the shading effect of high buildings. On the other hand, the relatively lower sun elevation angle could not let the surface being heated-up as much as on the previous date.

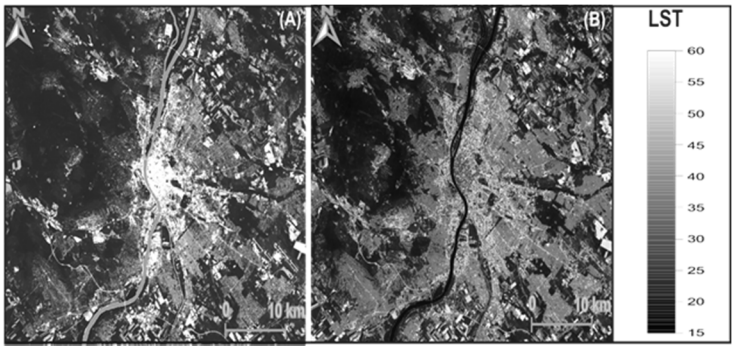

Fig. 3 Spatial distribution of the land surface temperature (LST; °C) in Budapest on 2 (a) and 18 (b) August 2014

The quantitative results suggest that the highest LST was 50–60 °C provoking a vast thermal load for the LCZ of compact midrise (Table 3). Compact low-rise (40.8 °C and 40.6 °C) and open midrise (40.0 °C and 38.6 °C) LCZs are also separated from the other groups due to their higher thermal exposure (Table 4). The substantially larger, but less populated classes like open low-rise (33.2 °C and 34.4 °C) and large low-rise (35.9 °C and 33.4 °C) were less affected by the high LST. Decrease of the impervious surface fraction delays the run-off, enhances the evaporation, the heat capacity and the albedo, and hence contributes to a huge (surface) temperature alteration. As a result of these impacts, the LST was about 40 °C lower in dense trees category on 2 August compared to the compact midrise class. The cooling potential of the three vegetation-related LCZs (dense trees, scattered trees, low plants) attained 12 °C and 9.43 °C on both dates, in contrast with the other 7 categories (except for the water class). After all, it must be highlighted that the green areas and parks not only play a role in urban planning, but also reduce the LST.

3.3. Cross-section diagrams of the land surface temperature

The LST maps extended for the entire city (or the study area) do not always give back the topographical aspect of the thermal field, so cross-section diagrams have to be created to analyze the cold and hot spots in Budapest (Fig. 1). Actually, we tried to concentrate on the first date (2 August), when the SUHI proved to be the most pronounced. The cross-sections move along a 29 km (20 km) long line from northwest to southeast (from southwest to northeast) by hitting 8 (6) well-separated area of the city.

Starting from northwest (Fig. 4), Pesthidegkút consists of medium-density residential areas, and characterized by an LST of about 25 °C, then the relief is dominated by the greatly vegetated Buda Hills, where the surface temperature decreased further (23 °C). A significant increase occured in Törökvész (30 °C) and Országút (35.1 °C) due to the existence of high-density residential and commercial areas. The maximum of LST together with the maximum of impervious and building surface fraction and the minimum of natural surface fraction produced a notable thermal load in the downtown (e.g. Lipótváros, Erzsébetváros). The equable course of LST dropped to up to 20–25 °C in the middle of the 'downtown' domain as a result of a large green space, called Szabadság Square. The same processes can be considered in Outer Ferencváros (e.g. Népliget Park at about 17.5 km), where housing estates, row housing, panel blocks and parks made the landscape diversified with approximately a 30 °C variation in LST. The external parts of southeast Budapest (Kispest, Pestszentlőrinc) displayed a decreasing magnitude of the thermal field.

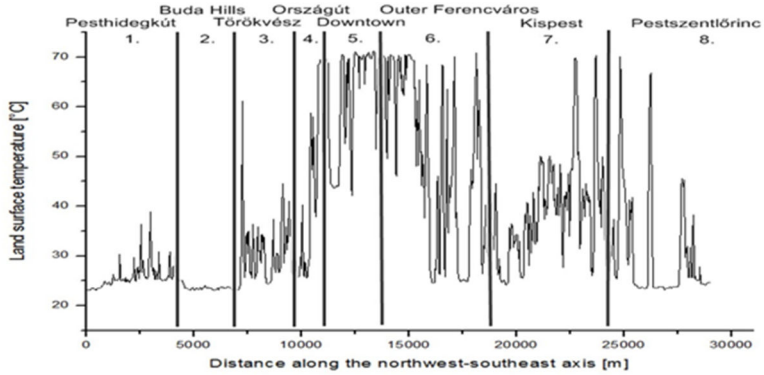

Fig. 4 Cross-section diagram of the land surface temperature along the northwest-southeast direction (02.08.2014. 09:30:53 UTC). The numbers (from 1 to 8) refer to the location of each places marked in Fig. 1

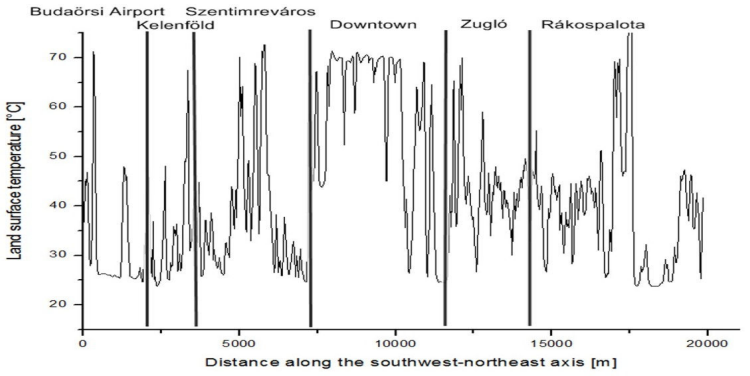

Fig. 5 Cross-section diagram of the land surface temperature along the southwest-northeast direction (02.08.2014. 09:30:53 UTC). The numbers (from 1 to 6) refer to the location of each places marked in Fig. 1

Similar to our previous case, an increasing trend is outlined along the southwest-northeast axis to the end of Downtown (Fig. 5) (Budaörsi Airport: 32.2 °C, Kelenföld: 33.5 °C, Szentimreváros: 37.9 °C, Downtown: 58.3 °C). The line, however, crosses cold spots such as the foreground of Sas Hill (at about 4.5 km) and Gellért Hill (at about 7000 m). Zugló consists of two major land cover zones: open midrise (housing estates, apartments, panel blocks) and open low-rise (family housing) resulting in a bimodal LST distribution. Rákospalota indicates a nearly constant value of LST, though the panel blocks (at about 17,000 m) trap the heat intensely during the summer months and consequently contribute to a huge thermal load. Based on the results of the two cross-sections, it is evident that the most decisive factor in the governing of the thermal field is the natural surface fraction and the elevation in Budapest.

4. CONCLUSIONS

In this study, the relationship of land-use and land surface temperature was examined using fine-resolution Landsat 7 ETM+ images taken on 2 and 18 August 2014 in Budapest. It is well known that intense urbanization and anthropogenic activity (e.g. transportation, industry, heating/cooling) generate a special climate on the meso- and microscales. The vegetation attenuates this environmental influence by shading, as well as a higher albedo and evapotranspiration related to the artificial surfaces. The goal of this analysis was to quantify the impact of greenery on LST reduction and to explore the cold and hot spots in the 11 Local Climate Zones (Stewart and Oke 2012) of Budapest. The NDVI values indicated a positive gradient towards the external areas. On 2 and 18 August 2014, the lowest NDVI was found in the LCZ of compact midrise with 0.15 and 0.02, respectively, while the dense trees category showed the highest (0.61 and 0.70) values. Due to the less phenologic development of the vegetation on the later date, NDVI, on average, decreased by 15% between the two observations. In three LCZs (compact midrise: 63.5 °C and 38.2 °C; compact low-rise: 40.8 °C and 40.6 °C; open midrise: 40.0 °C and 38.6 °C), the LST exceeded 40 °C at most times inducing a pronounced thermal field. Contrarily, the external areas (e.g. woodlands, meadows, agricultural parcels) and parks diminished the LST up to 25–35 °C. The results suggest that the thermal contrast between areas with different natural/building surface fraction became lower, when the meteorological conditions favoured a greater LST. Overall, it has to be noted that the LST alteration is primarily driven by the fraction of natural, impervious and building surfaces. Cross-section diagrams reveal that the magnitude of LST was higher in the Buda side in case of identical elevation as a result of the enhanced natural surface fraction. On the other hand, the territories on the Pest side have more complex surface structures, consequently the course of LST presents a large variety within a narrow region. Nevertheless, the importance of vegetation in LST reduction essentially depends on the season of the year, the period of the day and the location of the study area, thus our analysis cannot be generalized, but provides only site-specific information about the thermal field of Budapest.

REFERENCES

Alipour T, Sarajian MR, Esmaely A (2011) Land surface estimation from thermal band of Landsat sensor, case study: Alashtar city. Int Arch Photogramm Remote Sens Spat Info Sci 38/C7

Barsi JA, Barker JL, Schott JR (2003) An atmospheric correction parameter calculator for a single thermal band earth-sensing instrument. Proc IEEE IGARSS, 21–25 July 2003, Toulouse, France, 3014-3016.

Becker F, Li ZL (1990) Temperature-independent spectral indices in thermal infrared bands. Remote Sens Environ 32:17-33

Carlson TN, Ripley DA (1997) On the relation between NDVI, fractional vegetation cover and leaf area index. Remote Sens Environ 62:241-252

Census of Hungary (2013): 2011. évi népszámlálás. Területi adatok. [Census of Hungary (2011). Local data. (in Hungarian)] Budapest

Chandler G, Markham BL, Helder SL (2009) Summary of current radiometric calibration coefficients for Landsat MSS, TM, ETM+ and EO-1 ALI sensors. Rem Sens Environ 113:893-903

Chen F, Yang X, Zhu W (2014) WRF simulations of urban heat island under hot-weather synoptic conditions: The case study of Hangzhou City, China. Atmos Res 138:364-377

Cristóbal J, Jiménez-Munoz JC, Sobrino JA, Ninyerola M, Pons X (2009) Improvements in land surface temperature retrieval from the Landsat series thermal band using water vapor and air temperature. J Geophys Res 114:1-16

Field CB, Barros VR, Dokken DJ, Mach KJ, Mastrandrea MD, Bilir TE, Chatterjee M, Ebi LK, Estrada YO, Genova RC, Girma B, Kissel ES, Levy AN, MacCracken S, Mastrandrea PR, White LL (2014) Climate Change 2014 Impacts, Adaptation, and Vulnerability. Part A: Global and Sectoral Aspects. Contribution of Working Group II to the Fifth Assessment Report of the Intergovernmental Panel on Climate Change. Cambridge University Press, Cambridge, New York

Fricke C, Pongrácz R, Dezső Zs, Bartholy J (2014) A vegetáció szerepe a budapesti városi hősziget jelenségben. [The role of vegetation in urban heat phenomenon in Budapest (in Hungarian)]. Légkör 59:150-153

Gábor P, Jombach P (2009) The relation between the biological activity and the land surface temperature in Budapest. Appl Ecol Env Res 7:241-251

Gillespie AR (1985) Lithologic mapping of silicate rocks using TIMS. Proc TIMS Data Users' Workshop, Berkeley, CA

Gitelson AA, Kaufman YJ, Merzlyak MN (1996) Use of a green channel in remote sensing of global vegetation from EOS-MODIS. Remote Sens Environ 58:289-298

Gosling SN, McGregor GR, Páldy A (2007) Climate change and heat-related mortality in six cities. Part 1: Model construction and validation. Int J Biometeorol 51:525-540

Gu D, Gillespie AR (2000) A new approach for temperature and emissivity separation. Int J Remote Sens 21:2127-2132

Jordan CF (1969) Derivation of leaf-area index from quality of light on forest floor. Ecology 50:663-666

Ichinose T, Shimodozono K, Hanaki K (2009) Impact of anthropogenic heat on urban climate in Tokyo. Atm Environ 33:3897-3909

Jimenez-Munoz JC, Sobrino JA (2003) A generalized single-channel method for retrieving land surface remote sensing data. J Geophys Res 108:1-9

Jiménez-Munoz JC, Cristóbal J, Sobrino JA, Sória G, Ninyerola M, Pons X (2009) Revision of the single-channel algorithm for land surface temperature retrieval from Landsat thermal-infrared data. IEEE T Geosci Remote 47:339-349

Köppen W (1936) Das geographische System der Klimate. In: Köppen W, Geiger R (eds): Handbuch der Klimatologie. Verlag von Gebrüder Borntraeger, Berlin

Mallick J, Kant Y, Bharat BD (2008) Estimation of land surface temperature over Delhi using Landsat-7 ETM+. J Ind Geophys Un 12:131-140

Miao S, Chen F, LeMone MA, Tewari M, Li Q, Wang Y (2009) An observational and modeling study of characteristics of urban heat island and boundary layer structures in Beijing. J Appl Meteorol Clim 48:484-501

NASA (2015) Landsat 7 Science Data Users Handbook. National Aeronautics and Space Administrati on http://landsathandbook.gsfc.nasa.gov/pdfs/Landsat7_Handbook.pdf [accessed Dec 2015]

Oltra-Carrió R, Sobrino JA, Franch B, Nerry F (2012) Land surface emissivity retrieval from airborne sensor over areas. Rem Sens Environ 123:298-305

Peel MC, Finlayson BL, McMahon TA (2007) Updated world map of the Köppen-Geiger climate classification. Hydrol Earth Syst Sc 11:1633-1644

Pongrácz R, Bartholy J, Dezső Z (2006) Remotely sensed thermal information applied to urban climate analysis. Adv Sp Res 37:2191-2196
Pongrácz R, Bartholy J, Dezső Z (2010) Applications of remotely sensed information to urban of Central European cities. Phys Chemistry Earth 35:95-99
Probáld F (1974) Budapest városklímája [Urban climate of Budapest (in Hungarian)]. Akadémiai Kiadó, Budapest
Probáld F (2014) The urban climate of Budapest: past, present and future. Hun Geogr Bull 63:69-79
Qin Z, Karnieli A (1999) Progress in the remote sensing of land surface temperature and ground emissivity using NOAA-AVHRR data. Int J Rem Sens 20:2367-2393
Qin Z, Karnieli A, Berliner P (2001) A mono-window algorithm for retrieving land surface temperature from Landsat TM and its application to the Israel-Egypt border. Int J Rem Sens 22:3719-3746
Rouse JW, Haas RH, Schell JA Jr, Deering DW (1974) Monitoring vegetation systems in the Great Plains with ERTS. Third ERTS-1 Symposium Washington, DC, NASA, 309-317
Stewart ID, Oke TR (2012) Local Climate Zones for urban temperature studies. Bull Amer Meteor Soc 93:1879-1900
Senanayake IP, Welivitiya WDDP, Nadeeka PM (2013) Remote sensing based analysis of urban heat islands with vegetation cover using Landsat-7 ETM+ data. Urb Clim 5:19-35
Sobrino JA, Caselles V, Becker F (1999) Significance of the remotely sensed thermal infrared measurements obtained over a citrus orchard. ISPRS J Photog Rem Sens 44:343-354
Sobrino JA, Raissouni N, Li ZL (2001) A comparative study of land surface emissivity retrieval from NOAA data. Remote Sens Environ 75:256-266
Sobrino JA, Jiménez-Munoz JC, Paolini L (2004) Land surface retrieval from Landsat 5 TM. Remote Sens Environ 90:434-440
Sobrino JA., Jiménez-Munoz JC, Sória G, Romaguera M, Guanter L (2008) Land surface emissivity retrieval from different VNIR and TIR sensors. IEEE Trans Geos Rem Sens 46:316-327
Storey J, Scaramuzza P, Schmidt G, Barsi J (2005) Landsat 7 scan line corrector-off gap-filled product development. Proceedings of Pecora 16 Global Priorities in Land Remote Sensing. Sioux Falls, South Dakota
UN (2015) World Urbanization Prospects: The 2014 Revision. United Nations, Department of Economic and Social Affairs, Population Division
Walawender JP, Szymanowszki M, Hajto MJ, Bokwa A (2014) Land surface temperature patterns in the urban agglomeration of Krakow (Poland) derived from Landsat-7/ETM+ data. Pure Appl Geophys 171:913-940
Wang M, Yan X, Liu J, Zhang X (2013) The contribution of urbanization to recent extreme heat events and potential mitigation strategy in the Beijing–Tianjin–Hebei metropolitan area. Theor Appl Climatol 114:407-416
WHO (2004) Comparative quantification of health risks. Global and regional burden of disease attributable to selected major risk factors (Vol. I.). World Health Organization, Hong Kong
Zeng C, Shen H, Zhang L (2013) Recovering missing pixels for Landsat ETM+ SLC-off imagery using multi-temporal regression analysis and a regularization method. Remote Sens Environ 131:182-194
Zhang C, Li W, Travis D (2007) Gaps-fill of SLC-off Landsat ETM+ satellite image using a geostatistical approach. Int J Rem Sens 28:5103-5122

ACTA CLIMATOLOGICA ET CHOROLOGICA
Universitatis Szegediensis, Tomus 49-50, 2016, 63-80

URBAN CLIMATE ISSUES IN COMPLEX URBANIZED ENVIRONMENTS: A REVIEW OF THE LITERATURE FOR NOVI SAD (SERBIA)

S SAVIĆ[1], D MILOŠEVIĆ[1], D ARSENOVIĆ[2], V MARKOVIĆ[2], I BAJŠANSKI[3] and I ŠEĆEROV[2]

[1]*Climatology and Hydrology Research Centre, Faculty of Sciences, University of Novi Sad, Trg Dositeja Obradovića 3, 21000 Novi Sad, Serbia*
[2]*Departman of Geography, Tourism and Hotel Management, Faculty of Sciences, University of Novi Sad, Trg Dositeja Obradovića 3, 21000 Novi Sad, Serbia*
[3]*Department of Architecture and Urban Planning, Faculty of Technical Sciences, University of Novi Sad, Trg Dositeja Obradovića 6, 21000 Novi Sad*
E-mail: stevan.savic@dgt.uns.ac.rs

Summary: In the last five years more than 30 articles have been published in scientific journals and conferences focused on urban climate research in Novi Sad. These researches were led by members from the Climatology and Hydrology Research Centre at the Faculty of Sciences, University of Novi Sad (Republic of Serbia), together with demographers, architects, environmental researchers and experts from medicine and biostatistics. Novi Sad is a mid-sized city in the northern part of the Republic of Serbia with a built-up area of 112 km^2 and a population of 340,000 (data from 2015). All results were published in 7 scientific journals, one PhD dissertation, a few books and presented in 12 conferences. Furthermore, all research activities in the last few years were covered by one international project (EU-funded IPA project) and one national project (funded by the Autonomous Province of Vojvodina). This paper presents all research and results of urban climate in the Novi Sad built-up area. Up to now, the results have been mostly focused on urban surface issues, definition of Local Climate Zones (LCZ) and adequate station cites, the analysis of urban heat island (UHI), outdoor human thermal comfort and the interaction of urban climate and urbanization and mortality.

Key words: urban climate, Local Climate Zones, urban heat island, outdoor thermal comfort, urbanization, mortality, Novi Sad, Serbia

1. INTRODUCTION

Urban environments are becoming increasingly important and relevant to study since most of the world's population now inhabits towns and cities (UN 2009, Grimmond et al. 2010), and as such, the proportion of the world's land and water surface covered by built-up environment is constantly expanding. Therefore it is essential to better understand atmospheric processes and impacts in urban areas and how they will be affected by climate change (Muller et al. 2013).

In Central Europe (where Novi Sad is situated), climate change is expected to increase the frequency, duration and intensity of heat waves (IPCC 2012, Pongrácz et al. 2013), along with the thermal stress experienced by people (Tomlinson et al. 2011). With reduced nocturnal cooling, the climate of cities is expected to make these already adverse projections worse, as elevated heat loads are linked to higher morbidity and mortality rates (Petralli et al.

2012). Thus, monitoring the spatial and temporal patterns of the elevated urban temperature is an important task that can help both in the mitigation of and in the adaptation to the altered circumstances of the future (Lelovics et al. 2016).

Therefore, in the last five years urban climate research was expanded, mostly led by the members from the Climatology and Hydrology Research Centre at the Faculty of Sciences, University of Novi Sad (Republic of Serbia). Up to now 38 references have been published in scientific journals and conferences, focused on urban climate issues in Novi Sad. 11 papers have been published in 7 journals (such as Building and Environment, Advances in Meteorology, International Journal of Biometeorology, Időjárás) and 22 abstracts and extended abstracts have been presented on 12 different conferences (such as ICUC9 – 9th International Conference on Urban Climate, Fifth EUGEO Congress on the Geography of Europe, European Population Conference 2014, IGU regional conference – Changes, Challenges, Responsibility). Within the urban climate research group in Novi Sad, one PhD dissertation has been defended related with the impact of air temperature on the seasonal variation of human mortality in Novi Sad (Arsenović 2014) and one PhD dissertation is in preparation related with the temporal and spatial analysis of outdoor human thermal comfort in different LCZs of Novi Sad. From 2012 to 2014, two projects related with urban climate issues were conducted. The first one was an EU-funded project in the frames of the IPA Hungary-Serbia programme (project title: Evaluation and public display of URBAN PATterns of Human thermal conditions) and the second one was a regional project funded by the Autonomous Province of Vojvodina (project title: Analysis of urban climate in Novi Sad and its impact on the thermal comfort of urban population). The published papers have been focused on urban surface characteristics, delineations of LCZs and definition of representative station sites (Popov 1994, 1995, Popov and Savić 2010, Unger et al. 2011a, 2011b, Savić et al. 2012b, Savić et al. 2013a, Savić et al. 2013b, Savić, et al. 2013c, Savić et al. 2014a, Savić et al. 2014b, Unger et al. 2014, Jovanović et al. 2015, Unger et al. 2015a, Savić 2015, Šećerov et al. 2015a, Šećerov et al. 2015b), analysis of UHI and outdoor human thermal comfort (Lazić et al. 2006, Savić et al. 2012a, Marković et al. 2013, Marković et al. 2014a, Marković et al. 2014b, Milošević et al. 2015a, Skarbit et al. 2015, Savić et al. 2015; Marković 2015, Milošević et al. 2015b, Milošević et al. 2015c, Bajšanski et al. 2015, Basarin et al. 2016, Lelovics et al. 2016) and interaction of urban climate and urbanization, human mortality, tourism attractiveness (Stankov et al. 2013, Stankov et al. 2014, Arsenović 2014, Arsenović et al. 2014a, Arsenović et al. 2014b, Arsenović and Đurđev 2015, Savić et al. 2015, Bajšanski et al. 2015).

The main goal of this study is to present the results of all published journal papers, conference presentations and other publications related with the urban climate research of Novi Sad city and represent and propose some activities and investigations in the future according to the urban climate issues.

2. INVESTIGATED AREA

Novi Sad is a mid-sized city in the northern part of the Republic of Serbia (Fig. 1), located on a plain between 80 and 86 m a.s.l. Hence, the climate is generally free of orographic effects. Based on a population of 340,000 (data from 2015), Novi Sad is the second largest metropolitan region in Serbia with a built-up area of 112 km^2. The Danube River passes through the southern and eastern edges of the urban area; its width varies from

260 to 680 meters. The relatively narrow Danube-Tisza-Danube Canal passes through the northern part of the city. The northern slopes of the Fruška Gora Mountains (which have a maximum peak of 538 m a.s.l.) are located south of the Novi Sad urban area (Unger at al. 2011).

The Novi Sad region has a Cfb climate (temperate climate, fully humid, and warm summers, with at least four $T_{mon} \geq +10$ °C) according to the Köppen-Geiger climate classification (Kottek et al. 2006). The mean monthly air temperature ranges from -0.4 ºC in January to 21.7 ºC in July. The mean annual precipitation is 598 mm (based on data registered from 1949 to 2013).

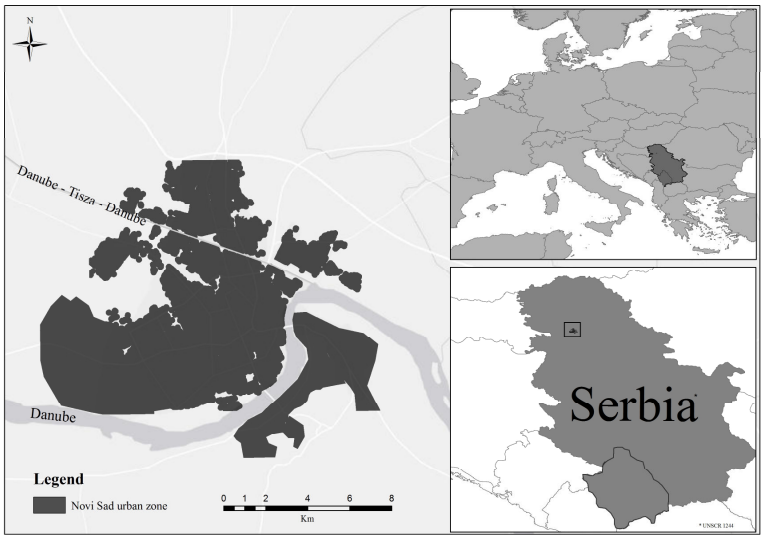

Fig. 1 Investigated built-up area of Novi Sad; its location in the Republic of Serbia and Europe

3. URBAN SURFACE ANALYSIS AND CLIMATE MONITORING NETWORK DEVELOPMENT

3.1. Local Climate Zones definitions

LCZ presents a comprehensive climate-based classification of urban and rural areas for temperature studies. This kind of analysis can contribute to the standardization of surface descriptions, the intercity comparison of UHI magnitude, the clear communication of station site metadata and the interdisciplinary transfer of urban climate knowledge (Stewart and Oke 2012). Therefore, the first papers of urban climate research in Novi Sad were focused on instead LCZ: urban built type definitions. The first definition and delineation of urban built types were made by Popov (1995) and Popov and Savić (2010). The eight urban built types (Fig. 2a) are defined based on various urban surface elements i.e. surface roughness, street width, sky view factor (SVF) and built-up ratio. The results showed that the coefficient of roughness of the terrain varies from about 0.4 m on the outskirts of the city, where about 20–30% of the surface is under family houses, to about 2.5 m in the center of the city, where 60–70% of the surface is under the high buildings. SVF decreases from about 0.9 at the

suburban settlement to about 0.35 in some narrow streets in the downtown. Further steps in LCZ definition were made in 2011 based on Stewart and Oke's (2010) classification system. Novi Sad was one of the first cities where this new LCZ classification method was applied. The urban area of Novi Sad (60 km^2) was established as a grid network of 240 cells (0.5 km × 0.5 km). A Landsat satellite image (from June 26, 2006) was used in order to evaluate Normalized Difference Vegetation Index (NDVI) and built-up ratio by cells. The built-up ratio ranged from near 0% (the River Danube) to over 90% (densely built-up centre). Large density was found in the central part and in eastern areas, near the Danube. Furthermore, built-up maxima were located in the western, northern, northeastern and eastern urban areas (Figure 7). Further analysis based on guidance given by Stewart and Oke (2010), information extracted from Google Maps and the authors' local knowledge of the study area have been used to define 7 LCZ classes (Fig. 2b) (Unger et al. 2011a, 2011b).

Table 1 Names and designation of the LCZ types (after Stewart and Oke 2012)

Built types	Land cover types	Variable land cover properties
LCZ 1 – compact high-rise	LCZ A – dense trees	b – bare trees
LCZ 2 – compact midrise	LCZ B – scattered trees	s – snow cover
LCZ 3 – compact low-rise	LCZ C – bush, scrub	d – dry ground
LCZ 4 – open high-rise	LCZ D – low plants	w – wet ground
LCZ 5 – open midrise	LCZ E – bare rock / paved	
LCZ 6 – open low-rise	LCZ F – bare soil / sand	
LCZ 7 – lightweight low-rise	LCZ G – water	
LCZ 8 – large low-rise		
LCZ 9 – sparsely built		
LCZ 10 – heavy industry		

Table 2 Spatial characteristics of LCZ built types and distribution of stations in each LCZs (Šećerov et al. 2015b)

LCZ types	Number of patches	LCZ proportion in %	Number of stations
2	6	9.6	3
3	5	5.2	2
5	8	15.1	6
6	19	42.3	9
8	6	10.1	1
9	5	13.0	3
10	4	4.7	1
A			1
D			1

According to the spatial distribution, the most dominant classes are open low-rise, open midrise and large low-rise. Within the framework of the URBAN-PATH project, during 2013 and 2014 a new spatial distribution of LCZs in urban area of Novi Sad based on Stewart and Oke's (2012) classification (Table 1) was created. In this research a new method based on the automated Geographic Information System (GIS) method developed by Lelovics et al. (2014) (Fig. 3) was used. The study area was divided into 47,000 lot area polygons (Gál and Unger 2009) consisting of a building and the area of influence around it as basic areas in the calculation of surface parameters necessary to characterize the LCZ types. The first step in the analysis was the LCZ classification in each lot area polygon. In order to obtain LCZ areas with appropriate size, they were aggregated and merged according to their LCZ category and their location relative to each other. The aggregation procedure was carried out

according to the recommendations of Stewart and Oke (2012) and Lelovics et al. (2014). Final results indicated the existence of 7 LCZ built classes within the city, named as: LCZ 2 – compact midrise, LCZ 3 – compact low-rise, LCZ 5 – open midrise, LCZ 6 – open low-rise, LCZ 8 – large low-rise, LCZ 9 – sparsely built and LCZ 10 – heavy industry. The types and areal distribution of these zones within the urban area of Novi Sad is supplemented by 2 land cover types (A – dense trees, D – low plants) (Fig. 4, Table 2) (Savić et al. 2013a, Savić et al. 2013b, Savić et al. 2014a, Savić et al. 2014b, Unger et al. 2014, Milošević et al. 2015a, Šećerov et al. 2015b).

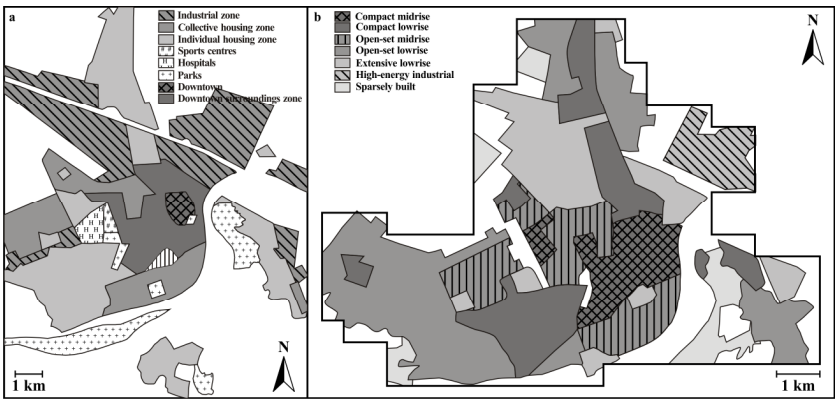

Fig. 2 Spatial distribution of urban built types a) Popov and Savić 2010 and LCZs b) Unger et al. 2011a in Novi Sad urban area

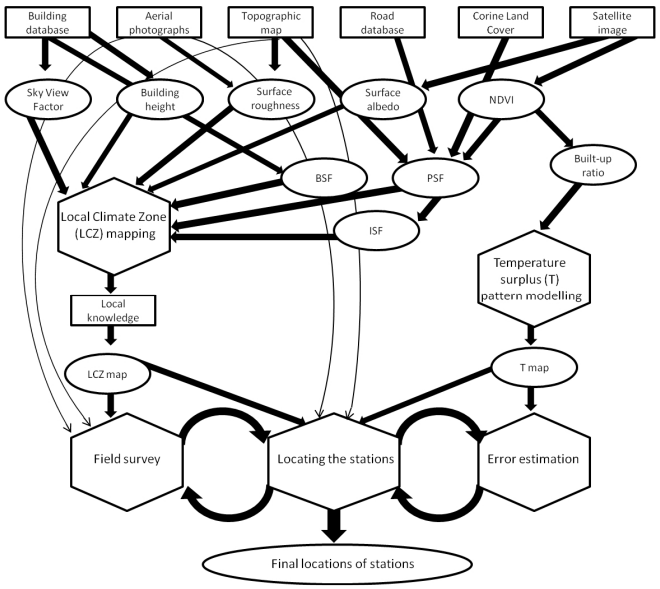

Fig. 3 Process of identifying and delineating LCZs and selecting the representative station sites for urban monitoring network in Novi Sad, Serbia (based on Lelovics et al. 2014). Note: NDVI – Normalized Difference Vegetation Index, BSF – Building Surface Fraction, PSF – Pervious Surface Fraction, ISF – Impervious Surface Fraction

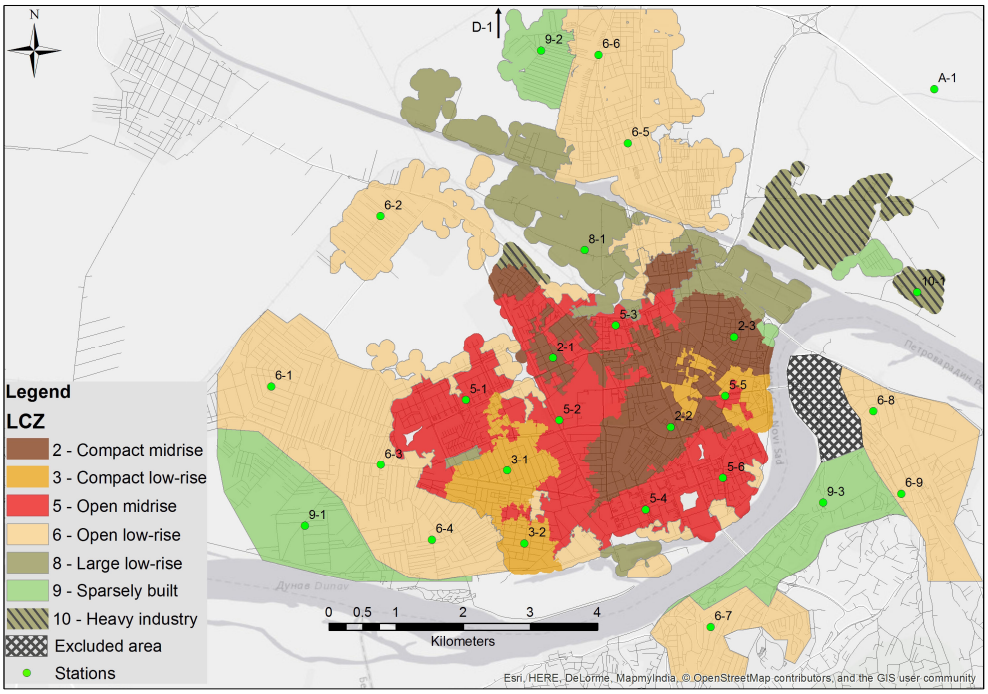

Fig. 4 The obtained LCZ classes and station locations of the urban monitoring network in Novi Sad (Serbia). Note (Station labels): first character – LCZ type; second character – station number in the given LCZ type (Unger et al. 2014, Šećerov et al. 2015b)

3.2. Urban station network development

The spatial and temporal variability of climate across whole cities or regions cannot be represented by individual monitoring stations while the precise allocation of any equipment is difficult (WMO 2006). Thus, the only appropriate way to monitor urban environments, such as the Novi Sad urban area, is with a dense sensor network. This kind of network maximizes the understanding of the urban environment, as well as any changes that are occurring and the likely impacts (Muller et al. 2013).

During 2010 and 2011 proposals have been published for an urban monitoring network containing 9–10 stations across the urban area (Popov 1995, Popov and Savić 2010, Unger et al. 2011a, 2011b) based on urban surface analysis and LCZs delineation. According to further publications (Savić et al. 2013a, 2013b, Unger et al. 2014, Lelovics et al. 2014) an urban monitoring network was developed in Novi Sad, financed by the EU-funded URBAN-PATH project. In order to have a representative urban monitoring network the locations of all stations were based on few criteria (Oke 2004, Lelovics et al. 2014): a) the sites had to be surrounded by at least 250 m wide homogeneous LCZ areas, and the number of stations per each LCZ had to be approximately proportional to the areas of different LCZs; b) the site's representativeness in terms of its microenvironment, i.e. the selected site had to be typical to the LCZ where the station was located; c) the sites had to be located near the areas where high and low temperature surpluses occurred, as well as near local maxima and around spatial temperature stretches, as indicated by the modelled temperature pattern; d) the site's

suitability for instrument mounting (for instance: safety, constant electricity supply, stability of lamppost); according to Stewart and Oke's (2012) classification (Table 2 in Lelovics et al. 2016).

The urban monitoring network in Novi Sad consists of 27 stations. 25 stations are located in the urban area and 2 stations are located in the land cover D and A classes and they represent general climate conditions in the non-urbanised areas (Fig. 4). The distribution of stations per LCZs is shown in Table 2.

Stations are installed at least 4 m above the ground (with exceptions ±0.2 m) on arms fixed to selected lampposts (Fig. 5) and equipped with air temperature (±0.3 ºC accuracy) and humidity (RH accuracy: ±2% at 20–80%) sensors covered with radiation protection screens with dimensions of 200 × 240 mm. All stations have power supply through the city lights system. The stations measure the parameters every minute and send the readings related to air temperature, relative humidity, battery voltage, status values and other technical information to the main server (installed at University of Novi Sad, Faculty of Science) at 10-minute intervals. The system time of the stations is in UTC (Unger et al. 2014, Šećerov et al. 2015b).

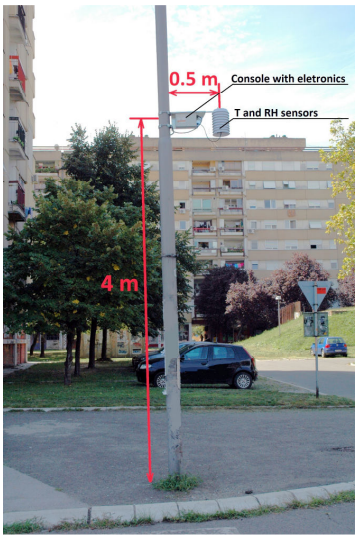

Fig. 5 Example of monitoring network station in Novi Sad (Serbia) mounted on a lamppost (Šećerov et al. 2015b)

3.3. Monitoring and public display system

It is very important to implement the method of data representation and communication between stations and servers, working with data stored in database and the real-time public availability of the data (Šećerov et al. 2015b) in order to adequately use the temperature and relative humidity values from stations.

In order to receive and store data into the database server and monitor system behaviour, the Urban Path System tool (UP-SYS_tool) was built. Further climate studies, and work with gathered data can be done using URBAN-PATH Portal. Data uploaded to the primary server are being processed by the UP-SYS_tool. All data are processed whether they contain climatological *measurement* or *debug* data with statistics about station work. Error detection and notification is performed through the entire UP-SYS_tool work. As a final result of the UP-SYS_tool work, data are stored into the database server. Using defined periods, UP-SYS_tool starts the archiving process to relocate and compress processed files to archive location. After that they can be used, if needed, for recovery. URBAN-PATH Portal is an application built to support all demands related with urban climate studies and for analyzing the entire systems' work. It can be used for two purposes: a) to get data from the database in the desired format and b) to monitor current system status.

The latest inserted data for each station *(stations monitor)* are shown together with their 'age'. If the last inserted data are older than the defined thresholds, the line containing it is coloured with a different warning colour. Next to the *stations monitor* is the *missing measurements monitor*, used to provide adequate information about the number of missing data per station (Fig. 6). Although the system is built to handle different levels of problems

whether they are hardware or software or related to connection problems, the final result is the data not being stored into the database server. The UP-SYS_tool periodically checks the database for missing data and stores results into a separate database, which is used for *missing measurements monitor* (Šećerov et al. 2015b).

The visualization of the measured values from the urban climate monitoring network in Novi Sad is provided by an automatic data procession system. This system was developed and installed at the Department of Climatology and Landscape Ecology of the University of Szeged. Every 10 minutes, the data from the monitoring network, stored into the main server at the Faculty of Science, University of Novi Sad, is transmitted to the main server at the University of Szeged and the automatic data procession system creates two final (site and spatial) databases in order to present these data as charts and maps on the public homepage of the URBAN-PATH project (http://en.urban-path.hu/monitoring-system.html). All of the measured and calculated values can be accessed in a way that the time of the maps and charts can be defined by the visitors. Additionally, public display is installed at a frequently visited place, i.e. in the main building of the University of Novi Sad (Savić and Unger 2014, Unger et al. 2015b).

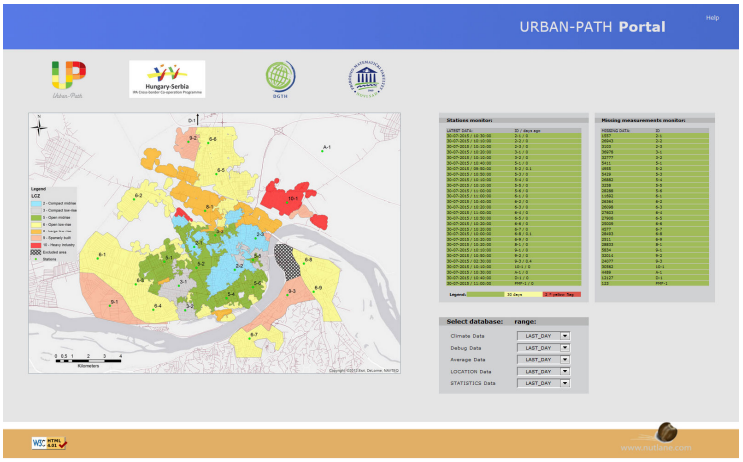

Fig. 6 URBAN-PATH Portal main page with data monitoring and database selection tool (Šećerov et al. 2015b)

4. URBAN HEAT ISLAND TEMPERATURE PATTERN AND OUTDOOR THERMAL COMFORT RESEARCH

4.1. Urban heat island analysis

Urban heat island occurs in almost all urban areas, large or small, in warm or cold climates. The traditionally described heat island is measured at standard screen height (1–2 m above ground), below the city's mean roof height in a thin section of the boundary layer atmosphere called the urban canopy layer. Air in this layer is typically warmer than that at screen height in the countryside. The main causes of the heat island are related to structural and land cover differences of urban and rural areas (Stewart and Oke 2012).

The results from the Novi Sad urban area show that the built-up ratio has a significant influence on the spatial pattern of the annual mean UHI intensity, i.e. the ΔT values follow the change in the built-up values (Fig. 7). The main feature of this pattern in the central study area is that the isotherms show concentric-like shapes with values increasing from the suburbs towards the inner urban areas with the highest ΔT (>4 °C) in the densely built-up centre. Deviations from this concentric-like shape occur in the western, northern and northeastern parts where the isotherm of 2 °C stretches towards the outskirts. Furthermore, three island-like local maxima appear in the northern, northeastern and eastern parts of the study area with values over 3 °C, 2.5 °C and 2 °C, respectively. The largest area with very low ΔT values, due to the influence of the River Danube, can be found in the southeastern part of the study area (Unger et al. 2011a, 2011b). The applied method for the determination of the suspected spatial structure of the mean annual UHI intensity in Novi Sad is based on the study of Balázs et al. (2009). The main advantage of this regression method was to predict the spatial distribution of the annual mean UHI using just a few input parameters which can be determined in a simple way (remote sensing) without having detailed local information about the city. For the evaluation of the model estimation a comparison has been made using the datasets of the Rimski Šančevi (rural) and Petrovaradin (urban) stations (1956–1992). Since there were no night-time measurements, the daily minimum temperature data was used for the comparison. The differences (ΔT_{min}) of the measured daily minimum temperature were calculated for each day and the average of these differences can be considered as an approximate value of the annual mean UHI intensity. Finally, the ΔT value of Petrovaradin calculated by the statistical model is 1.66 °C and the measured (ΔT_{min}) is 1.8 °C. This insignificant difference proves that the accuracy of the model estimation meets the requirements of the aim of the study (Unger et al. 2011a).

The first intra-urban and inter-urban comparisons from Novi Sad (Serbia) and Szeged (Hungary), based on daily minimum and maximum temperature values were made by Lelovics et al. (2016). The research period was three summer months (June, July and August) in 2014, i.e. during two time periods with prevailing anticyclonic conditions with 72 (July 3 to 5) and 48 (July 19 to 20) hours in length, respectively. In Novi Sad, the temperatures were slightly higher, but the classes differ less compared to Szeged. The greatest temperature surpluses occurred in LCZ 2 and LCZ 6 (between 5–7 °C), while LCZ 5, LCZ 3 and LCZ 8 remained somewhat cooler. The cycles of LCZ A and LCZ D were similar. The temperature difference between the two types remained within the ±3 °C interval, with the largest values occurring around 0 UTC (Fig. 8). According to Fig. 9 for the most time, the UHI intensity remained positive with highest values at night, while negative values occurred predominantly during the day (urban cool island). The dividing line between these two periods was around

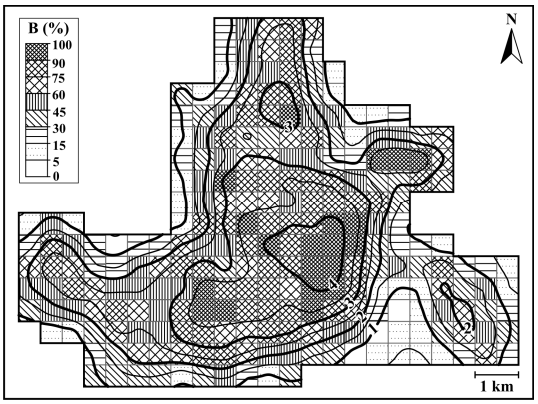

Fig. 7 Spatial distribution of the built-up ratio (B) and the modelled annual mean UHI intensity (°C) in the study area of Novi Sad (Unger et al. 2011a)

6 UTC and 12 UTC in both cities. The range of UHI intensity was between -1.48 °C and 5.22 °C in Szeged, and between -3.70 °C and 6.85 °C in Novi Sad. Urban cool islands occurred in both cities during the day. It was typically around -1 °C in Szeged and -2 °C in Novi Sad (Lelovics et al. 2016).

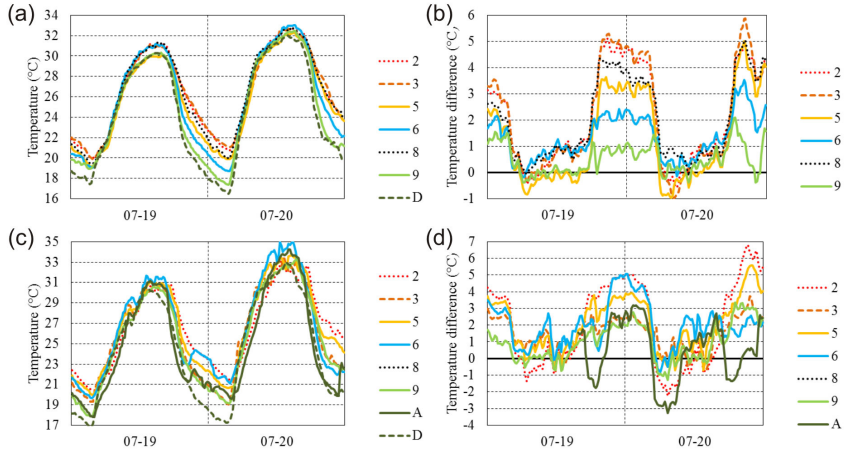

Fig. 8 Absolute and relative (difference from LCZ D) temperature variations at selected sites in Szeged (a, b) and Novi Sad (c, d) (3 to 5 July 2014) (Lelovics et al. 2016)

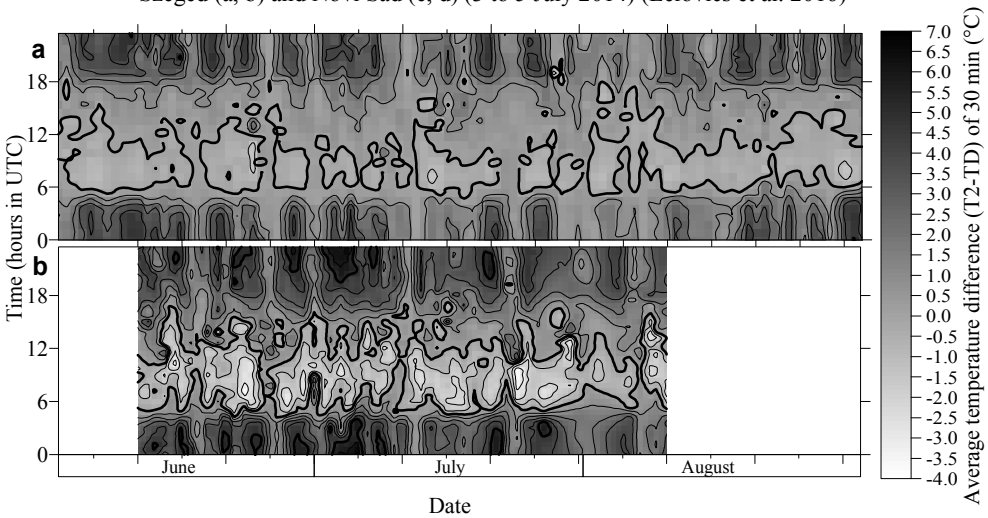

Fig. 9 Average temperature differences (°C) between LCZ 2 and LCZ D (a) in Szeged and (b) Novi Sad in summer 2014 (thin isotherms – integer °C, thick isotherms – 0 and 5 °C) (Lelovics et al. 2016)

4.2. Outdoor thermal comfort outcomes

People living in urban areas experience various kinds of thermal stress during the year. Extreme weather events, e.g. heat waves and cold spells, are especially stressful. With the usage of field measurements and models it is possible to quantify the outdoor thermal

conditions in urban areas. These are important input data for architects and urban planners in order to create comfortable urban areas for their residents (Milošević et al. 2015a).

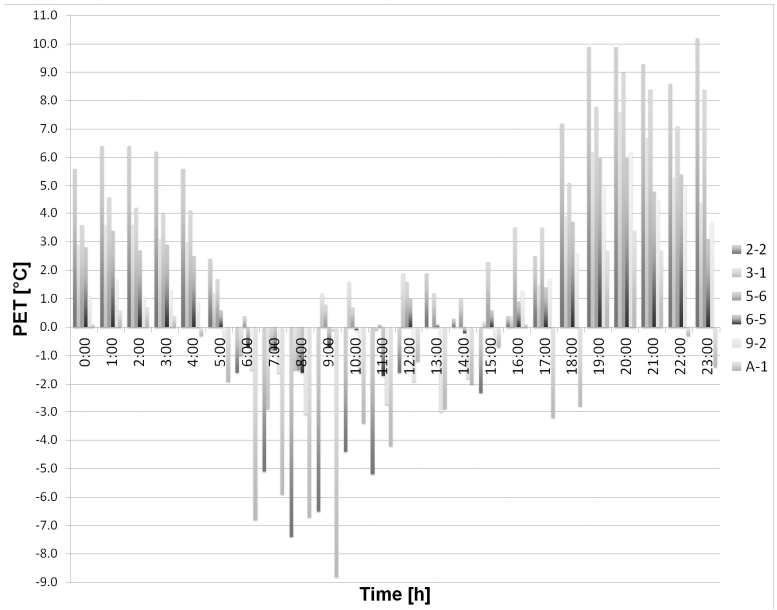

Fig. 10 Mean hourly PET differences between selected LCZs and LCZ D (ΔPET_{LCZx-D}) in Novi Sad during the tropical day (13th August 2014) (Milošević et al. 2015b)

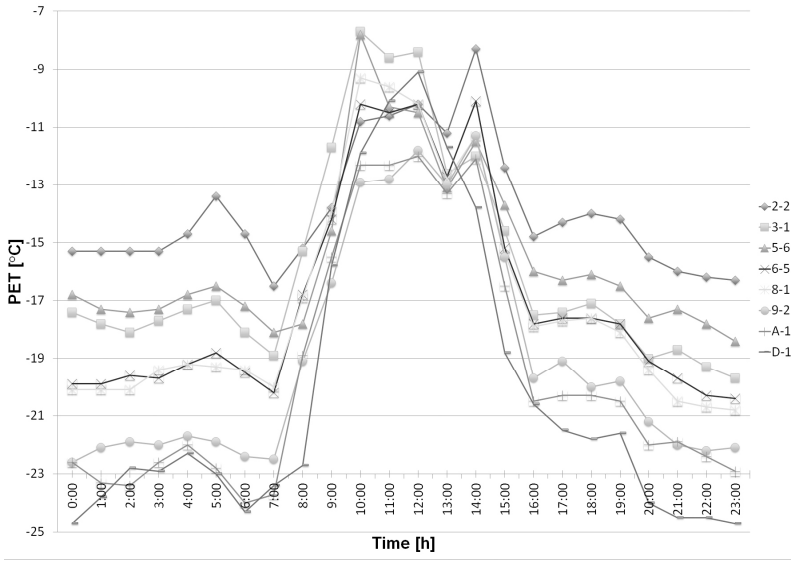

Fig. 11 Diurnal variation of human bioclimatic characteristics expressed via PET index in selected LCZs in Novi Sad on icy day (31st December 2014) (Milošević et al. 2015b)

The first analysis related with outdoor thermal comfort conditions in different LCZs of the Novi Sad and its surroundings was based on the calculated Physiologically Equivalent Temperature (PET) values for 13th August (the hottest day in 2014) and 31st December (the coldest day in 2014). Comparing hourly PET values in each selected LCZ with hourly PET values in LCZ D (low plants), all LCZs, in general, had higher PET values compared to LCZ D during late afternoon and nocturnal hours. Maximum PET difference was 10.2 °C between LCZ 2 and LCZ D at 23 UTC. This suggests that urban areas are substantially more uncomfortable during the night compared to the low plant (rural) areas in the vicinity of the city. In the early morning hours (7–8 UTC) all LCZs had smaller heat loads compared to LCZ D and this continued until the midday hours for all LCZs except LCZ 3 and LCZ 5. LCZ D had higher heat loads (up to 8.8 °C) during the majority of the day when compared with LCZ A (dense trees) (Fig. 10). On the coldest day, urban LCZs were warmer compared to the LCZ D during most of the day with smaller diurnal temperature ranges. Maximum PET difference (9.6 °C) occurred between LCZ 2 and LCZ D in the period 5–6 UTC. Only in the period 11–13 UTC did the majority of the urban LCZs have lower PET compared to the LCZ D (Fig. 11). Intra-urban analysis for an icy day showed that the smallest difference in average daily PET occurred between similar LCZs and the largest difference between urban and non-urban LCZs (Milošević et al. 2015a).

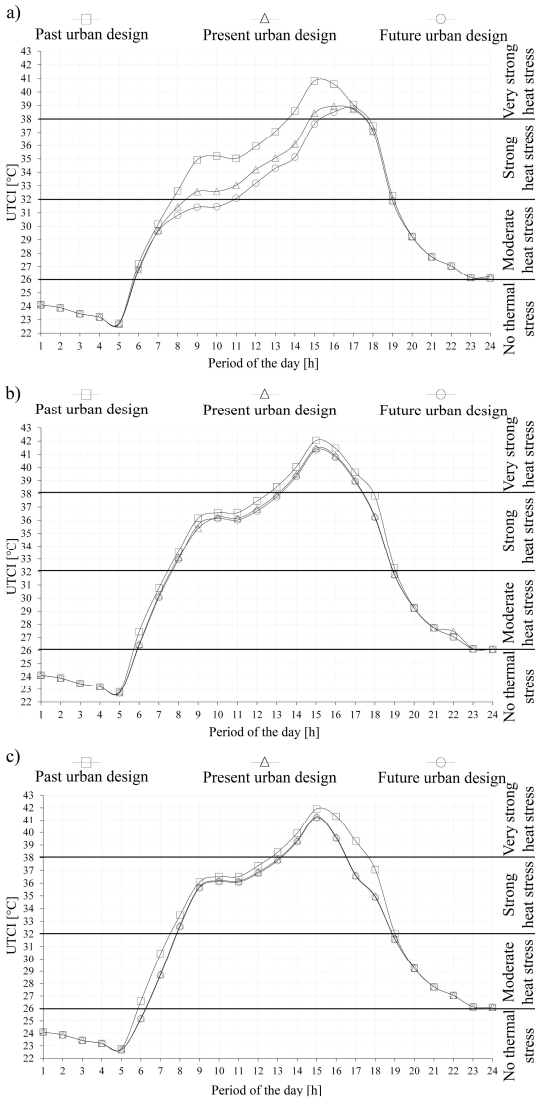

Fig. 12 The average UTCI values for 7th July 2014 at all predetermined body locations at: a) the northern footway, b) the middle of the street, and c) the southern footway (Bajšanski et al. 2015)

In order to quantify relative differences in diurnal thermal comfort conditions during heat wave period (from 5th to 8th July 2014), the average hourly PET in each selected LCZ was compared with average hourly PET values in LCZ D. Fig. 10 shows that all LCZs (except

LCZ A – dense trees) had higher PET values compared to LCZ D (low plants) from 17 UTC to 5 UTC. Maximum PET difference of 7.1 °C is noticed between LCZ 2 (compact midrise) and LCZ D (low plants) at 0 UTC. Contrary to this, LCZ D (low plants) had higher PET values compared to the majority of LCZs in the period 7–16 UTC with maximum difference of 8.5 °C compared to LCZ A (dense trees) at 9 UTC (Milošević et al. 2015b).

Built urban environment creates a climate that influences outdoor thermal comfort conditions and this is a well-established fact (Bajšanski et al. 2015). Therefore, during 2015 the first common research of urban climatologists and architects was carried out in order to create new possibilities for the evaluation and improvement of outdoor human thermal comfort in built urban environments using different software packages and parametric approach. Algorithms were developed and applied for the evaluation and improvement of non-stationary outdoor thermal comfort conditions and one street and one station from a compact midrise built-up area (LCZ 2) was used as database. The evaluation of thermal comfort in urban designs of linear street showed that periods with very strong heat stress have decreased on s hot summer day by up to 9.8% (Fig. 12). In contrast, the greatest thermal stress in winter (strong cold stress) increased by up to 3.5%. Universal Thermal Climate Index (UTCI) values decreased by up to 6.1 °C at 10 UTC when comparing past and future urban designs on hot summer day. On a cold winter day, the greatest UTCI decrease of 3.2 °C was observed at 11 UTC. Maximum UTCI changes were detected in shadowed body locations. The improvement of outdoor thermal comfort between future planned and proposed urban design of linear street is a consequence of up to 2.9 °C UTCI decrease on summer day and up to 1.7 °C UTCI increase on winter day. The UTCI decrease in non-linear streets between future planned and proposed urban designs was up to 3.9 °C on summer day and increase was up to 1.1 °C on winter day (Fig. 13). The developed automatic algorithms showed to be suitable for evaluating and improving the outdoor thermal comfort sensation in any built urban environment with appropriate weather data (Bajšanski et al. 2015, Savić et al. 2015).

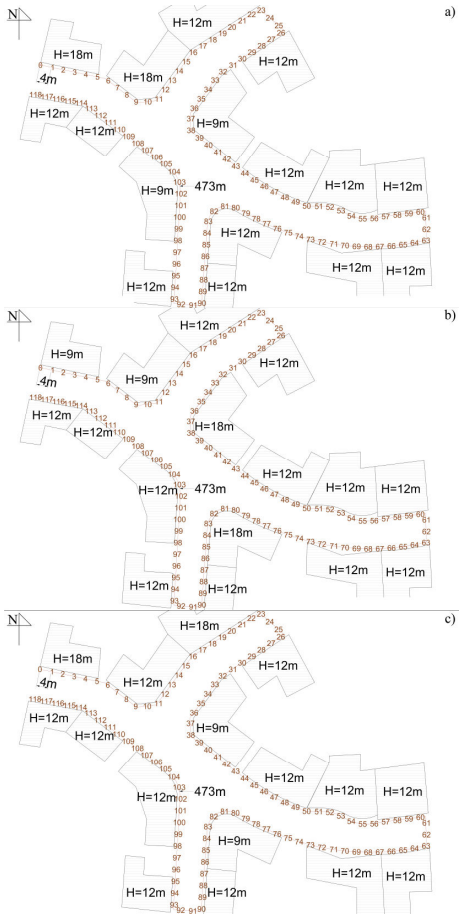

Fig. 13 The buildings heights arrangement of the non-linear streets: a) future planned urban design, b) proposed urban design in summer and c) proposed urban design in winter (Bajšanski et al. 2015)

5. AIR TEMPERATURE AND MORTALITY IN URBAN AREA

Strong evidence exists that seasonal variations of mortality are caused by different physiological parameters, e.g. haemostatic factors, blood pressure, as well as malnutrition (Stout and Craword 1991, Woodhouse et al. 1993). Several research articles suggested that these changes are consequences of the seasonal variation of temperature (Rose 1966, Kalkstein and Greene 1997). Strong relation between mortality and temperature was found during heat wave occurrences (Arsenović et al. 2014a). Therefore, in 2011 the urban climate research group from Novi Sad started with first analysis related with the seasonal variation of mortality caused by air temperature pattern in urban area. The first published papers (Đurđev et al. 2012, Arsenović et al. 2012) focused on air temperature and crude death rate (CDR) in the Belgrade urban area for the period 1988–2008.

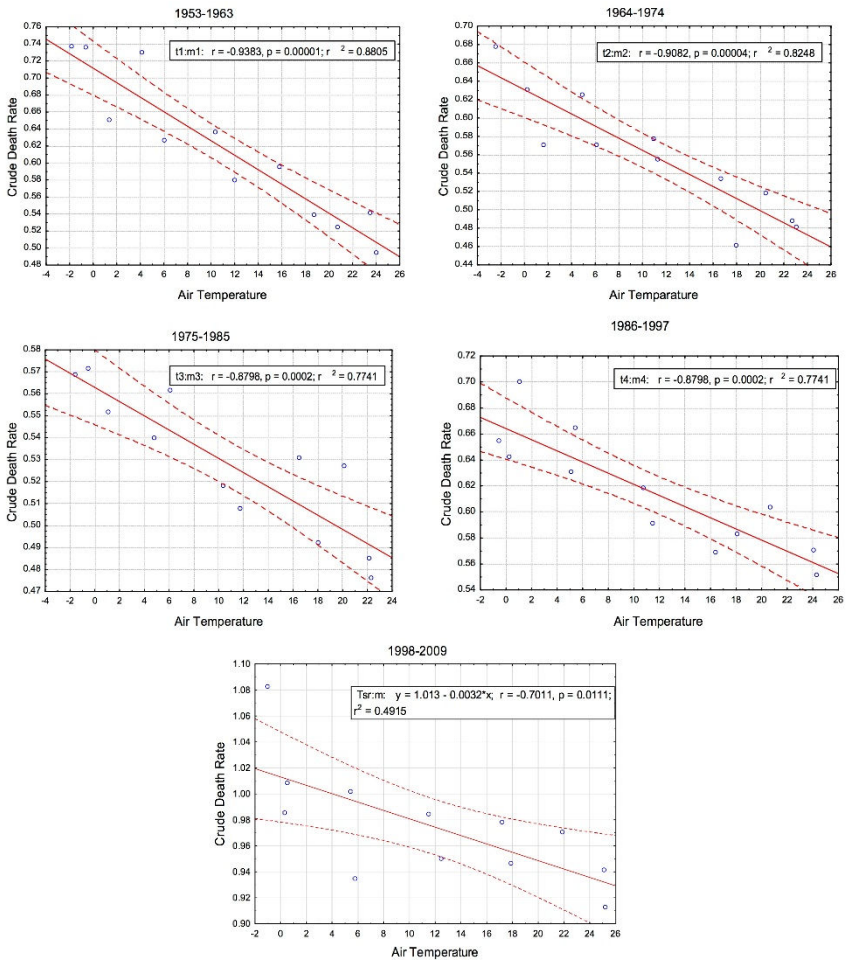

Fig. 14 Trends of crude death rate (CDR) in winter and non-winter periods (preceding and following period) (Arsenović et al. 2014a, Arsenović and Đurđev 2015)

The first results for Novi Sad are presented in the papers of Arsenović (2014) and Arsenović et al. (2014a, 2014b) and Arsenović and Đurđev (2015). Winter mortality in Novi Sad in the period from 1953/54 until 2008/09 was about 15% higher than in the preceding and following period and the results of regression analysis indicated that crude death rate and temperature are negatively associated; the decrease of average temperature is followed with an increase of crude death rate. During the last observed period, results show lower statistical significance in regression (Fig. 14). The results of Healy for the period 1988–1997 show that winter mortality in region EU 14 is about 16% higher than in non-winter period. The population in Novi Sad is more sensitive during the colder period of the year and the seasonal pattern of mortality has changed during the observed period. During the analysis it was noticed that in January, May, June, July and August, the average temperature has been increasing. Such trend of average temperature may alter balance between mortality in the winter and non-winter period. In regions with temperate climate, such as Novi Sad, even small changes of temperature could influence the seasonal fluctuations of mortality during year. Similar results for Belgrade also show that during the second half of the 20th century and the first decade of the 21st century, the population is less sensitive to cold periods (Đurđev et al. 2012).

6. CONCLUSIONS

According to the analysis of the reviewed papers in the last five years a substantial contribution has been made to urban climate research in Serbia, i.e. in the Novi Sad urban area, which is the second largest city in the country. In order to provide detailed research of morphologically heterogeneous urban environments it is necessary to implement multidisciplinary and interdisciplinary approaches.

Up to now the urban climate research group from Novi Sad was focused on LCZ classifications and development of urban climate network in order to analyze in fine detail UHI and outdoor human thermal comfort patterns in Novi Sad. Outcomes from these urban climate researches should play an important role in urbanization, demography and health issues. Therefore, this kind of common research can contribute to the understanding of weather and climate interactions and impacts in urban areas.

Further research will be focused on the improvements of the urban surface classifications. The members of the Novi Sad research group are a part of the WUDAPT (World Urban Database and Access Portal Tools) group (http://www.wudapt.org). The main activities through the WUDAPT group are to create LCZ maps of important cities in South-East Europe using a new approach of LCZ mapping. Outdoor human thermal comfort is connected with the quality of life in urban areas, urbanization and mortality of the population. Therefore, spreading activities related with these issues is an important task. Our urban climate research group joined the Working Group on Protocols for the Assessment and Reporting of Outdoor Thermal Comfort that is initiated by Professor Rohinton Emmanuel.

Today, increased energy consumption is a huge problem in urban areas, mostly during the extreme temperature events (heat and cold waves). Research from Savić et al. (2014c) showed that extreme air temperature spells impact electrical energy consumption, not only in large-sized cities, but also in small-sized too. Therefore, correlation of air temperature and energy consumption in the Novi Sad urban area will be one of the research goals in further years.

Urban climate survey can provide detailed spatial and temporal data and outcomes of temperature and thermal comfort patterns in order to help local authorities in urban planning strategies and to counterattack the adverse effect of urban climate and climate change.

Acknowledgement: This research has been funded by the Ministry of Education, Science and Technological Development of the Republic of Serbia through Project No. 176020.

REFERENCES

Arsenović D, Đurđev B, Savić S (2012) The time course of temperature related mortality. Međunarodni naučni skup – Problemi i izazovi savremene geografske nauke i nastave, Univerzitet u Beogradu-Geografski fakultet, Beograd, 281-286

Arsenović D (2014) Impact of air temperature on seasonal variation of human mortality in Novi Sad. PhD dissertation. University of Novi Sad, Faculty of Sciences, Novi Sad http://www.cris.uns.ac.rs/record.jsf?recordId=85691&source=DARTEurope&language=en

Arsenović D, Đurđev B, Savić S (2014a) Seasonal variation of mortality in Novi Sad (Serbia): a role of air temperature. In: Proc European Population Conf 2014, Budapest, Hungary, 7

Arsenović D, Dolinaj D, Stankov U (2014b) Changing excess mortality during summer months: evidence for urban population in Novi Sad. in: Proc IGU Regional Conf – Changes, Challenges, Responsibility, Krakow, Poland

Arsenović D, Đurđev B (2015) Changes in seasonal pattern of mortality and its relation with temperature: result for urban area of Novi Sad. In: Proc Fifth EUGEO Congress on the Geography of Europe, Budapest

Bajšanski I, Milošević D, Savić S (2015) Evaluation and improvement of outdoor thermal comfort in urban areas on extreme temperature days: Applications of automatic algorithms. Build Environ 94:632-643

Balázs B, Unger J, Gál T, Sümeghy Z, Geiger J, Szegedi S (2009) Simulation of the mean urban heat island using 2D surface parameters: empirical modelling, verification and extension. Meteorol Appl 16:275-287

Basarin B, Lukić T, Matzarakis A (2016) Quantification and assessment of heat and cold waves in Novi Sad, Northern Serbia. Int J Biometeorol 60:139-150

Đurđev SB, Arsenović D, Savić S (2012) Temperature-related mortality in Belgrade in the period 1888-2008. Acta Geogr Slov 52: 385-401

Gál T, Unger J (2009) Detection of ventilation paths using high-resolution roughness parameter mapping in a large urban area. Build Environ 44:198-206

Grimmond CSB, Roth M, Oke TR, Au YC, Best M, Betts RCG, Cleugh H, Dabbert W, Emmanuel R, Freitas E, Fortuniak K, Hanna S, Klein P, Kalkstein LS, Lui CH, Nickson A, Pearlmutter D, Sailor D, Voogt J (2010) Climate and more sustainable cities: climate information for improved planning and management of cities (producers/capabilities perspective). Procedia Environ Sci 1:247-274

IPCC (2012) Managing the Risk of Extreme Events and Disasters to Advance Climate Change Adaptation. A Special Report of Working Groups I and II of the IPCC. Cambridge University Press, Cambridge, New York

Jovanović D, Govedarica M, Sabo F, Sladić D, Ristić A (2015) Spatial analysis of high-resolution urban thermal patterns in Vojvodina, Serbia. Geocarto Int 30:483-505

Lelovics E, Unger J, Gál T, Gál CV (2014) Design of an urban monitoring network based on Local Climate Zone mapping and temperature pattern modelling. Clim Res 60:51-62

Lelovics E, Unger J, Savić S, Gál T, Milošević D, Gulyás Á, Marković V, Arsenović D, Gál CV (2016) Intra-urban temperature observations in two Central European cities: a summer study. Idojaras (accepted)

Kalkstein SL, Greene JS (1997) An evaluation of climate/mortality relationships in large U.S. Cities and possible impacts of a climate change. Environ Health Persp 105:84-93

Marković V, Savić S, Arsenović D, Stankov U, Dolinaj D (2013) Quantification of artificial surfaces impact on urban heat island of Novi Sad (Vojvodina, Serbia). Geogr Pannon 17:69-73

Marković V, Stankov U, Savić S, Klaučo M, Pavlović M (2014a) A GIS analysis of artificial surfaces impact on urban heat islands of Novi Sad, Serbia. In: Proc 5th Jubilee Int Conf on Cartography and GIS, Riviera, Bulgaria

Marković V, Savić S, Milošević D, Arsenović D, Stankov U (2014b) A GIS analysis of Local Climate Zones and human thermal condition patterns in Novi Sad: Preliminary results. In: Proc The Third Romanian-

Bulgarian-Hungarian-Serbian Conf 'Geographical Research and Cross-border Cooperation within the Lower Basin of the Danube', Veliko Gradište, Serbia
Marković V (2015) Heat wave risk mapping in Novi Sad (Serbia). In: Proc Fifth EUGEO Congress on the Geography of Europe, Budapest, Hungary
Milošević D, Savić S, Unger J, Gál T (2015a) Urban climate monitoring system suitability for intra-urban thermal comfort observations in Novi Sad (Serbia) – with 2014 examples. In: Proc 9th Int Conf on Urban Climate and 12th Symp on Urban Environ, Toulouse, France
Milošević D, Unger J, Gál T (2015b) Thermal comfort observations in the City of Novi Sad (Serbia) in 2014. In: Proc Fifth EUGEO Congress on the Geography of Europe, Budapest, Hungary
Milošević D, Savić S, Marković V, Šećerov I (2015c) Temperature characteristics of Novi Sad during extreme temperature days. In: Proc 4 Srpski kongres geografa, Kopaonik, Serbia
Muller CL, Champan L, Grimmond CSB, Young DT, Cai X (2013) Sensors and the city: a review of urban meteorological networks. Int J Climatol 33:1585-1600
Oke TR (2004) Initial Guidance to Obtain Representative meteorological Observations at Urban Sites. IOM Report 81, WMO/TD no. 1250, Geneva
Petralli M, Morabito M, Cecchi L, Crisci A, Orlandini S (2012) Urban morbidity in summer: ambulance dispatch data, periodicity and weather. Cent Eur J Med 7:775-782
Pongrácz R, Bartholy J, Bartha EB (2013) Analysis of projected changes in the occurence of heat waves in Hungary. Adv Geosci 35:115-122
Popov Z (1995) The proposal for setting station network to monitor urban climate of in Novi Sad. Republic Hydrometeorological Service, Belgrade
Popov Z, Savić S (2010) The urban climate of Novi Sad. In: Proc Drugi Kongres geografa Srbije, Srpsko geografsko društvo-Departman za geografiju, turizam i hotelijerstvo, Novi Sad, Serbia
Rose G (1966) Cold weather and ischaemic heart disease. Brit J Prev Soc Med 20:97-100
Savić S, Mitrović M, Lazić L (2012a) Analiza novosadskog urbanog ostrva toplote. [Analysis of urban heat island in Novi Sad (in serbian)] Zbornik radova, Univerzitet u Novom Sadu, PMF, Departman za geografiju, turizam i hotelijerstvo, 41:18-28
Savić S, Unger J, Gál T, Milošević D, Popov Z (2012b) Urban heat island research of Novi Sad (Serbia): A review. In: Proc Geographical Research and Cross-border Cooperation within the Lower Basin of the Danube, Eger, Hungary
Savić S, Milošević D, Arsenović D, Marković V (2013a) Evaluation and public display of urban patterns of human thermal conditions (URBAN-PATH). In: Proc Int Symp – Geography for Sustainable Development; West University of Timisoara, Faculty of Chemistry, Biology and Geography; Timisoara, Romania
Savić S, Milošević D, Lazić L, Marković V, Arsenović D, Pavić D (2013b) Classifying urban meteorological stations sites by 'Local Climate Zones': preliminary results for the City of Novi Sad (Serbia). Geogr Pannon 17:60-68
Savić S, Unger J, Gál T, Milošević D, Popov Z (2013c) Urban heat island research of Novi Sad (Serbia): A review. Geogr Pannon 17:32-36
Savić S, Unger J, Milošević D, Lelovics E, Gál T (2014a) Mapping of Local Climate Zones in two neighbouring Central-European city located in similar geographical environments. In: Proc IGU regional conference – Changes, Challenges, Responsibility, Kraków, Poland
Savić S, Milošević D, Marković V, Arsenović D (2014b) Urban heat island and human thermal comfort monitoring system in Novi Sad (URBAN-PATH project). In: Proc The Third Romanian-Bulgarian-Hungarian-Serbian Conf 'Geographical Research and Cross-border Cooperation within the Lower Basin of the Danube', Veliko Gradište, Serbia
Savić S, Selakov A, Milošević D (2014c) Cold and warm air temperature spells during the winter and summer seasons and their impact on energy consumption in urban areas. Nat Hazards 73:373-387
Savić S, Unger J (2014) Evaluation and public display of urban patterns of human thermal conditions (URBAN-PATH project). Urb Clim News 51:12-18
Savić S (2015) Urban climate monitoring network in Novi Sad (Serbia). In: Proc Fifth EUGEO Congress on the Geography of Europe, Budapest, Hungary
Savić S, Bajšanski I, Milošević D (2015) Evaluation of outdoor thermal comfort in urban transformations of Novi Sad (Serbia). In: Proc Fifth EUGEO Congress on the Geography of Europe, Budapest, Hungary
Skarbit N, Unger J, Gál T, Savić S (2015) Intra-urban climate observations in two Central European cities based on one year network datasets. In: Proc Fifth EUGEO Congress on the Geography of Europe, Budapest, Hungary
Stankov U, Savić S, Marković V, Pašić M, Dolinaj D, Arsenović D (2013) Spatial distribution of tourism resources in urban heat island of Novi Sad. In: Proc The Int Conf – Contemporary Trends in Tourism and Hospitality, Novi Sad, Serbia

Stankov U, Marković V, Savić S, Dolinaj D, Pašić M, Arsenović D (2014) Tourism resources in urban heat island: A GIS analysis of Novi Sad, Serbia. In: Proc 5th Jubilee Int Conf on Cartography and GIS, Riviera, Bulgaria

Stewart ID, Oke TR (2010) Thermal differentiation of Local Climate Zones using temperature observations from urban and rural field sites. In: Proc Ninth Symp on Urban Environment, Keystone, Colorado

Stewart ID, Oke TR (2012) Local Climate Zones for urban temperature studies. Bull Am Meteorol Soc 93:1879-1900

Stout RW, Crawford V (1991) Seasonal variation in fibrinogen concentrations among elderly people. Lancet 339:9-13

Šećerov I, Savić S, Milošević D (2015a) Urban climate research based on an automated monitoring network sensors in Novi Sad (Serbia). In: Proc 4 Srpski kongres geografa, Kopaonik, Serbia

Šećerov I, Savić S, Milošević D, Marković V, Bajšanski I (2015b) Development of an automated urban climate monitoring system in Novi Sad (Serbia). Geogr Pannon 19:174-183

Tomlinson CJ, Chapman L, Thornes JE, Baker CJ (2011) Including the urban heat island in spatial heat health risk assessment strategies: a case study for Birmingham, UK. Int J Health Geogr 10:1-14

UN (2009) World urbanization prospects. The 2007 Revision Population Database. Available at http://esa.un.org/unup

Unger J, Savić S, Gál T (2011a) Modelling of the annual mean urban heat island pattern for planning of representative urban climate station network. Adv Meteorol 2011, ID 398613

Unger J, Savić S, Gál T (2011b) Method for representative siting of urban climate station network – Novi Sad (Serbia) as an example. In: Proc Climate and Constructions, Int Conf, Karlsruhe, Germany

Unger J, Savić S, Gál T, Milošević D (2014) Urban climate and monitoring network system in Central European cities. University of Novi Sad, University of Szeged, Novi Sad, Szeged

Unger J, Savić S, Gál T, Milošević D, Marković V, Gulyás Á, Arsenović D (2015a) Urban climate monitoring networks based on LCZ concept. In: Proc 9th Int Conf on Urban Climate and 12th Symp on Urban Environ, Toulouse, France

Unger J, Gál T, Csépe Z, Lelovics E, Gulyás Á (2015b) Development, data processing and preliminary results of an urban human comfort monitoring and information system. Időjárás 119:337-354

WMO (2006) Initial Guidance to Obtain Representative Meteorological Observations at Urban Sites. Instruments and Observing Methods Report No. 81, WMO/TD-No. 1250, Geneva

Woodhouse PR, Khaw KT, Plummer M (1993) Seasonal variation of blood pressure and its relationship to ambient temperature in an elderly population. J Hypertens 11:1267-1274

ACTA CLIMATOLOGICA ET CHOROLOGICA
Universitatis Szegediensis, Tomus 49-50, 2016, 81-90

CARBON SEQUESTRATION MODELING IN A TEMPERATE NEAR-NATURAL BEECH FOREST USING CO2FIX

E TANÁCS, T KRIZSÁN and M KISS

Department of Climatology and Landscape Ecology, University of Szeged, P.O.Box 653, 6701 Szeged, Hungary
E-mail: nadragulya@geo.u-szeged.hu

Summary: As climate change becomes a more and more pressing issue, the role of forests as carbon sinks will increase further. Carbon sequestration models can be a useful tool in planning future management strategies, but only if they are properly calibrated for the ecosystem in question. In our study we used data from the literature and other publicly available data for the parameterisation of the CO2Fix model and compared the model results to reference estimations based on data from a field survey carried out in autumn 2015 in some beech and hornbeam-dominated stands of Haragistya-Lófej forest reserve (Aggtelek Karst). Due to the less favourable site conditions, effects of earlier management and the relatively young age of the stands the carbon content of the biomass was found to be somewhat lower than in other beech forests. We also examined the effect of using different mortality settings on the results. The model with 'no mortality' settings was found to give the best results, however the performance was species-dependent. The model tends to underestimate the carbon content of the biomass for beech-dominated plots, but the higher the proportion of hornbeam, the higher the chance that the model overestimates the carbon content.

Key words: carbon sequestration, CO2Fix, near-natural forest, forest reserve, Fagus sylvatica

1. INTRODUCTION

Climate change, as one of the most important contemporary environmental issues, draws attention to the global climate regulation ecosystem service of the natural vegetation, in which forests play an outstanding role. In the process of photosynthesis carbon dioxide is fixed in different compartments of living biomass (stems, branches, foliage and roots) and in the soil. After timber harvesting and industrial processing, the carbon content of wood may be stored further in wood products with different life spans. In the end, it returns to the atmosphere as a result of turnover or logging. Earlier it was generally thought that ageing forests should be at best considered carbon-neutral (Odum 1969). This was based (among others) on the assumption that the growth trends of individual trees and even-aged monospecific stands can be directly extended to natural forests. However, it was found that growth and carbon acquisition in old natural forests cannot be extrapolated from the productivity of even-aged stands (Carey et al. 2001, Harmon 2001). Recently, research on the effects of forest management intensity has shown that forest management and disturbances affect forest soils and biomass carbon stocks and emissions to the atmosphere (Luyssaert et al. 2011). Harvesting frequency and structural retention significantly affect mean carbon storage, and the mean carbon sequestration is significantly greater for non-managed stands compared to any of the active management scenarios (Nunery and Keeton

2010). Of the harvest treatments, those favouring high levels of structural retention and decreased harvesting frequency have been shown to store the greatest amounts of carbon (Neilson et al. 2006; Taylor et al. 2008; Nunery and Keeton 2010). Greater harvest intensity results in less carbon storage, and the carbon in wood products does not make up for harvest losses (Nunery and Keeton 2010, Fischer 2013). Carbon sequestration models, particularly those including a wider context (e.g. wood products, avoided emission, carbon accounting schemes) provide an opportunity for decision-makers to consider the effects of a management decision on the ecosystem services of a forest in a more complex manner. However in order to be used that way, the models must be sound concerning the function and the natural carbon fluxes of the particular ecosystem in question. Empirical data needed for model calibration are generally scarce and poorly representative across forest biomes (Keith et al. 2010) therefore some of the complexity needs to be traded for more general usability. However, too much simplification may lead to the underestimation of the carbon sequestration capacity of near-natural forests, which in turn could lead to erroneous management decisions.

One aim of the present study is to test the performance of the biomass module of the relatively simple, widely used CO2Fix model (Masera et al. 2003) against stand-level empirical data from a forest reserve (unmanaged for the last 20 years) using the literature and widely accessible data for model parameterisation. When using CO2Fix in a previous study we found that mortality rates (not including management mortality) strongly affected the model results (Kiss et al. 2011). It is known that mortality rates in a stand are not constant over time, they are highly stochastic and the most probable cause of death differs according to the size and role of a tree (Holzwarth et al. 2013, Tanács and Barta 2014). Mortality is often higher in young stands, followed by a phase of relatively lower rates and then it increases again in old age (e.g. Holzwarth et al. 2013). Major disturbances (due e.g. to climate events like a major thunderstorm or a lasting heat wave) can locally additionally modify the mortality rate. We used three different approaches in order to find out how best to include mortality in the model.

2. MATERIALS AND METHODS

2.1. Study area

Haragistya-Lófej Forest Reserve is situated in the north-western corner of Aggtelek National Park, NE Hungary. Except for a part of its buffer zone in the south, the area is under strict protection. Haragistya is a continuation of Silická planina, and it bears all the hallmarks of a typical karst plateau. Its surface is dry and highly varied, covered by series of dolines and dry valleys. The 90 ha sample area is situated in the south-eastern part of the plateau. Wetterstein Limestone and Dolomite make up the bedrock, dolomite being more typical within the selected study area. However, in the bottom of hollows such as dolines, valleys and slope curves, Cretaceous red clay sediments have accumulated, and in certain places serve as a basis for soil formation. The tops and ridges are characterised by extremely shallow black rendzinas, and the slopes by slightly deeper brown rendzinas. On the red clayey patches red rendzinas and deeper brown forest soils developed.

The zonal forest types of the karst plateaus of the Aggtelek Mts. are xerotherm sessile oak forests (*Quercetum petraeae-cerris*, but mainly without the turkey oak), which occupy the lower hilltops, ridges and southern-facing slopes, while mesophilous sessile oak-

hornbeam forests (*Carici pilosae-Carpinetum*) are the characteristic association of the high plateaus and northern-facing slopes. Submontane beech forests (*Melitto-Fagetum*) can be found in small patches, mainly in valleys and on north-facing slopes. According to the forest inventory, the age of the forests in the sample area varies between 60 and 110 years. Management activity in the last decades mostly consisted of thinning; however some of the area has not been actively managed for at least 40 years. Recruitment and early regeneration dynamics are currently strongly affected by the high number of browsing game.

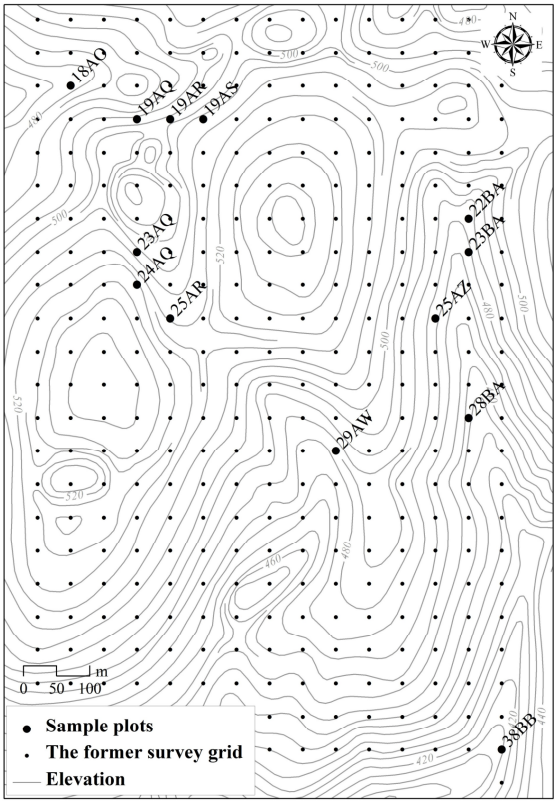

Fig. 1 The study area

For the purposes of long-term structure monitoring in the forest reserve, a 50 m resolution grid of 361 permanent plots was established in 2006, each consisting of a 10 m radius circle (Fig. 1). The plots were divided in 3 age groups (61–80, 81–100 and 101–120 yrs) based on the inventory data and 3 broad forest types (dry oak, mezophilous oak and beech stands).

2.2. Data

In the course of the baseline survey in 2006–2007 we recorded the position, diameter at breast height (dbh) species and crown class (according to the Kraft-classification) of every living tree and snag exceeding a dbh of 5 cm or a height of 5 m within the 10 m-radius circle plots. Tree heights were measured for a few hundred individuals (Zboray et al. 2007). The survey was partly repeated in autumn 2015, in 53 of the original plots. For the present study we used the data of 13 sample plots from beech stands, representing each of the 3 age groups (Fig. 1, Table 1). The chosen stands are mainly dominated by beech or hornbeam, accompanied mainly by *Sorbus torminalis* and downy oak (*Quercus petraea*). We chose plots where signs of earlier thinning (e.g. tree stumps) were not evident.

For both model parameterisation and as reference we used some results and equations from the baseline survey of 2006–2007, data from the repeated survey, and also from the literature. Wood density data came from the Chave et al. (2009). For the estimation of the species-specific C-content of dry matter in the different biomass compartments and the

proportion of C stored in the roots and the foliage compared to the stem and the branches we used the results of Führer and Jagodics (2009) who carried out specific measurements in beech stands in Hungary.

Table 1 Stand characteristics of the examined plots

Plot ID	Age (y)	No. of trees (2015) in the plot	Proportion			Yield class		
			Fagus s.	*Carpinus b.*	other	*Fagus s.*	*Carpinus b.*	other
19AS	105	19	0.26	0.53	0.21	5	4	4
23AQ	105	17	0.41	0.24	0.35	2	5	5
24AQ	105	13	0.77	0.08	0.15	4	5	4
25AR	105	13	0.38	0.46	0.15	6	5	5
18AO	100	18	0.39	0.28	0.33	5	5	5
19AQ	100	19	0.53	0.16	0.32	5	5	5
19AR	100	18	0.39	0.61	0.00	4	4	5
28BA	100	14	0.29	0.71	0.00	5	4	5
22BA	75	12	0.67	0.00	0.33	4	5	4
23BA	75	17	0.76	0.18	0.06	5	5	5
25AZ	70	18	0.83	0.11	0.06	4	5	5
29AW	70	18	0.39	0.28	0.33	6	5	5
38BB	75	14	0.43	0.29	0.29	5	4	5

Estimations serving as reference data for the C-content of the tree stem and branches were calculated using tree volume, density and species-specific C-content. In order to calculate the volume of each individual tree, Király's tree volume equation was applied (see Veperdi 2008). Tree height, which is a necessary input to this equation, was estimated on the basis of species-specific diameter-height equations set up using data from the first survey of 2006 (Tanács 2011). The C-content of the roots and foliage were then estimated on the basis of their above-mentioned proportions. The results were up-scaled to a 1-ha area for each plot.

2.3. Carbon sequestration modeling

2.3.1.Brief description of the CO2Fix model

CO2Fix (v. 3.2) is a simulation model developed as part of the CASFOR II project. It quantifies the carbon stocks and fluxes in the forest biomass, the soil organic matter and the wood products chain (Masera et al. 2003; Schelhaas et al. 2004). These are estimated with a time-step of one year using the 'cohort' as a unit, where each cohort is defined as a group of individual trees assumed to exhibit similar growth. The model consists of six modules: biomass, soil, wood products, bioenergy, financial and carbon accounting. The total carbon content of the system is obtained by adding up the amount of live biomass and soil carbon content and the carbon stored in wood products. The overall effect on the climate system depends on the changes of the carbon content and the so-called avoided emission. Avoided emission characterizes how much less carbon dioxide is released into the atmosphere through substituting fossil fuels with biomass; it is also calculated by the bioenergy module. Since the present analysis aims to find the appropriate parameterisation for the biomass module, which is the basis of the model calculations, only the biomass module was used. It uses the following equation to calculate carbon content:

$$Cb_{it+1} = Cb_{it} + Kc\,[Gb_{it} - Ms_{it} - T_{it} - H_{it} - Ml_{it}] \quad (\text{tC ha}^{-1}) \qquad (1)$$

where
- Cb_{it}: C-content of the living biomass of cohort 'i' at time 't'
- Kc: constant to convert biomass to carbon content (MgC per Mg biomass dry weight).
- Gb_{it}: biomass growth
- Ms_{it}: tree mortality due to senescence
- T_{it}: turnover of branches, foliage and roots
- H_{it}: amount of harvest
- Ml_{it}: mortality due to logging

2.3.2.Model parameterisation

The model calculates the biomass increment using the following equation:

$$Gb_{it} = (Kv_i \; Ys_{it} \; (1 + \Sigma \; (F_{ijt}))) \cdot Mg_{it} \qquad (\text{Mg ha}^{-1} \text{ yr}^{-1}), \tag{2}$$

where:
- Kv_i: basic wood density (Mg dry biomass per m^3 of fresh stemwood volume) for each cohort 'i'
- Ys_{it}: is the volume yield of stem wood for each cohort 'i' (m^3 ha^{-1} yr^{-1}),
- F_{ijt}: is the biomass allocation coefficient of each living biomass component 'j' (foliage, branches, and roots) relative to stems, for each cohort 'i' at time 't' (Mg per Mg stemwood), and
- Mg_{it}: is the growth modifier due to interactions among and within cohorts (dimensionless).

Wood density data came from the Wood Density Database (Chave et al. 2009). The annual yield of stem wood was derived from the national yield tables (Sopp 1974, Béki 1986, Mendlik 1986, Béki 1987). These are available for the commercially significant tree species of Hungary. Yield classes were determined according to the maximum height for each species at the plot and checked against the increment between 2006 and 2015. Since the eroded karstic soils do not provide a favourable environment for growth, we generally worked with the tables for classes 4 or 5 (in a few cases 3 or 6). In order to calculate the relative growth of the other biomass compartments (roots and foliage) we used data from Führer and Jagodics (2009). They measured the amount of C-content/ha in the different compartments of a beech stand and we used the proportions as a constant value for relative growth. For the relative growth of branches, we used the small branches' proportions tables available along with the yield tables. Percentages for each species and age group were given based on the typical dimensions (dbh and height) of the appropriate yield class. Each species for each yield class was handled in a separate model and the results were added up for each plot after being weighted according to the species composition. Therefore interactions between the cohorts were not (directly) included in the model (correction number was left at the default: 1). For rare species without yield information we used the parameters of the most similar commercial species, mainly pedunculate oak.

Turnover rates were defined on the basis of the paper of Wutzler and Mund (2007). As the products module was not used, the amount of harvest and mortality due to logging were not considered – the status of the area ('forest reserve') means that active management is limited to its buffer zone.

As described in the introduction, the mortality rate parameter was earlier found to be a critical point of the parameterisation. In order to find the best approach, we ran the model

with 3 different mortality settings. In the first case ('no mortality') we set the mortality rates to 0 as is the model default. In the second case ('yield table mortality') we used the volume of trees proposed for removal in the yield tables, supposing that since thinning aims to optimize growth, the volume of wood proposed for removal would be similar to that lost to mortality in a natural forest. This means relatively high, although continuously decreasing rates. In the third case (3) we used the species-specific mortality statistics calculated from our own dataset for the examined beech stands for the period between 2006 and 2015. In this case for stands younger than 50 years, mortality rates were set to 0.

3. RESULTS AND DISCUSSION

3.1 Model results

When estimating the actual carbon content of the stands based on the survey data, we got on average 188 t ha^{-1} for the 100–105-year-old stands and 148 t ha^{-1} for the 70–75 year-old ones (Fig. 2). Of the 13 plots examined, 18AO had to be omitted; shortly after the baseline survey, a gap formed in the vicinity of the plot, where most of the trees (representing 87% of the volume in 2006) died by the autumn of 2015; thereore the amount of carbon stored in the remaining living biomass is much lower at this plot than at others around it. Although the C content of living biomass at the plot increases with stand age, other factors (e.g. species composition and local mortality) also influence its value.

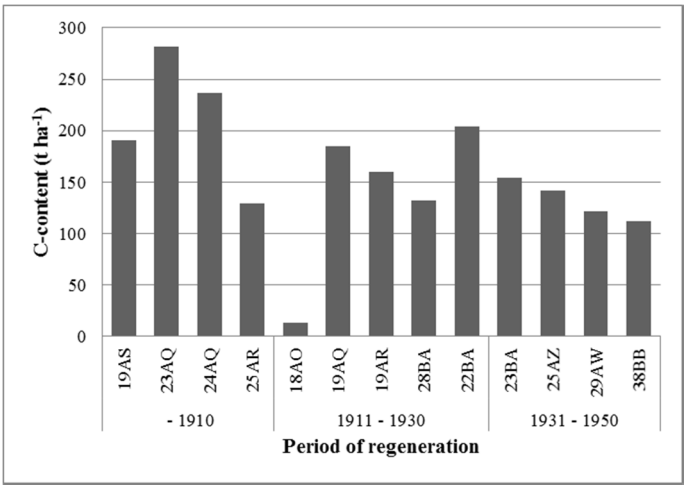

Fig. 2 C-content of the biomass (t ha^{-1}) at the plots estimated using survey data from 2015. Dates show the time of the last stand regeneration based on forest inventory data

Since most of the stands in the reserve have been subject to management in the past, their natural development has only recently begun and their structure retains traces of earlier human impact (Tanács et al. 2007). Therefore the amount of biomass (and carbon) stored in the stands was expected to be between those of managed stands and naturally developed forests. Führer and Jagodics (2009) carried out detailed measurements in a managed beech forest at a high-quality site and as a result found the C-content of the living biomass to be

292 t ha^{-1}. Juhász et al. (2008) measured and estimated the C-content of an old-growth natural beech forest (Kékes-Észak forest reserve) and got 231 t ha^{-1} as a result. Our results are typically lower than both, however the stands in our survey are younger and the site is less favourable. 2 of our plots (23AQ and 24AQ) show values that are similar to the above-mentioned results, these are situated in a rather remote part of the study area, where stands with the most natural structure can be found (Tanács 2011).

Fig. 3 shows the model results together with the reference values. All those calculations where mortality is included tend to underestimate the carbon content, except in the case of plot 18AO, where locally mortality was extremely high in recent years and regrowth has not occurred yet. Calculations without including mortality seem to give the best estimations for the carbon content of the biomass. The reason for this could be that the loss of a dominant tree also means modified light conditions resulting in the accelerated growth of the surviving individuals around it. Whereas it is possible to include mortality in the model, it is not possible to directly include the effect of the resulting increased growth. The average difference between the model results and the reference values is -8.38 t ha^{-1} (25.8 t ha^{-1} if the absolute values are averaged), which means an average -2.69% of the reference values (15.44% for the absolute values).

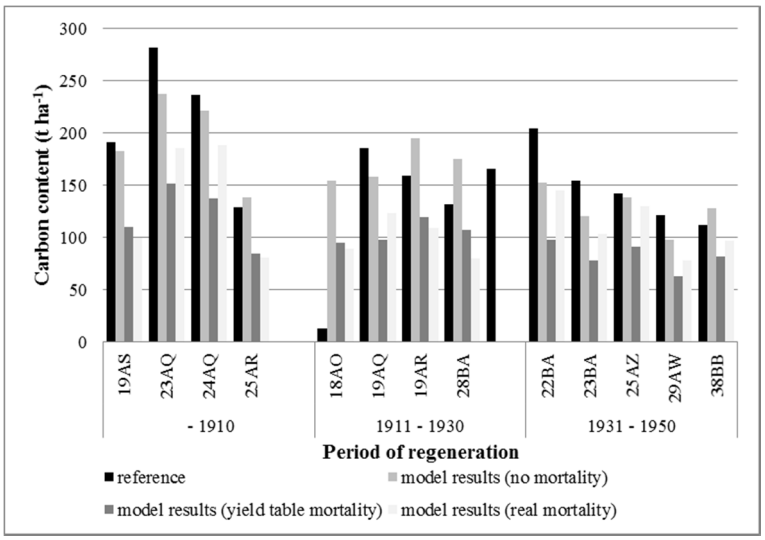

Fig. 3 The carbon content of the biomass (t ha^{-1}) at the plots using different mortality settings in the model

As the averages show, the no-mortality model results are in most cases also lower than the reference values (see also Fig. 4). One reason for the underestimation could be that the yield tables applied were created on the basis of national-level data; no matter how carefully the yield class is chosen, in most locations the actual growth rates are different. This is especially true in the extremely diverse karstic environment where growing conditions may significantly change within very short distances (Tanács 2011). Also, the yield tables contain data for monospecific stands whereas interactions between species could result in increased growth rates (such an effect was demonstrated in another Hungarian forest reserve for beech by Veperdi (2010)).

In some cases the model with the 'no-mortality' setting overestimates the carbon content of the biomass, usually for those plots where the proportion of hornbeam is high (Fig. 4).

Since in these forests hornbeam generally forms a second crown layer, overshadowed by the bigger beech trees, its growth is considerably slower than it would be in a monospecific stand such as those represented by the yield table. Mortality is higher among the suppressed individuals (Tanács and Barta 2014) but the disappearance of a small tree from the second crown layer probably does not generate so much excess light as to induce faster growth in the vicinity.

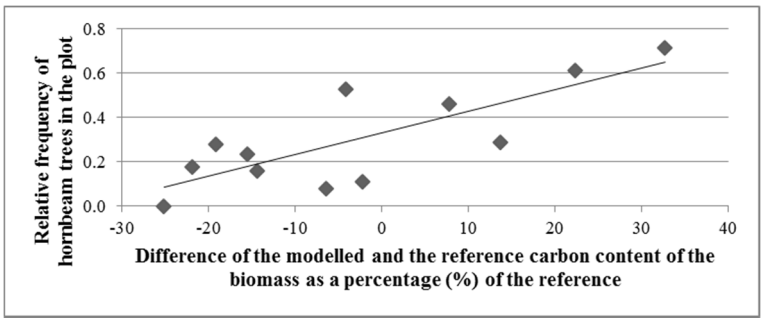

Fig. 4 The effect of species composition on the performance of the 'no mortality' model

4. CONCLUSIONS

Hungarian forests are considered important carbon sinks (Somogyi 2008); in fact, they are the only significant sinks in the greenhouse gas balance of Hungary (Kis-Kovács et al. 2011). As climate mitigation becomes a more and more pressing issue, the role of forests as carbon sinks will increase even further and management decisions will need to increasingly take this into account. Carbon sequestration models can be useful tools in planning future management strategies, but only if they are properly calibrated for the ecosystem in question. In our study we used data from the literature and other publicly available data for the parameterisation of the CO2Fix model and compared the model results to reference estimations based on data from a field survey carried out in autumn 2015 in some beech and hornbeam-dominated stands of Haragistya-Lófej forest reserve. Due to the less favourable site conditions, effects of earlier management and the age of the stands the actual carbon content of the biomass was found to be somewhat lower than expected in a near-natural beech forest. We also examined the effect of using different mortality settings on the results. The model with 'no mortality' settings was found to give the best results in almost all the plots, however the performance was species-dependent. The higher the proportion of hornbeam is at the site, the higher the chance that the model overestimates the carbon content. This draws attention to the fact that growth is much affected by the status of the individual within the canopy (expressed e.g. by the crown class) therefore the model performance could perhaps be further enhanced by taking this into account as well.

It is important to note that empirical data (even appropriate yield tables) for setting up even a relatively simple carbon sequestration model are scarce even for the most researched

tree species and forest types and there are several of these (usually economically less important) for which practically no data are available.

Acknowledgements: The authors express special thanks to Tamara Faragó and Adrienn Okner for their participation in the field work and dr. Ferenc Szmorad for his support.

REFERENCES

Béki A (1986) A gyertyán növekedése, fatermése és faállományszerkezete. [Growth, yield and structure of hornbeam (in Hungarian)] – In: Bondor A (ed) A gyertyán. Akadémiai Kiadó, Budapest

Béki A (1987) Növekedés, fatermés. [Growth and yield (in Hungarian)] In: Bondor A (ed) A kocsánytalan tölgy. Akadémiai Kiadó, Budapest

Carey EV, Sala A, Keane R, Callaway RM (2001) Are old forests underestimated as global carbon sinks? Global Change Biol 7:339-344

Chave J, Coomes DA, Jansen S, Lewis SL, Swenson NG, Zanne AE (2009) Towards a worldwide wood economics spectrum. Ecol Lett 12:351-366

Fischer PW (2013) The effects of forest management intensity on carbon storage and revenue in western Washington: a model and Monte Carlo-based case study of tradeoffs at pack forest. Master Thesis, University of Washington, https://dlib.lib.washington.edu/researchworks/handle/1773/22918

Führer E, Jagodics A (2009) A klímajelző fafajú állományok szénkészlete. [Carbon content of stands consisting of climate indicator species (in Hungarian)] Klíma-21 Füzetek 57:43-55.

Harmon ME (2001) Carbon sequestration in forests. Adressing the scale question. J Forest 4:24-29

Holzwarth F, Kahl A, Bauhus J, Wirth C (2013) Many ways to die–partitioning tree mortality dynamics in a near-natural mixed deciduous forest. J Ecol 101:220-230

Juhász P, Bidló A, Heil B, Kovács G, Patocskai Z (2008) Bükkös állományok szénmegkötési potenciálja a Mátrában [The carbon sequestration potential of beech forests in the Mátra Mountains, Hungary (In Hungarian)]. In: Proc of the Hungarian Conf on Soil Science, Bessenyei György Könyvkiadó, Nyíregyháza

Keith H, Mackey B, Berry S, Lindenmayer D, Gibbons P (2010) Estimating carbon carrying capacity in natural forest ecosystems across heterogeneous landscapes: addressing sources of error. Glob Change Biol 16:2971-2989

Kis-Kovács G, Hidy D, Tarczay K, Nagy E, Borka Gy, Lovas K, Kottek P, Somogyi Z, Zsembeli J (2011) National inventory report for 1985–2009, Hungary. Hungarian Meteorological Service, Budapest

Kiss M, Tanács E, Keveiné Bárány I (2011) Karsztos erdők szénmegkötésével kapcsolatos számítások egy erdőrezervátum adatai alapján [Calculations of carbon sequestration of karst forests using the data of a forest reserve (in Hungarian)]. Karsztfejlődés 16:157-166

Luyssaert S, Hessenmoller D, Von Lupke N, Kaiser S, Schulze ED (2011) Quantifying land use and disturbance intensity in forestry, based on the self-thinning relationship. Ecol Appl 21:3272-3284

Masera O, Garza-Caligaris JF, Kanninen M, Karjalainen T, Liski J, Nabuurs GJ, Pussinen A, de Jong BJ (2003) Modelling carbon sequestration in afforestation, agroforestry and forest management projects: the CO2FIX V. 2 approach. Ecol Model 164:177-199

Mendlik G (1986) A bükkösök fatermése. [The yield of beech stands (in Hungarian)] In: Bondor A (ed) A bükk. Akadémiai Kiadó, Budapest

Nabuurs GJ, Van Putten B, Knippers TS, Mohren GMJ (2008) Comparison of uncertainties in carbon sequestration estimates for a tropical and a temperate forest. Forest Ecol Manag 256(3):237-245

Neilson ET, MacLean DA, Arp PA, Meng FR, Bourque CPA, Bhatti JS (2006) Modeling carbon sequestration with CO2Fix and a timber supply model for use in forest management planning. Can J Soil Sci 86:219-233

Nunery JS, Keeton WS (2010) Forest carbon storage in the northeastern United States: net effects of harvesting frequency, post-harvest retention, and wood products. Forest Ecol Manag 259:1363-1375

Odum EP (1969) The strategy of ecosystem development. Science 164:262-270

Schelhaas MJ, van Esch PW, Groen TA, de Jong BHJ, Kanninen M, Liski J, Masera O, Mohren GMJ, Nabuurs GJ, Palosuo T, Pedroni L, Vallejo A, Vilén T (2004) CO2FIX V 3.1–a modelling framework for quantifying carbon sequestration in forest ecosystems. ALTERRA Report 1068. Wageningen

Somogyi Z (2008) A hazai erdők üvegház hatású gáz leltára az IPCC módszertana szerint [Greenhouse gas inventory of forests in Hungary using the IPCC methodology (in Hungarian)]. Erdészeti Kutatások 92:145-162

Sopp L, Kolozs L (eds) (2000) Fatömegszámítási táblázatok. [Forest yield tables (in Hungarian)]. Állami Erdészeti Szolgálat, Budapest

Tanács E (2011) Az erdőszerkezet tér- és időbeli mintázatainak vizsgálata a Haragistya-Lófej erdőrezervátum (Aggteleki-karszt) területén. [Spatial and temporal patterns of forest structure in Haragistya-Lófej forest reserve (Aggtelek Karst, Hungary) (in Hungarian)] PhD thesis, Szegedi Tudományegyetem, Szeged http://doktori.bibl.u-szeged.hu/753/

Tanács E, Barta S (2014) A mortalitás és a fafajösszetétel rövid távú változásai a Haragistya-Lófej erdőrezervátum üde erdőiben. [Mortality and short-term changes of species composition in the mesophilic forests of Haragistya-Lófej forest reserve (in Hungarian)] In: Tóth V (ed) Kutatások az Aggteleki Nemzeti Parkban II.

Tanács E, Szmorad F, Bárány-Kevei I (2007) A review of the forest management history and present state of the Haragistya karst plateau (Aggtelek Karst, Hungary). Acta Carsologica 36:441-451

Taylor AR, Wang JR, Kurz WA (2008) Effects of harvesting intensity on carbon stocks in eastern Canadian red spruce (Picea rubens) forests: an exploratory analysis using the CBM-CFS3 simulation model. Forest Ecol Manag 255:3632-3641

Veperdi G (2008) Erdőbecsléstan; oktatási segédanyag [The measurement of individual trees and stands; educational material (in Hungarian)]. University of West Hungary, Sopron

Veperdi G (2010) Természetközeli erdőnevelési eljárások faterméstani alapjainak kidolgozása. [Final report of the project Working out the basics of nature-based silviculture (in Hungarian)] http://real.mtak.hu/586/1/38415_ZJ1.pdf

Wutzler T, Mund M (2007) Modelling mean above and below ground litter production based on yield tables. Silva Fenn 41:559-574

Zboray Z, Tanács E, Bárány-Kevei I (2007) The accuracy and possible uses of a stand height map derived from a digital surface model. In: Proc of the ForestSat 2007 Conf, Montpellier, France